

17-7-2019

MSc thesis report

Techno-economic feasibility of Hydro-
power at weir-complex Driel with
assessment method for low-head run-of-
river powerplants

Ing. S.R. van Erp
TU DELFT & ARCADIS NL

Techno-economic feasibility of Hydro-power at weir-complex Driel with assessment method for low-head run-of-river powerplants

By

Ing. S.R. (Stefan) van Erp

MSc student Civil Engineering
Structural Engineering track
specialisation Hydraulic Structures

In partial fulfilment of requirements for the degree of

Master of Science
in Civil Engineering

at the Faculty of Civil Engineering and Geoscience of
the Delft University of Technology,
in the Netherlands

to be defended publicly on Wednesday July 24th, 2019 at 9:30 AM

Thesis Committee:

Chairman:

Dr. ir. J.D. (Jeremy) Bricker

TU Delft - Hydraulic Structures and Flood Risk
section

Dr. ir. drs. C.R. (René) Braam

TU Delft - Concrete Structures section

Ir. W.F. (Wilfred) Molenaar

TU Delft - Hydraulic Structures and Flood Risk
section

Additional member:

Dr. ir. M. (Miroslav) Marenc

UNESCO – IHE Institute for Water Education and
guest-lecturer Hydro-power Engineering at TU Delft

Company supervisor:

Dr. ir. H.G. (Hessel) Voortman

Arcadis NL

Company daily supervisor:

Ir. P. (Patrick) Buijs

Arcadis NL

An electronic version of this thesis is available at <http://repository.tudelft.nl/>.

PREFACE

As a final project this thesis is written as a part of the Master Structural engineering and specialization Hydraulic structures at the faculty of Civil Engineering and Geoscience of the Delft University of Technology in the Netherlands.

Arcadis NL provided the opportunity to undertake the research at their office and with their (hard and software) resources.

READING GUIDE

Starting with the introduction in chapter 1 after which the considered problem and scope of the research are stated in chapter 2 and chapter 3 respectively. A literature review summary is given in chapter 4 detailing the relevant theory and existing technologies. This chapter is a summary of the more elaborate literature review that is added in Appendix 2.

In chapter 5 the location is analyzed where subjects like the available flow and space are determined. The conceptual design has been worked out in chapter 6, where first a generic turbine and then three assigned turbine types: Kaplan, Venturi enhanced Kaplan and Archimedes screw have been analyzed. The financial performance of the designs are situated in chapter 7 and to round things off in chapter 8 the conclusions and recommendations can be found.

Behind that are the references and the appendices, to which have been referred throughout the report. They are both ordered by occurrence of reference in the text.

ACKNOWLEDGEMENTS

First I'd like to thank my thesis committee who have been very patient with me and given valuable feedback as well as directed me to many useful sources. Also I want to thank Patrick Buijs and Hessel Voortman for their advice, guidance and opportunity to work at Arcadis. Their regular input and feedback has helped shape this thesis greatly.

From the company Pentair Fairbanks Nijhuis I'd like to thank Raymond Meijnen for providing very useful information about their fish friendly Kaplan turbines. Using information from the manufacturer gives the results extra realism that cannot always be achieved by working from theoretical sources alone.

Then I'd like to thank Wim Schoonderbeek and Albert Bloem from the Hevea Initiative, without whom this research might not even have come about. Their creative idea has instigated this research and helping them get closer to achieving a more sustainable future has been a great experience.

Many others, like friends and family, have helped me with this research and gave me the opportunity and/or supported me in completing my studies at the TU Delft. Thank you very much, I am very proud of achieving this degree, but couldn't have done it without you.

*S.R. van Erp
Delft, July 2019*

ABSTRACT

The goal of this research is to assess technical and economic feasibility of hydropower at the weir-complex of Driel. A local initiative opting to improve the environment gained interest in the idea and asked Arcadis NL for help.

The weir complex at Driel lays in a key position in the Dutch river Delta and regulates the flow to the IJssel and Nederrijn, both important parts of the flood protection and important shipping routes. In the Nederrijn 2 other hydro-power plants have been built at weirs. Driel was considered as well, but at the time could not be made feasible due to the low head difference at Driel. Developments in low-head hydro-power have given new possibilities and reason for reassessment.

First the location has been analysed, in particular the flow situation. Except for the low head difference, the location lends itself well for a hydroelectric plant. The crux of the research is therefore in making the most of the available head.

4 variants have been worked out: a copy of the downstream hydro-power plant of Maurik as a reference, several variations on low head Kaplan turbines and an Archimedes screw have been assessed. A special variation of the Kaplan is the Venturi enhanced Kaplan, which uses part of the discharge to increase the head difference over the turbine.

To estimate the annual production, first a simple approach, assuming a turbine can create a certain head difference, and later a hydraulic model incorporating hydraulic losses and using turbomachinery theory, has been used for the Kaplan design variants.

The result of the comparison is that the regular Kaplan variant number 4 with 5 turbines, a combined capacity of 3.160kW and a LCOE of 0,154 € per kWh (using interest rate of 3,3%), has the best economic performance and is therefore recommended for further development. A good second option with a lower initial investment (9,6 million euros versus 20,5 of variant nr. 4) is design variant number 1 with a set of 2 Kaplan turbines having a combined capacity of 1.475kW and a LCOE of 0,161 € per kWh.

Despite the regular Kaplan performing better economically, the Venturi Enhanced Kaplan Turbine certainly has potential for low head run of river hydropower and is therefore recommended for further research as well. The increase in power and produced energy gives reason to believe that further optimisation and detailing will lead to a competitive design compared to the regular Kaplan turbines.

Key words: Low head, hydro power, Kaplan, Archimedes Screw Turbine, Venturi Enhanced Kaplan, Economic feasibility.

TABLE OF CONTENTS

Preface	ii
Reading guide	ii
Acknowledgements	ii
Abstract	iii
Table of contents	iv
List of symbols	viii
1 Introduction	1
2 Problem analysis, Research goal and question	2
2.1 Problem statement	2
2.2 Main goal	2
2.3 Research question	2
2.4 Problem analysis	3
2.4.1 Scale level 1 – Human activity	3
2.4.2 Scale level 2 – The Netherlands	4
2.4.3 Scale level 3 – Location Driel	9
2.5 Expected result	10
3 Research scope	11
3.1 Project area	11
3.2 Research method/plan	12
4 Literature study summary	13
4.1 Introduction of hydro-power-formulae and principles	13
4.2 Head-discharge-relation	15
4.2.1 Hydraulic losses	15
4.2.2 Quadratic resistance coefficient	16
4.2.3 Energy extraction	17
4.2.4 Turbine theory	19
4.2.5 Optimisation of power output and the Speed ratio r_s	20
4.2.6 Annual energy production	26
4.3 Cavitation limits	27
4.4 Existing Low-head-hydro-power-technologies	28
4.4.1 Reference project HPP Maurik	29
4.4.2 Reference project Dommelstroom	31
5 Location analysis	33
5.1 Location in Delta	33
5.2 Stakeholders around weir-complex Driel	33
5.3 Flow data analysis	33
5.3.1 Discharge data analysis	34

5.3.2	Discharge analysis results	34
5.3.3	Average values over time	37
5.3.4	Water level data analysis	38
5.3.5	Water-level-analysis results	39
5.3.6	Combining discharge and head-difference	40
5.3.7	Operation of the weir	41
5.4	Elevation and Subsoil analysis	44
5.4.1	Elevations	44
5.4.2	Subsoil	45
5.5	Shipping movements	45
5.6	Power grid connections	46
5.7	Protected areas and nature reserves	46
5.8	Requirements and design goals	47
5.8.1	Requirements	47
5.8.2	Economic design goals	48
5.8.3	Technical and secondary design goals	49
6	Conceptual design	50
6.1	Potential locations	50
6.1.1	Potential locations for head-based turbines	50
6.1.2	Free flow hydro-power schemes	51
6.2	Variant generation	53
	Longlist	53
	Shortlist	53
6.3	Generic turbine	54
6.3.1	Discharge duration curve	54
6.3.2	Discharge area	56
6.3.3	Power and energy production	57
6.3.4	Design variants	59
6.4	Free flow turbines	66
6.5	Regular Kaplan Turbine	67
6.5.1	First estimate of costs	67
6.5.2	Hydraulic model Kaplan	68
6.6	Venturi Enhanced Kaplan	72
6.6.1	Head discharge relation	73
6.6.2	Design variants	75
6.6.3	Head gain	76
6.6.4	Power output VET	77
6.6.5	Cost estimation VET	77

6.6.6	Conclusions VET	78
6.7	Archimedes screw turbine (AST)	79
6.8	Construction depth	82
6.9	Financial analysis	83
6.9.1	Magnitude of investment	83
6.9.2	Levelized cost of electricity (LCOE)	83
6.9.3	Internal rate of return	84
7	Results table	85
8	Conclusion and recommendations	87
8.1	Conclusions	87
8.1.1	Location	87
8.1.2	Flow analysis	87
8.1.3	Kaplan turbines	88
8.1.4	Venturi turbines	88
8.1.5	Archimedes screw turbines	88
8.1.6	Overall conclusions	89
8.2	Recommendations	89
	References	91
	Appendices	1
	Appendix 1 – Mind-map Problem analysis	3
	Appendix 2 – Literature review	5
	Hydro-power theory	5
	Introduction of hydro-power-formulae and principles	5
	Head-discharge-relation	8
	Loss-coefficients	9
	Sum of energy-head-losses in the system	18
	Energy extraction	18
	Turbine theory	21
	Optimisation of power output and the Speed ratio r_s	24
	Cavitation limits	32
	Annual Energy production	34
	Appendix 3 – Turbo-machinery-theory	35
	Appendix 4 – Existing Turbine technologies	37
	Kaplan	38
	Archimedes Screw Turbine (AST)	39
	Pump enhanced AST	42
	Waterwheel	44
	Oryon watermill	47

Appendix 5 – Stakeholders	48
Appendix 6 – Data quality and filtering method	50
Quality of the data	50
Discharge data quality	50
Water-level-data quality	51
Method of Loading and filtering the data:	52
Appendix 7 – Flow and water-level data analysis	56
Appendix 8 – A3 detailed flow duration curve	64
Appendix 9 – Net Present Value, LCOE and IRR explanation	66
Appendix 10 – Sub-soil profiles and info	70
Appendix 11 – Nature reserves and protected areas	71
Appendix 12 – Reverse engineered Maurik power isobars	74
Appendix 13 – Location and topography	80
Appendix 14 – Hydro-power-scheme variants	82
Appendix 15 – Output Energy calculation generic turbine (0.)	84
Appendix 16 – Hydraulic model Kaplan-bulb	86
Appendix 17 – Hydraulic model VETT	88
Appendix 18 – Output Energy calculation AST	90

LIST OF SYMBOLS

Ordered in alphabetical order where: lower case symbols precede upper case ones and Latin symbols precede Greek symbols.

Symbol	Description
A	(Cross-sectional) Area in square meters.
A_{ct}	Common tube discharge area in meters squared.
A_t	Cross-sectional area in square meters of the turbine at the location of the rotor, available for flow.
A_{tt}	Turbine tube discharge area in meters squared.
C	Quadratic resistance coefficient in seconds squared over meters to the 5th power. Equal to head difference over discharge squared.
C_{bpt}	Discharge resistance coefficient of the bypass tube in the Venturi Enhanced turbine in cubic meters per second
C_{ct}	Discharge resistance coefficient of the common tube in the Venturi Enhanced turbine in cubic meters per second
C_{Maurik}	Quadratic discharge coefficient that is valid for Maurik
C_{tt}	Discharge resistance coefficient of the turbine tube in the Venturi Enhanced turbine in cubic meters per second
CF	Capacity factor, amount of full load hours with respect to the amount of hours in a year
D	Rotor diameter
D_{in}	Inner diameter of the rotor where the blades attach, in meters
D_{out}	Outer diameter of the rotor in meters
D_t	Turbine diameter in meters
E	Energy in joule or kilowatt-hours
E_{annual}	The amount of energy in Joules or kilowatt-hours produced in a year by the considered system
g	Gravitational acceleration in meters per second squared
H	Energy head, the sum of hydraulic head (h) and velocity head (h_v).
h	Hydraulic head, the sum of pressure head and elevation head (z)
h_{at}	atmospheric pressure head in meters.
h_f	usable fall head in meters
H_{NPS}	Net positive suction head in meters
$h_{s,adm}$	admissible head in meters
h_v	Velocity head in meters, velocity squared over two times gravitational acceleration
h_{vap}	Vapour pressure head in meters

i_{river}	Inclination of the water surface (in free flow situation)
IRR	Internal rate of return
$LCOE$	Levelized Cost of Electricity, price per kilowatt-hour of produced energy such that the Net Present Value at the end of a chosen life-time is zero.
N	Rotation speed of the (turbine) system in revolutions per minute (rpm)
n_b	Number of blades of the turbine
n_p	Number of pole pairs
N_s	Specific speed in revolutions per minute (rpm)
N_{sp}	Power specific speed in revolutions per minute (rpm)
N_{ss}	Suction specific speed. Specific speed with as input the H_{NPS} and related discharge.
n_t	Number of turbines
NAP	"Normaal Amsterdams Peil", reference water level equal to sea level.
NPV	Net Present Value. Value of an amount of money spent or received in the future translated to present day value of said amount.
p	Lower case p , pressure in Pascal or newton per square meter.
P	Power of considered system in kilowatt
\hat{P}	Dimensionless power coefficient
p_0	The absolute stagnation pressure in Pascal
$P_{free-flow}$	Theoretical power of a free flow turbine in kilowatt
P_{rated}	The rated (maximum) design power output of the turbine in Joules per second or Watts
p_v	The vapour pressure in Pascal
PoT	Price of the turbine in euros per kilowatt
Q	Discharge in cubic meters per second
Q_{100}	100 day exceedance discharge in cubic meters per second. Discharge is equal or larger than this value 100 days in a year.
Q_{ava}	Available discharge for hydro power production in cubic metres per second
Q_{bpt}	Discharge of the bypass tube in the Venturi Enhanced turbine in cubic meters per second
Q_{buc}	Bucket discharge for an archimedes screw turbine in cubic meters per second
Q_{ct}	Discharge of the common tube in the Venturi Enhanced turbine in cubic meters per second
Q_{max}	maximum discharge in cubic meters per second going through the turbine while producing power

$Q_{max,total}$	Maximum discharge in cubic meters per second going through the entire set of turbines while producing power
Q_{NoLoad}	Discharge through the system when no load is applied by the turbine. I.e. the resistance of the turbine is zero.
Q_{sys_avg}	Average discharge through the entire system in cubic meters per second
Q_t	Discharge through the turbine when the rotor gives resistance to the flow, i.e. when load is applied by the turbine. This occurs when power is being generated by the turbine.
$Q_{t,20\%}$	20% of the maximum discharge Q_{max}
Q_{tt}	Discharge of the turbine tube in the Venturi Enhanced turbine in cubic meters per second
r_A	Discharge area ratio of the Venturi Enhanced turbine. Turbine tube discharge area over common tube discharge area.
r_h	Dimensionless head ratio or in short head ratio. Equal to the head over the turbine divided by the head over the system.
r_P	Product of head ratio and discharge ratio, with the idea that product of the discharge and head is proportional to the power.
r_Q	Dimensionless discharge ratio, or discharge ratio. Equal to the discharge through the turbine divided by the discharge through the system without any load
r_s	Speed ratio. Dimensionless ratio of rotation speed N over specific speed N_s or power specific speed N_{sp}
Re	Reynolds number
$t_{full-load}$	Equivalent amount of time in a year in seconds, or more commonly in hours, that the turbine runs at rated power. Annual energy divided by rated power.
t_{load}	Number of hours that the turbine has been active.
t_{year}	Total amount of time in a year (about 8760 hours)
u	flow velocity in meters per second
V_{buc}	Bucket volume for an archimedes screw turbine in meters cubed
W	Heat exchange within the system in Joules per second or Watts
z	elevation head, height of the considered flow line above the reference level
ΔH	Head difference. Difference between two head-levels in meters.
ΔH_{ava}	Available head difference for hydro power production in meters
ΔH_{avg}	Average occurring head difference in meters
ΔH_{bpt}	Head difference of the bypass tube in the Venturi Enhanced turbine in meters
ΔH_{ct}	Head difference of the common tube in the Venturi Enhanced turbine in meters
ΔH_{loss}	Energy head losses in the system in meters

ΔH_{max}	Maximum occurring head difference in meters
ΔH_{sys}	Head difference over the entire considered system in meters. The available head difference in meters.
ΔH_{sys_thres}	Threshold, minimum Head difference for the turbine to start over the entire considered system in meters. Derived from threshold head difference over turbine.
ΔH_t	head difference over the turbine in meters.
ΔH_{t_thres}	Threshold, minimum head difference over the turbine in meters for which the turbine will work or start.
ΔH_{tt}	Head difference of the turbine tube in the Venturi Enhanced turbine in meters
η	(Greek letter ieta/eta) Efficiency factor of a considered system
μ	(Greek letter mi/mu) Dimensionless discharge coefficient that scales the cross-sectional area A such that the correct head-discharge relation is given
ν_{dyn}	(Greek letter ni/nu) Dynamic fluid viscosity in Pascal. Constant for a given fluid and temperature.
ν_{kin}	(Greek letter ni/nu) Kinematic viscosity in meters squared per seconds squared, equal to dynamic viscosity over the mass density of the fluid.
ξ_{eq}	Equivalent loss coefficient, replaces a summation of loss coefficients over their related areas squared such that its value over the turbine area squared gives the same quadratic discharge coefficient C
ξ_i	(Greek letter xi) Dimensionless head-loss-coefficient for particular part "i" in the system, scaling the velocity head to be equal to the head-loss.
Π_i	(Greek kapital letter pi) The "i"th Buckingham's PI dimensionless group of parameters
ρ	(Greek letter rho) mass density in kg per cubic meter
σ_{Ts}	Thoma's cavitation coefficient
τ_i	(Greek letter tav/tau) Fluid thermodynamic internal energy per unit mass at location "i" in Joule per kg
φ	(Greek letter phi) Dimensionless volumetric flow coefficient
ψ	(Greek letter psi) Dimensionless Head coefficient (or sometimes also referred to as "Energy transfer coefficient")
ω_{screw}	(Greek letter omega) Screw rotation speed in rpm

1 INTRODUCTION

In the Netherlands there is a local initiative called the "Hevea Initiative" (HI, formerly known as "Heveadorp Energie Initiative"), that wants to implement sustainable energy applications and ideas in and around their village of Heveadorp (about halfway between Arnhem and Wageningen). HI suggested a plan to apply some form of hydro-power at the weir-complex of Driel.

The complex at Driel is 1 of the 3 weirs in the river "Nederrijn" or Lower Rhine (as shown in **Figure 1**). The river Rhine/Rijn enters from Germany. The bifurcation near Nijmegen is called "Pannerdenschekop". The bifurcation at Arnhem is called "IJsselkop". Downstream of the weir of Hagestein the "Nederrijn" becomes the river "Lek".

What makes this one special is that it controls the amount of water that flows into the IJssel river, especially in situations of low discharge. The reason to do this is to keep the IJssel navigable for shipping and also to make sure the IJssel-lake is being fed with sufficient water.

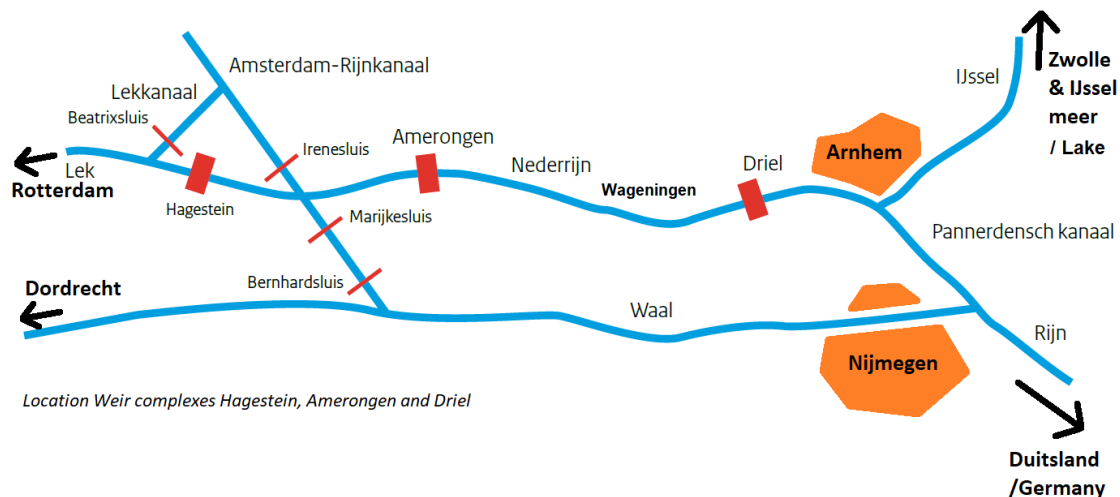


Figure 1 - Nederrijn with 3 weir-locations.

HI participated in a contest for sustainable energy ideas, where the prize was funding for the idea, and had noticed a technology called the "Oryon watermill" [1]. They proposed this technology to implement at weir-lock-complex Driel. Unfortunately they didn't win with this idea and they want to work the idea out in more detail.

HI wants to investigate by having a feasibility study performed. They contacted the "Koninklijke Nederlandse Heidmaatschappij" (abbreviated by KNHM). KNHM noted that they didn't have the required knowledge about hydro-power and thus contacted the engineering consultancy firm Arcadis NL. The three parties together then decided that for various reasons it would be best to have a student do the feasibility study and that's where this research comes in.

2 PROBLEM ANALYSIS, RESEARCH GOAL AND QUESTION

In this problem analysis 3 scale levels are considered. Level 1 on a global level considering human activity in general, level 2 is at a national level and level 3 considers the local situation. An attempt to capture the problem analysis in a mind map has been made and can be found in **Appendix 1**.

2.1 PROBLEM STATEMENT

The core problem is that Hevea Initiatief (HI) wants to apply hydro-power at and/or near the Weir-complex Driel and to provide sustainable electricity to the local community of Heveadorp, but has to overcome that:

1. Low head hydro power is technically challenging to get to work and the location of Driel sees very low head differences compared to other low head hydro power.
2. Any solutions found must also be economically feasible.
3. Both HI and KNHM don't have the required technical knowledge regarding civil and in particular hydro-power engineering to assess previous two points for hydro-power at Driel

When combined these form the following problem statement:

"Arcadis and the HI have developed interest in the techno-economic feasibility of hydro-power at weir-complex Driel, but this has to be reinvestigated due to developments in technology for low-head-run-of river hydro-power."

2.2 MAIN GOAL

"To assess the technical and economic feasibility of current state of the art hydro-power technologies at low-head run of river locations such as the weir complex Driel."

Which can be broken down into the following sub-goals:

1. Finding the technologies that are able to generate power from very low head situations present in Driel.
2. Determining the designs for technical feasible hydro power at Driel
3. Assessing economic feasibility for these designs

2.3 RESEARCH QUESTION

For which the research question is:

"What is the most optimal design of a hydropower plant at Driel in terms of economic performance while remaining technical feasibility, and what conclusions can be drawn that are also valid for similar locations?"

The sub-questions:

1. What functional requirements does the weir complex Driel have when hydro-power is added?
2. What are the technical requirements for head based power-plants when applied at Driel?
3. What are the economic requirements for hydro-power at Driel to be economically feasible?
4. What scoring criteria determine which variant/hydro-power schemes scores better at Driel?
5. Where are the best locations for free-flow turbines?
6. Where are the best locations for the head based turbines?
7. What is the most optimal design in terms of energy production?
8. What is the most optimal design in terms of economic yield?
9. What are the investment costs for the developed variants?
10. Which variant scores best for the situation of Driel?

2.4 PROBLEM ANALYSIS

2.4.1 Scale level 1 – Human activity

At a very high level of abstraction the situation is that the human population has been making and will keep making several demands of both itself and their environment. These demands are often supplied by human activity/exploits.

Three major demands often made are:

1. Economic growth or gain
2. Useful work to be done
3. Safe living environment

Economic growth or gain covers most of the wishes and needs of people. It works on the basis of doing work in return for money, which gives the possibility to purchase almost anything of choice, e.g. food, a place to live, etc.

With the term useful work in this case is the physical version is meant (force traveling over a distance, having the unit of joules). Work can be done for several reasons, for instance economic reasons or safety, etc. A good example for safety reasons could be a light illuminating the road. This is not done for economic reasons. Useful work is often done by converting stored energy into the desired form. This is commonly chemically stored energy converted into electrical work via several conversions (i.e. from chemical to thermal to mechanical to electrical energy, e.g. an engine powering a generator).

A safe living environment is a demand that cannot always be covered by the economic demand, because certain risks cannot be carried by one person alone. For instance flooding is something that a large group of people can be victim of and also requires quite an investment to protect against. That is often where government- and semi-government-agencies are called for, to bear this responsibility for many people in a certain region e.g. a nation or a province.

All these demands lead to human activities that have an influence on the environment. Land is being used and occupied to perform all these activities, resources are extracted and pollutants can be introduced into the environment.

Another influence that has been a topic of discussion for quite some time is human induced climate change, where so named "greenhouse gasses" are released that have an effect that is greater than natural occurring fluctuations in the climate. Large emissions of these greenhouse gasses are often linked to the use of fossil fuels in order to produce energy or work. Especially because they bring stored greenhouse elements back into the cycle. Both human induced climate change and the use of fossil fuels in general have a bad influence on the environment.

These effects of human activity on the environment are considered by many as a threat to natural life, including human life. As such this conflicts with the 3rd major demand. Requests for reduction of this human influence on the climate increase in size and frequency, as can be seen by actions such as the Paris agreement [2, p. 3], where 171 of the 195 countries in the world signed an agreement to do just that.

2.4.2 Scale level 2 – The Netherlands

Within the Netherlands the previously described principles are also at work. The energy accord and climate agreements are actions that are similar as the one of the Paris agreement. They aim at stimulating the so called "Energy-transition" where the goal is to change from fossil fuels to renewable energy like wind-, solar-, hydro-power, etc.

Renewable energy in general is not a very large contributor to the country's annual energy consumption of 3.150,6 PJ (in 2017) [3]. Of this amount 945 PJ [4] is being used for production of electricity, of which **419 PJ is actual electrical energy** [4]. The other portion is turned into heat (which is often used by industry or heating of greenhouses). In **Figure 2** the contributions to production of 2017 can be seen. Only 16,9% of total energy used for electric energy is powered by non-fossil-fuel-sources of which large parts are covered by nuclear power (3,5%) and burning of biomass (7,7%). Unsurprisingly the contribution of hydro-power in the Netherlands is therefore not very large, only 0,6% [5] of the total electrical energy production.

Energy sources for electricity in NL in 2017

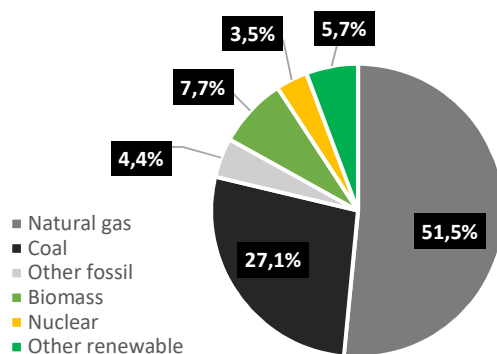


Figure 2 - Pie chart of energy sources for electricity in 2017 in the Netherlands (100%=945 PJ). - CBS [4]

% of total renewable electric energy production in NL in 2017

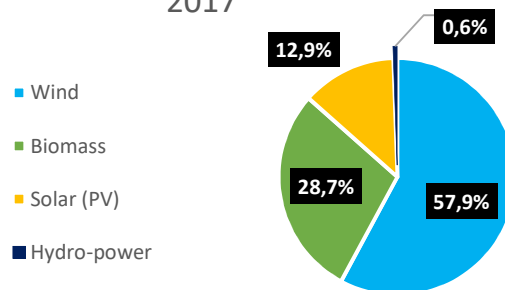


Figure 3 - Electric power production in % of total (100% = 60PJ). - Source: CBS [6]

Available energy for hydro-power in the Netherlands

The low-land rivers like the Rhine don't have much energy left after flowing down from the Alps all the way through Switzerland, Lichtenstein, Austria, France, Luxemburg and Germany, losing energy mostly through (bed) friction and some hydro-power-plants along the way as well.

Examples of such plants are the hydro-power-station in the rhine are Iffezheim (run-of-river, 146MW) near Karlsruhe, station Wyhlen (run-of-river, 38,5MW) near Basel at the Swiss-German Border, Rheinfelden (run of river, 100MW) and Ryburg-Schwörstadt (run-of-river, 60MW) all run by TransnetBW GmbH [7]. Let's consider at an abstract level for a moment the amount of energy going through the Netherlands: At Lobith the river Rhine enters the Netherlands.

From **Figure 5** it can be seen that between the years 1901 and 1960 the average 100 day exceedance discharge is about $Q_{100} = 2300m^3/s$, that for the this case will be assumed constant.

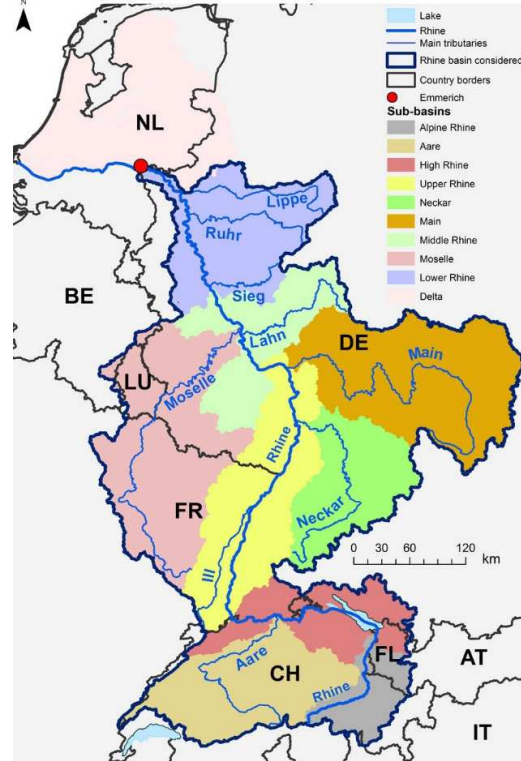


Figure 4 – Map of the Rhine basin - Source: [8, pp. 4231, Figure 1]

Note that 100 day average exceedance is equal to the 265 day subscedance discharge.

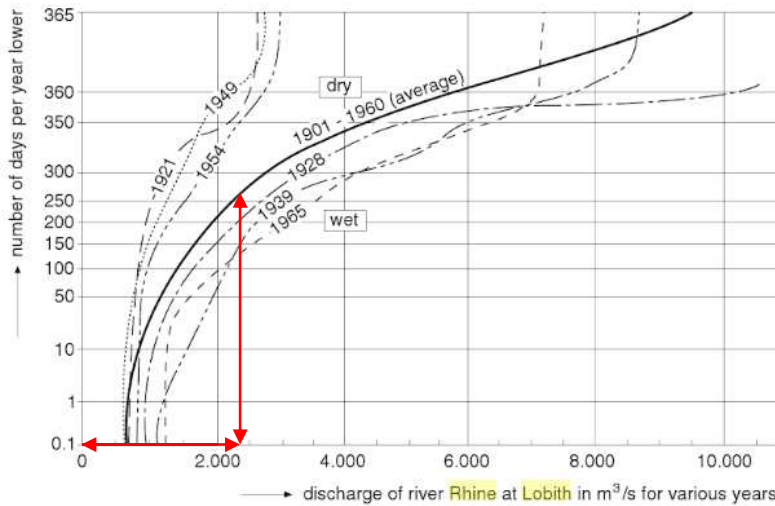


Figure 5 – Discharge subscedence curve for various years at Lobith. - Source: [9, pp. 135, figure 4.65]

Imagine a tube that takes all this discharge from Lobith in the East of the Netherlands, in a straight line, all the way to the North-sea in the West of the Netherlands. Assuming that the water-level at Lobith is on average 10m above NAP (Normaal Amsterdams Peil, sea-level), the resulting water-level-difference will then be $\Delta H = 10m$. See also **Figure 6** for a sketch of this situation.

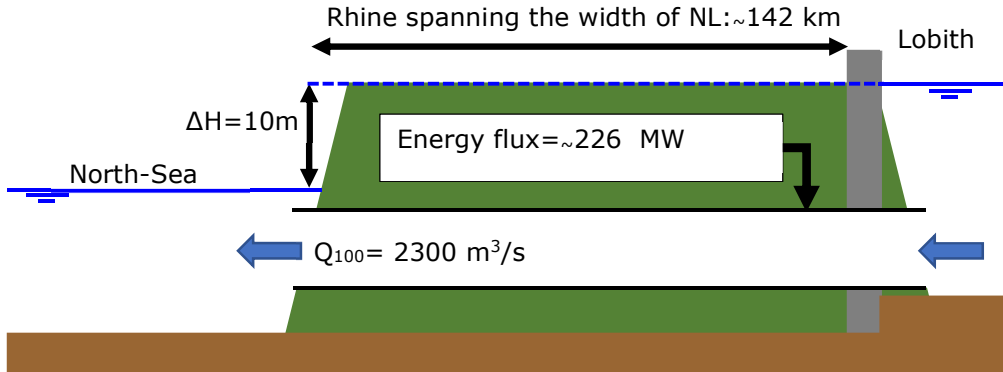


Figure 6 - Schematic theoretical turbine diverting all Rhine flow at Lobith to the turbine flowing out in the North-sea representing energy content Rhine Delta.

Further in the report, in the "Literature study summary" in **Chapter 4** a few important formulas have been clarified, which are used for this short analysis (hence the number 4 in the formula references "(4 - #)"). The formulas are explained there.

In **Figure 7** a schematic representation of a generic low-head hydro-power plant that is being referred to below, is shown. Here it is important to distinguish Energy-head (H), pressure-head (h) and velocity head ($\frac{u^2}{2g}$), where the first mentioned is the sum of the latter two as given by Bernoulli's law:

$$H = \left(\frac{p}{\rho g} + z + \frac{u^2}{2g} \right) = h + \frac{u^2}{2g} = h + \frac{Q^2}{2g * A^2} \tag{4 - 3}$$

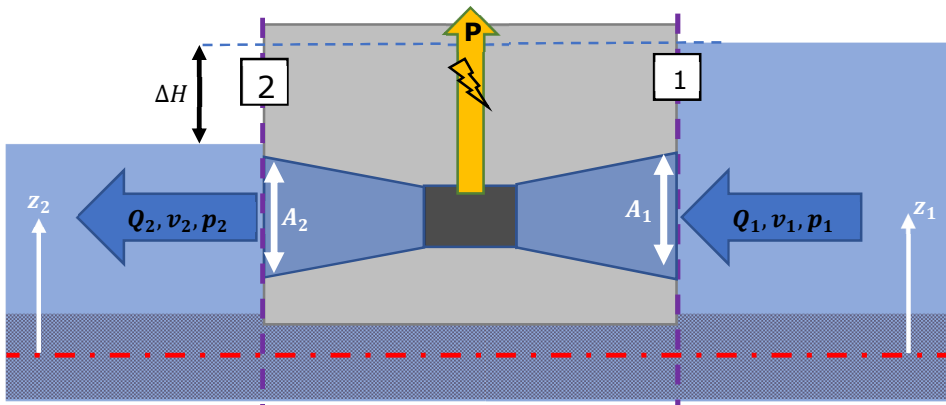


Figure 7 - Simplified hydropower system

The "hydro-power equation" is as follows:

$$P = \eta \cdot \rho \cdot g \cdot Q \cdot \Delta H_t \tag{4 - 2}$$

Where:

- $P =$ Power output of the considered system in [W]
- $\eta =$ efficiency factor of the considered system, dimensionless, $[0,0 \geq \eta \geq 1,0]$
- $g =$ Gravitational acceleration (in this report assumed to be constant with a value of 9,81) in $[m/s^2]$
- $\rho =$ Mass density of the fluid in $[kg/m^3]$ (assumed constant)
- $Q =$ Discharge through the considered system in $[m^3/s]$
- $\Delta H =$ Water-level-difference over the considered system in $[m]$,
i.e. $\Delta H = H_2 - H_1$

With that the energy flux or power from Lobith to the sea is:

$$P = 100\% \cdot 1000 \cdot 9,81 \cdot 10 \cdot 2300 \cdot \frac{1}{1000} = 225.630 \text{ kW} \approx 226 \text{ MW}$$

To get an idea of the amount of energy going through the Rhine with previous assumptions and also assuming that the average flow is present every hour of a year the annual energy production of a turbine can be calculated with **(4 - 23)**:

$$E_{\text{annual}} = \int_0^{t_{\text{year}}} P(t) dt \quad (4 - 23)$$

Where:

$P(t) =$ The instantaneous power output of the considered system at time t in [kW]

The energy produced in a year should the turbine run at full capacity is then:

$$E_{\text{annual}} = 24 \text{ hours} \cdot 365 \text{ days} \cdot 225.630 \text{ kW} = 1.976.518.800 \text{ kWh} = 7,12 \text{ PJ}$$

That is about 1,70% of the annual gross electrical energy produced of 2017 and equals 564.720 households^(3500kWh/year).

Also an important figure is the capacity factor shown below.

$$CF = \frac{E_{\text{annual}}}{t_{\text{year}} \cdot P_{\text{rated}}} = \frac{t_{\text{full-load}}}{t_{\text{year}}} \quad (4 - 24)$$

Where:

$CF =$ Capacity factor in [%]

$E_{\text{annual}} =$ The amount of energy produced in a year by the considered system in Joules [J] or more commonly in kilo-Watt-hours [kWh]

$P_{\text{rated}} =$ The rated (maximum) power-output of the considered system in Joules per second [J/s] or more commonly in kilo-Watts [kW]

$t_{\text{year}} =$ Amount of time in a year in [s] or more commonly in [hours], about 8760 hours.

$t_{\text{full-load}} =$ Equivalent amount of time in a year in [s] or more commonly in [hours], that the turbine runs at rated power P_{rated}

A global average capacity factor for hydro power, according to IPCC report on hydro-power of 2015, is 44% [10], based on a combined capacity of 926 GW (gigawatt) and combined annual energy production of $3,551 \cdot 10^6$ GWh/year (Gigawatt hours per year).

Assuming that the CF is indeed 44% and a system efficiency is 100%, the theoretical energy that can be produced in a year would be 869.668.272 kWh = 3,13 PJ or 0.75% of the annual-gross-electrical-energy-production²⁰¹⁷ in the Netherlands.

That is 248.477 households^(3500kWh/year).

This ignores several facts that reduce the actually available energy like:

- The flow from Lobith is divided over several different rivers (visualised in **Figure 8**);
- Friction, which can be quite considerable over the distance from Lobith to the sea (about 142km);
- The fact that a part of the head-difference is needed to create a discharge;
- Other energy losses in the system (inflow/outflow).
- Fluctuations in sea-level, discharge, water-level, etc.

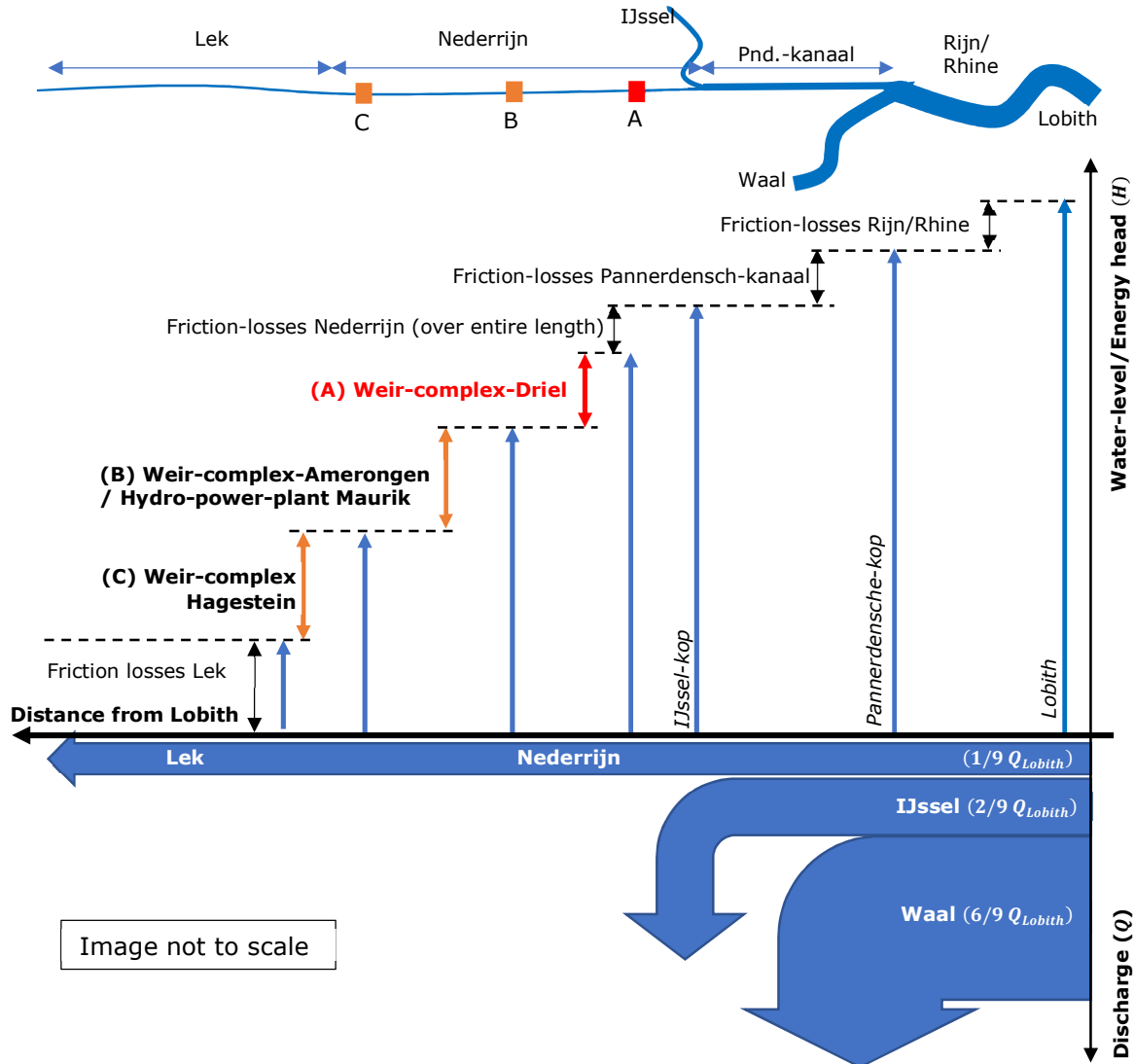


Figure 8 – Sketch of water levels (for the situation that all weirs are closed) and below the discharge distribution starting from Lobith.

Note: Right side of the picture is upstream, going to the left is downstream.

Pannerdensche-kop and IJssel-kop are the two bifurcation points of the river. Both are indicated in **Figure 8**.

Like other renewable energy sources, the amount of energy available for hydro-power is therefore not something that can be relied on completely and will always need to be backed-up by other sources of power.

River-delta-system

The river Rhine has an important function within the Netherlands. It is of course a source of fresh-water, enables shipping, prevents inflow of salt water in the cities close to the coast like Amsterdam, Rotterdam, Den Haag and Schiedam to name a couple (see **Figure 9**) and controls the ground-water-table along the river. The ground-water-level is important for agriculture, nature, but also for foundations of houses near the river.

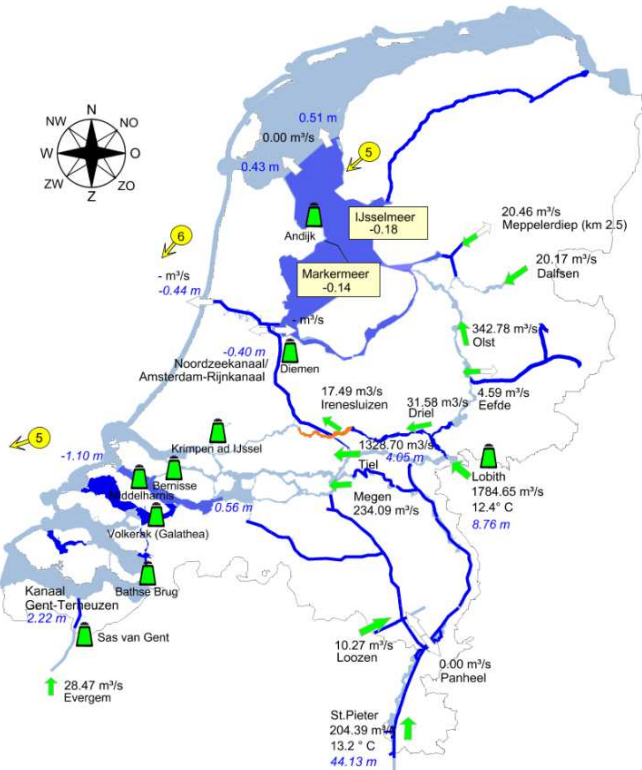


Figure 9 - Screen-shot of Real-time National Water-level and discharge overview. – Source: RWS [11] – accessed 10-04-2019 at 14:46 hr
Orange areas have a below target water-level.
Green arrows indicate in-/outflow discharges.

2.4.3 Scale level 3 – Location Driel

Downstream of Lobith the Rhine bifurcates after only a short distance into the Waal and Pannerdensch-kanaal. The latter bifurcates at Arnhem into the Lower Rhine (Nederrijn, in Dutch) going west and the IJssel going North to the IJssel lake. The weir at Driel regulates the discharge into the IJssel for low discharges from Lobith and is thus an important structure for the water level and distribution management.

This water level management is of paramount importance for flood-protection, shipping and fresh-water supply. For that reason the owner, RWS values this structures function highly.

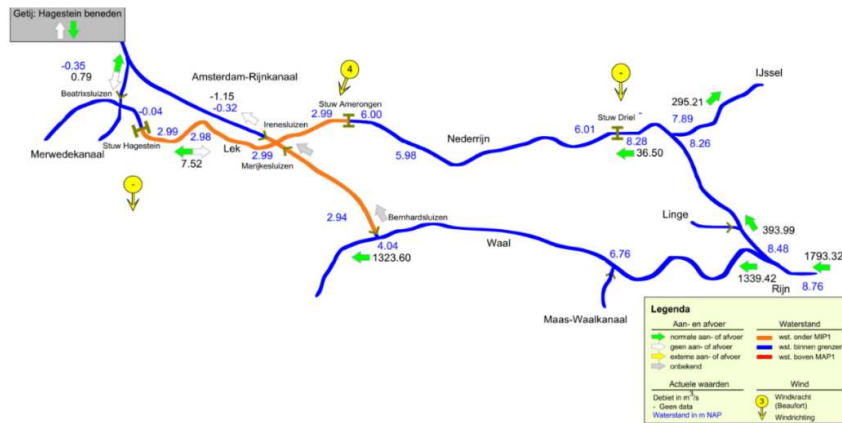


Figure 10 - Screen-shot of Real-time Water-level and discharge overview of the Nederrijn and Lek. . – Source: RWS [12] – accessed 10-04-2019 at 15:32 hr
Legend: same as **Figure 9**

For about 80% of the time in a year, the weir gate at Driel is closed, creating a water level difference. In that sense it is an ideal location to apply hydropower. This is also what HI concluded.

The potential for hydropower at Driel has been assessed before in its life-time, in 1968 and at the time the conclusion was drawn that it is not feasible at Driel, where it was at the two downstream weirs of similar build (Amerongen and Hagestein).

Hagestein has Hydro-power from the time it was built (1958) in the shape of an experimental smaller turbine (the syphon Kaplan technology at the time was quite unique) and not really designed for large scale electric power production.

The power-house at Amerongen has more "serious" proportions and has been built in 1968, after completion of the weir. The complex has a capacity (rated power) of 10MW with 4 bulb-Kaplan-turbines.

2.5 EXPECTED RESULT

The hypothesis of this research is that with development of new technologies and hydro-power schemes it may now be possible to apply hydro-power at Driel cost-effectively.

Royal Haskoning DHV (RH-DHV) has performed a study [13] for the Province of Gelderland (the provincial government) to check economic feasibility based on "reverse financial engineering" using financial goals like Internal rate of return (IRR) and payback periods. The study is aimed mostly at mapping the potential locations for the province of Gelderland.

The company also mentioned that, on one hand it is harder to design economically feasible hydropower projects in the Netherlands. This due to the lack of elevation differences. On the other hand there is new potential in new technologies, especially in the field of smaller hydro-power projects (capacity < 1MW).

RH-DHV calculated that with a 1,8 MW hydro-power-plant the theoretical energy production would be 4739 MWh (energy for about 1.247 families/3.800kWh), which is assuming about 2.633 full-load-hours (~110 days). With an internal rate of return (IRR) of 10 to 12 percent RH-DHV estimated that the maximum investment amount is between 3,028 million and 3,905 million euros. Using existing projects as reference they estimated a required investment of 7,2 million euros, leaving a 3,3-4,3 million euro investment gap.

They claim this has mostly to do with the available resource, however analysing the flow data, this is not necessarily true. RH-DHV assumes the weir is opened 100 days a year, where RWS claims this to be 75 days a year.

None-the-less, RH-DHV suggests that Driel might still be a feasible location in case the powerhouse construction is combined with maintenance and repairs of the weir and if existing structure is used for support.

Thus, both the fact that RH-DHV may have taken a conservative assumption for the amount of operation days and the possibility of combining the construction with repair and maintenance makes further analysis of this location worth the effort.

Besides that, whatever the result may be regarding Driel, this case-study can still be used to make assessments for other similar locations.

3 RESEARCH SCOPE

One only has limited time and resources to conduct a research, therefore it is important to state the intended scope, what will be part of the research and, arguably more important, what will not be part of it.

3.1 PROJECT AREA

The project initial aim is to power houses in (the neighbourhood of) Heveadorp. Especially when considering free-flow turbines, potentially the whole river could be used for that. The main limitation being transportation of the power to the local grid. However, chosen is to limit this research to the Nederrijn river, no further upstream than the IJsselkop bifurcation and also no further downstream than Amerongen weir, which lies 31km from the weir of Driel. This gives a $12,5+31=43,5$ km stretch of river and of course the weir itself to analyse for power production (see also **Figure 11**).

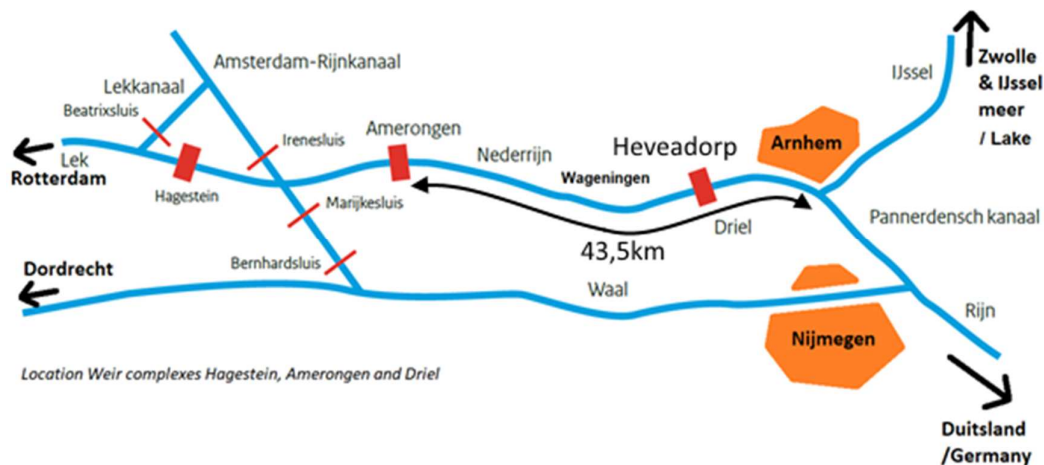


Figure 11 - Schematic map of weir-locations in the Nederrijn river

Besides this physical/geographic scope some limitations will be made that are also mentioned in the program of requirements in **paragraph 5.8**.

A wide variety of designs and hydro-power schemes can be thought of in this situation, but only the most promising variants have been worked out in detail as shown and described in paragraph **6.1**.

3.2 RESEARCH METHOD/PLAN

The method used consists of the following steps:

1. First information and data is gathered about the location.
2. Based on gathered information layouts or hydropower schemes were made, making provision for both free-flow and head-based hydro.
3. A generic turbine will be considered, where no specific type is chosen yet. This to determine the available energy in the flow and to make an estimate of the amount of turbines and their size.
4. Various turbine techniques will be considered in the considered layouts. A quick assessment is made to determine the most promising techniques and these are worked out in further detail, which entails making an hydraulic model for the losses in the used system to determine what is left for power production. The calculation is based on literature and is verified by software that is commonly used in civil engineering practise at Arcadis.
5. Once the power and energy production calculation method is ready, the variants developed by the generic turbine are run through their respective model to find the optimal configuration for each considered technique.
6. When the designs and dimensions are determined, a cost estimation is made to find the initial investment required to make a certain hydropower scheme with a certain technique. This is used, along with the energy production, to determine the levelized cost of electricity and internal rate of return.
7. With this known the variants are compared and the preferable variant(s) advised to the reader. From these actions conclusions are drawn, recommendations made and the research concluded.

4 LITERATURE STUDY SUMMARY

The hydraulic theory involved with calculating the energy production of a hydro-power-plant is quite extensive. Therefore the literature study is summarized here and the full review can be found in **Appendix 2 – Literature review**.

Also the existing technologies are briefly discussed.

4.1 INTRODUCTION OF HYDRO-POWER-FORMULAE AND PRINCIPLES

The hydropower equation can be derived by starting with the commonly known 1st (first) rule of thermodynamics and making the following assumptions:

1. Flow goes through a restricted volume, a pipe-system, from the upstream end to the downstream end;
2. Changes in temperature while the water flows through the system are negligible (i.e. thermal energy content before and after is equal and change is zero);
3. The fluid is incompressible (constant mass-density);
4. At any section in the pipe-system the cross-sectional area multiplied with the velocity equals discharge (i.e. $Q = v \cdot A$);
5. the energy flux through this system is only dependent on the loss of potential energy in terms of elevation.

Assumption number 5 also means that at the system boundaries there is no change in kinetic energy. Meaning the flow velocity is equal between the inflow boundary, a cross-section some distance before the inflow, and the outflow boundary, a cross-section some distance after outflow of the pipe-system.

With these assumptions the energy flux is defined as follows:

The energy flux $\frac{d}{dt}E$ is determined by the amount of mass flowing through the system per second ρQ , being accelerated by gravity g , thus creating impulse (force per second) and traveling in the same direction as this impulse (vertically downwards) over a distance ΔH thus producing work per second commonly known as power.

The so called "hydro-power-equation" **(4 - 2)** is derived from this energy flux **(4 - 1)**, by introducing an efficiency factor of the system η_{sys} :

$$\frac{d}{dt}E = \rho \cdot g \cdot \Delta H \cdot Q \quad (4 - 1)$$

$$P = \eta_{sys} \cdot \rho \cdot g \cdot \Delta H \cdot Q \quad (4 - 2)$$

Where:

$\frac{d}{dt}E =$	Energy flux in Joules per second [J/s] or Watt [W]
$\rho_i =$	Mass density of the fluid at location "i" in the system in [kg/m^3]
$g =$	gravitational acceleration (in this report assumed to be constant with a value of 9,81) in [m/s^2]
$Q =$	Discharge through the considered system in [m^3/s]
$\Delta H =$	Water-level-difference over the considered system in [m]
$P =$	Power output of the system in [kW]
$\eta_{sys} =$	System efficiency factor of the considered system, for a turbine is the effectively produced power per present energy flux. Dimensionless, [$0,0 \leq \eta \leq 1,0$]

Also important to clearly define is Bernoulli's equation, where assuming no energy losses, at any point along a streamline the following holds:

$$H(x) = \frac{p(x)}{\rho g} + z(x) + \frac{(u(x))^2}{2g} = h(x) + h_v(x) = \text{constant} \quad (4 - 3)$$

Where at location x along the system axis (flow line):

- $H(x)$ = Energy-head in [m]
- $\frac{p(x)}{\rho g}$ = Pressure-head in [m]
- $z(x)$ = Elevation-head in [m] with respect to a pre-defined constant reference level (see also **Figure 12** below)
- $h_v(x) = \frac{(u(x))^2}{2g}$ = Velocity head in [m] with $u(x)$ being the flow velocity in [m/s]
- $h(x)$ = Hydraulic head, sum of pressure- and elevation-head, in [m]
i.e. $h(x) = \frac{p(x)}{\rho g} + z(x)$

When including losses between two points along the stream-line the Bernoulli-equations needs to be altered slightly, by adding a loss-term. This loss term can be a change in velocity head and/or hydraulic head.

$$\Delta H = H(x_2) - H(x_1) = \Delta h + \Delta h_v \quad (4 - 4)$$

Where ΔH = Water-level-difference over the considered system in [m]

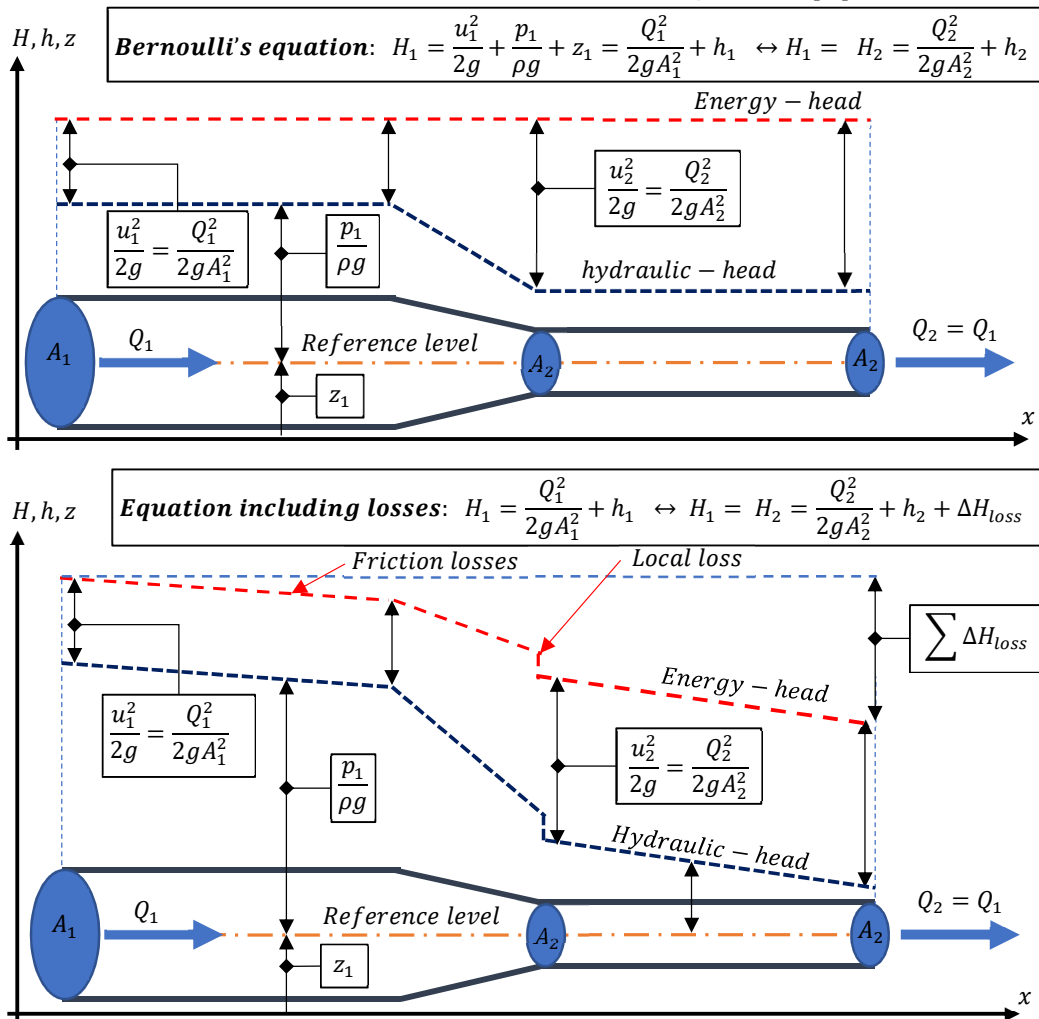


Figure 12 - Bernoulli's equation visualised both with and without losses.

4.2 HEAD-DISCHARGE-RELATION

From **(4 - 2)** it is clear that the amount of energy for a hydro-power turbine is dependent on both the discharge and the head-difference over the turbine. However, these quantities are different from available head difference and discharge. Therefore, the following relations are required:

$$\Delta H_t = f_1(Q_{ava}, \Delta H_{ava}) \quad (4 - 5)$$

$$Q_t = f_2(Q_{ava}, \Delta H_{ava}) \quad (4 - 6)$$

Where:

$\Delta H_t =$	Head difference over the turbine in [m]
$Q_t =$	The discharge going through the turbine in [m ³ /s]
$f(Q_{ava}, \Delta H_{ava}) =$	A function of Q_{ava} and ΔH_{ava} resulting in the head-difference over the turbine in [m]
$Q_{ava} =$	The available discharge in [m ³ /s]
$\Delta H_{ava} =$	The available head difference in [m]

Note: Both Q_{ava} and ΔH_{ava} are boundary conditions for the design of the powerplant.

Formula **(4 - 7)** can be derived from Torricelli's law (see also "Head-discharge-relation" in **Appendix 2**), giving the exit velocity of a fluid from a orifice (hole or opening in an container) at a certain height below the fluid-surface, and using assumption nr. 4. This formula gives the discharge for a system that has (turbulent) flow through a pressurised (pipe) system.

$$Q = \mu \cdot A \cdot \sqrt{2 \cdot g \cdot \Delta H} \quad (4 - 7)$$

Where:

$Q = A \cdot u$	Discharge through the considered system in [m ³ /s]
$A =$	Physical cross-sectional-area through which the water flows in [m ²]
$\mu =$	Dimensionless discharge coefficient that scales the cross-sectional area A such that the correct discharge is found.
$\Delta H =$	As defined before in (4 - 2) , the water-level-difference over the considered (part of the) system in [m]

4.2.1 Hydraulic losses

Hydraulic losses, or also called head losses, are expressed such that they are proportional to the velocity head (see **(4 - 8)**). This can be derived by rewriting **(4 - 7)**. The losses can be categorised in several ways. For instance if they occur locally or over a distance. Most important is that the sum of them determines the discharge through the whole system. Most common losses that occur in pipe-systems are: inflow, contraction, expansion, outflow and friction.

The head-loss in each part of the system can be determined by the related loss-coefficient ξ_i (X_i), that are being used in the design of sewage systems and other pipe-flow situations. These X_i factors can be found in many literature references, among which Deltares 's guide for designing and maintaining sewage-transport-systems [14], and more in depth in W.H. Hager's "Wastewater Hydraulics - chapter 2 Losses in flow" [15].

The head-loss scales quadratically with the flow-velocity, as can be seen below:

$$\Delta H_i = \xi_i \cdot \frac{u_i^2}{2g} = \xi_i \cdot \frac{Q_i^2}{2g \cdot A_i^2} \quad (4 - 8)$$

Where:

$\Delta H_i =$	The head-loss in a particular part "i" of the system in [m]
----------------	---

$\xi_i =$	The dimensionless loss-coefficient that determines what fraction of the velocity head results in loss of energy head. (Note the energy-head is not necessarily reduced, but the losses scale with the velocity-head).
$u_i =$	The flow-velocity in [m/s] at point "i" in the system that governs the losses, sometimes this is the velocity before, at or sometimes after the point of interest. Is Determined by discharge Q_i and cross-sectional area A_i at point "i"

Hager also references the book about hydraulic losses from I.E. Idel'cik [16], which is an extensive work that uses both theory and experimental data for determining loss-coefficients and has been reprinted and updated several times.

In **Appendix 2** in the paragraph "Loss-coefficients" the relevant factors have been described in further detail. The losses included in the hydraulic models for this thesis are:

1. Wall-friction losses
2. Expansion losses
3. Contraction losses
4. Inflow losses
5. Combining conduit losses (Y-junction)
6. Outflow losses
7. Trash-rack losses

4.2.2 Quadratic resistance coefficient

In the case of a system with elements in series, like the turbine system in **Figure 14**, the sum of the losses ΔH_i must be equal the total head-difference over the system. With that in mind the following equations can be formed:

$$\Delta H_{sys} = \sum_{i=1}^N \Delta H_i = \frac{Q^2}{2g} \cdot \sum_{i=1}^N \frac{\xi_i}{A_i^2} \quad (4 - 9)$$

Where:

$\Delta H_{sys} =$	The head-difference over the entire system, the total available head-difference in [m]
$\sum_{i=1}^N \Delta H_i =$	The sum of all the head-losses due to elements "1" up to and including element "N"

Due to continuity ($Q_{in} = Q_{out}$, because flow of mass is equal, and due to density remaining constant also volume V must be equal: $m_{in} = m_{out} (=) V_{in} = V_{out}$), the discharge in the entire system is the same for each entry ($Q_i = Q_t$). Therefore, writing out the sum and solving for Q_t , gives the relation for Q_t in terms of ΔH_{sys} .

For shorter writing the equivalent loss coefficient " ξ_{eq} " and the quadratic resistance coefficient " C " are defined as:

$$\xi_{eq} = A_t^2 \cdot \sum_{i=1}^N \frac{\xi_i}{A_i^2} \quad (4 - 10)$$

$$C = \frac{\Delta H_{sys}}{Q_t^2} = \frac{1}{2g} \cdot \sum_{i=1}^N \frac{\xi_i}{A_i^2} = \frac{\xi_{eq}}{2g \cdot A_t^2} \quad (4 - 11)$$

Where:

$\xi_{eq} =$	The equivalent loss coefficient.
$C =$	The Quadratic resistance coefficient in [s ² /m ⁵]

Note that most ξ_i values are dependent on the diameter and geometry of the turbine and thus ξ_{eq} too.

4.2.3 Energy extraction

When involving energy extraction, not all of the changes in head are due to friction or turbulence any more. A "head-difference" caused by the turbine is introduced. The discharge for all terms is the same Q and gravitational acceleration g is also assumed constant. The sum off head-differences is then:

$$\Delta H_{sys} = \sum_{i=1}^M \Delta H_i = \Delta H_t + Q_t^2 \cdot C \tag{4 - 12}$$

Where:

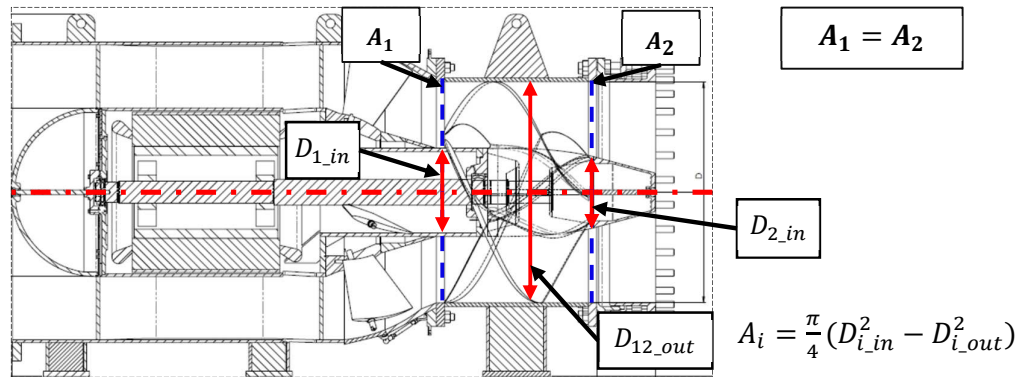
- $\Delta H_{sys} =$ The head-difference over the entire system, the total available head-difference in [m]
- $\sum_{i=1}^M \Delta H_i =$ The sum of all the head-differences due to elements "1" up to and including element "M"
- $Q_t^2 \cdot C =$ The sum of all the head losses, sometimes also referred to as "minor-losses", caused by friction, turbulence and the like, in [m].
- $\Delta H_t =$ The head-difference over the turbine in [m]

The head over the turbine is determined by turbo-machinery theory.

In **Figure 14** a simplified pipe-system with turbine is schematised. In this schematisation some assumptions have been made:

1. The cross-sectional area A_1 before (upstream) and after A_2 (downstream) of the turbine blades are assumed equal ($A_1 = A_2$)
2. Ignoring internal workings of the turbine with interaction with the rotor blades, the head-difference over the turbine is equal to the hydraulic-head-difference (i.e. $\Delta H = \Delta H_t = h_1 - h_2 = \Delta h$, see also formulas in **Figure 13**). The useable head over the turbine is not dependent on change in velocity head.

This isn't such a strange assumption for reaction turbines considering designs like shown in **Figure 13**. Even if the area's aren't exactly the same (e.g. $A_2 > A_1$), the head-difference is $\Delta H = \Delta H_A + \Delta H_t$, where ΔH_A is due to the geometry and ΔH_t due to the turbine, see also formulas in **Figure 13**).



$$H_1 = H_2 - \Delta H_{12} \quad \rightarrow \quad h_1 + \frac{Q_1^2}{2g \cdot A_1^2} = h_2 + \frac{Q_2^2}{2g \cdot A_2^2} - \Delta H_t, \quad \text{Bernoulli's equation}$$

$$h_1 + \frac{Q^2}{2g \cdot A_1^2} = h_2 + \frac{Q^2}{2g \cdot A_2^2} + \Delta H_A - \Delta H_t, \quad (\text{with } Q_1 = Q_2 = Q)$$

From that: $\Delta H_t = h_1 - h_2$ and $\Delta H_A = \frac{Q^2}{2g} \left(\frac{1}{A_2^2} - \frac{1}{A_1^2} \right)$, thus: $\Delta H_{12} = \Delta H_t + \Delta H_A$

If $\Delta H_A = 0$ ($A_1 = A_2$), then: $\Delta H = \Delta H_t = h_1 - h_2 = \Delta h$

Figure 13 - Pentair Fairbanks Nijhuis fish-friendly-turbine and formulas regarding head-difference assumptions - source: image used with permission from Pentair Fairbanks Nijhuis

With these assumptions **Figure 14** shows what happens with the Energy head, velocity head and hydraulic head for both the situation when energy is extracted and when it is not.

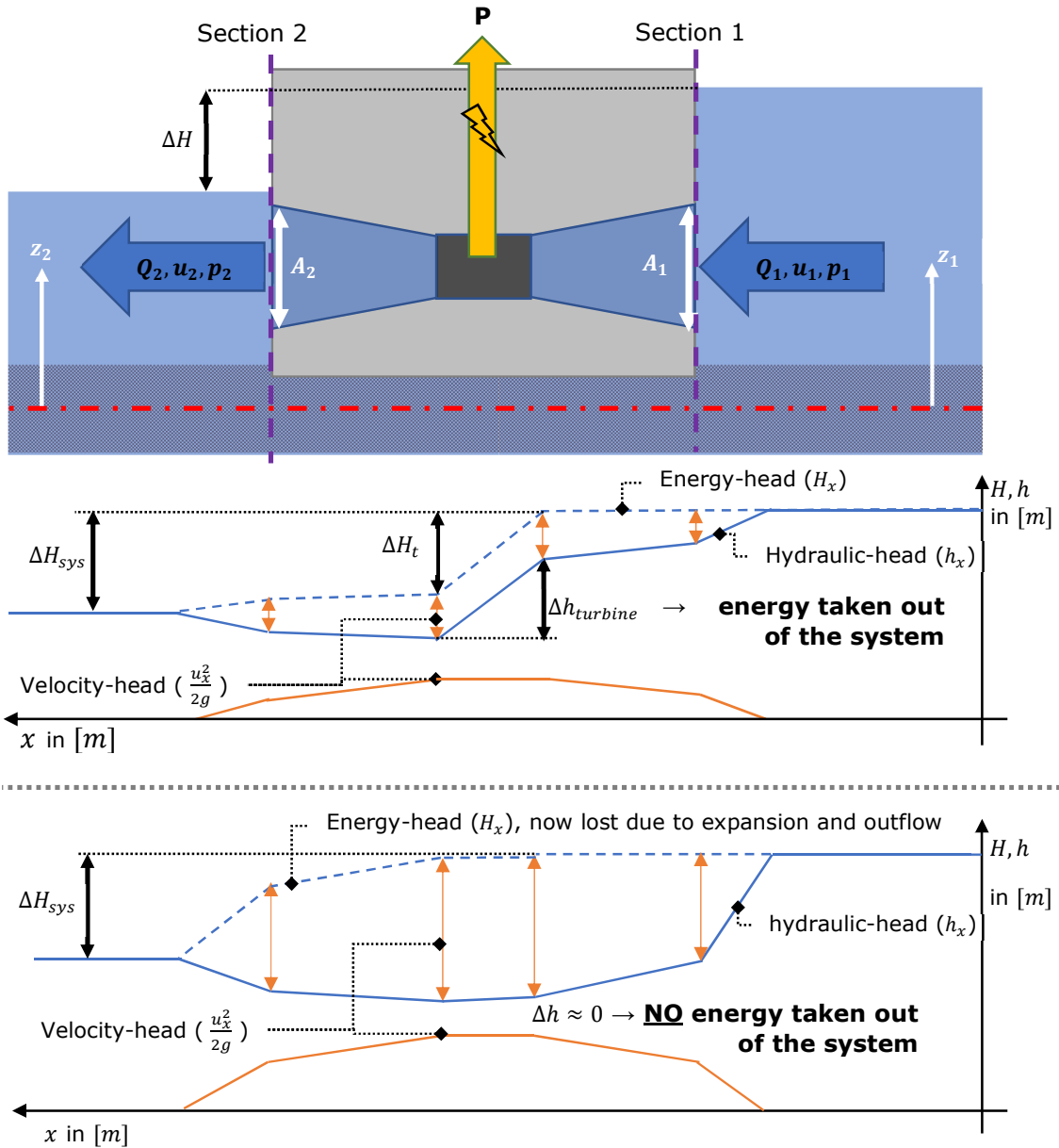


Figure 14 – Simplified, ideal hydropower system. Wall friction, inflow and contraction losses considered negligible.

Comparing the situation schematised in the bottom graph of **Figure 14** (without energy extraction), it can be seen that the velocity head in this case is much higher than in the case of the top graph (with extraction).

This is also the reason why, when the generator is not enacting any resistance/load on the rotor, the turbine will free-spin, which leads to a much higher rotational speed than when the turbine is experiencing load.

4.2.4 Turbine theory

A turbine is a machine that falls in the group called "turbo-machines". The definition of which, according to Dixon 1998 [17], is as follows:

"We classify as turbomachines all those devices in which energy is transferred either to, or from, a continuously flowing fluid by the dynamic action of one or more moving blade rows." - Dixon, S.L. 1998 [17]

The turbine obviously taking energy from the flow. From this theory a head-discharge relation is derived in **Appendix 3 – Turbo-machinery-theory**. The method uses the specific speed derived with the dimensional approach known as the Buckingham's Pi theory. Using two dimensionless terms, such that the diameter cancels out of the equation, the power specific speed and from that the specific speed relations are derived as shown below:

$$N_{sp} = \frac{(\hat{P})^{\frac{1}{2}}}{(\psi)^{\frac{5}{4}}} = \frac{N \cdot \left(\frac{P}{\rho}\right)^{\frac{1}{2}}}{(g \cdot \Delta H_t)^{\frac{5}{4}}} \xrightarrow{\text{Subst.}(P=\eta \cdot \rho \cdot g \cdot \Delta H_t \cdot Q_t)} \frac{N \cdot \left(\frac{\eta \cdot \rho \cdot g \cdot \Delta H_t \cdot Q_t}{\rho}\right)^{\frac{1}{2}}}{(g \cdot \Delta H_t)^{\frac{5}{4}}} = N_s = \frac{N \cdot (\eta \cdot Q_t)^{\frac{1}{2}}}{(g \cdot \Delta H_t)^{\frac{3}{4}}} \quad (4 - 13)$$

Where:

$\hat{P} = \frac{P}{\rho \cdot N^3 \cdot D^5}$	The dimensionless power coefficient
$\psi = \frac{g \cdot \Delta H}{(N \cdot D)^2}$	The dimensionless head or energy transfer coefficient
$N_{sp} =$	The (power) specific speed in [rpm] or "revs"
$\Delta H_t =$	The head-difference over the turbine in [m]
$Q_t =$	The discharge through the turbine in [m ³ /s]
$P =$	Turbine power in [kW]
$N =$	Rotations speed of the turbine in [rpm] or "revs"
$N_s =$	The specific speed in [rpm] or "revs"
$\eta =$	The turbine efficiency in [%]

The specific speed can be seen as the comparing two similar turbines where, for instance, one is a prototype and the other is the full-scale turbine. The dimensionless coefficients will stay the same for both.

When for instance the diameter changes with factor x, to keep the same specific speed, the produced power will change with factor x to the 5th power.

The prototype is defined in such a way that it will generate 1W of power at 1m of head and have a discharge of 1 m³/s (hence the name "specific", this means per unit discharge, power, and head).

Turbine discharge from specific speed

Due to the fact that both head-difference and discharge are in this relation for specific speed, the function can be used to determine the head-difference over the turbine when combined with the head-losses in a pipe-system. The $\Delta H_{turbine}$ in formula (4 - 17) was still unknown as of now. Rewriting (4 - 13) a relation between the turbine discharge and head-difference is found:

$$\Delta H_t = \frac{(\eta \cdot Q_t)^{\frac{2}{3}}}{g} \left(\frac{N}{N_s}\right)^{\frac{4}{3}} \quad (4 - 14)$$

Where:

$\Delta H_t =$	The head-difference over the turbine in [m]
----------------	---

Combining above with **(4 - 17)**:

$$\Delta H_{sys} = \Delta H_t + Q_t^2 \cdot C \xrightarrow{\text{substitute}} \Delta H_{sys} = (Q_t)^{\frac{2}{3}} \cdot \frac{\eta^{\frac{2}{3}}}{g} \left(\frac{N}{N_s} \right)^{\frac{4}{3}} + Q_t^2 \cdot C \quad \text{(4 - 15)}$$

Where:

ΔH_{sys} = The head-difference over the entire system, the total available head-difference in [m]

$Q_t^2 \cdot C$ = The sum of all the minor losses in the pipe-system in [m].

To find the relation to be found suggested in **(4 - 6)** (that is: $f_2(Q_{ava}, \Delta H_{ava})$), the equation **(4 - 15)** needs to be solved for Q_t . This can be done numerically by means of Newton-Raphson method [18].

In the hydraulic models in this thesis where the turbo machinery theory is used, this is written as a loop and gives a numerical function $Q_t(\Delta H_{sys}, C, N, N_s)$, that can be used in other formulae to plot graphs and calculate other quantities like power output or the head over the turbine.

To make the relation complete the discharge of the complex is limited to the available discharge:

$$Q_{plant} = \min(Q_{ava}, n_{t,active} \cdot Q_t(\Delta H_{ava}, C, N, N_s)) \quad \text{(4 - 16)}$$

Where:

Q_{plant} = The total discharge going through the power house in [m^3/s]

Q_{ava} = The available discharge in [m^3/s]

$Q_t(\Delta H_{ava}, C, N, N_s)$ = The discharge through the turbine for a particular available head difference $\Delta H_{sys} = \Delta H_{ava}$ over the system and geometry determined by C, N, N_s

$n_{t,active}$ = The number of active turbines

4.2.5 Optimisation of power output and the Speed ratio r_s

To achieve the highest annual energy production the turbine should run on as high a power-output as possible for as long as possible. Knowing where the peak-power is found within certain ranges of the parameters is therefore useful.

The numerical function of $Q_t(\Delta H_{ava}, C, N, N_s)$ that is found in the previous paragraph is now dependent on 4 variables, namely: $\Delta H_{ava}, C, N$ and N_s . To reduce the number of variables it is practical to define a speed ratio r_s as N over N_s .

$$r_s = \frac{N}{N_s} \left(\text{or } r_{sp} = \frac{N}{N_{sp}} \right) \quad \text{(4 - 17)}$$

Where:

r_s = The speed ratio [dimensionless].

When a fixed rotation speed N is assumed the amount of variables Q_t is dependent on is reduced to 3 of which:

1. ΔH_{ava} is a boundary condition given by the flow regime;
2. r_s is a design parameter.
In the case of a (double regulated) Kaplan turbine, this variable can also be a configuration parameter as the geometry can be altered during production.
3. C is another design parameter dependent on the chosen geometry

The discharge for a given head-difference ΔH_{ava} and Quadratic resistance coefficient C can then be plotted as function of the speed-ratio r_s (see **Figure 15**).

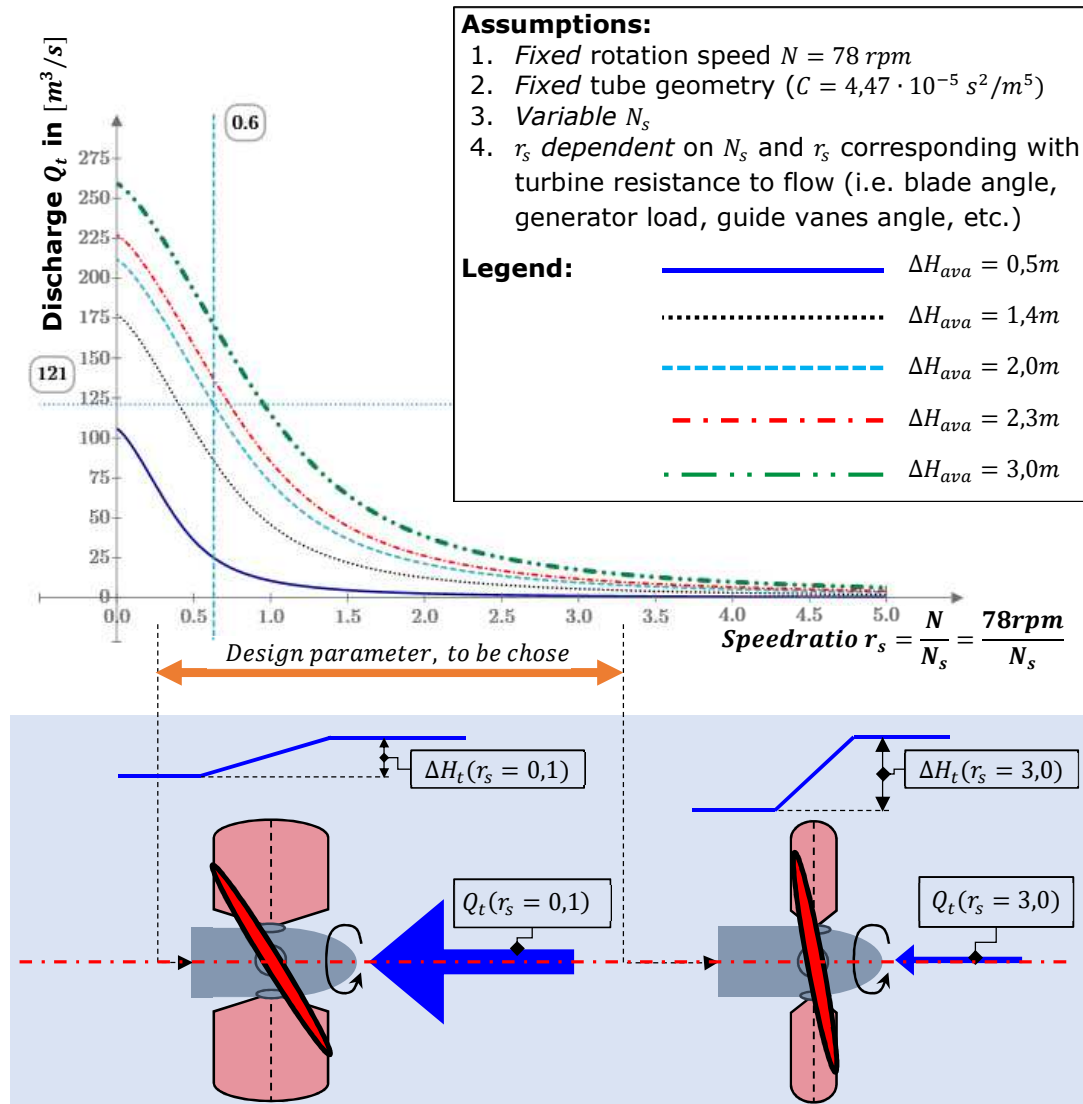


Figure 15 - Discharge as function of speed ratio for a fixed C coefficient and available head

This can also be done with the head difference over the turbine, as equation (4 - 14) can be written with the speed ratio r_s as well:

$$\Delta H_t = \frac{(Q_t)^2}{g} \cdot (r_s)^4 \tag{4 - 18}$$

In Figure 16 on the next page the turbine head (ΔH_t), discharge (Q_t) and power (P_t) have been plotted for various available head differences (ΔH_{ava}) and a chosen quadratic resistance coefficient (C), that is based on the system installed in Maurik¹ (value of C shown below). This shows the influence of the speed ratio as explained in **Important note 1** after that.

$$C_{Maurik} = \frac{1}{2g} \cdot \sum_{i=1}^N \frac{\xi_i}{A_i^2} = \frac{\xi_{eq}}{2g \cdot (A_t)^2} = \frac{0,102}{2 \cdot 9,81\text{m/s}^2 \cdot (10,80\text{m}^2)^2} \approx 4,47 \cdot 10^{-5} \text{ s}^2/\text{m}^5$$

¹ The more detailed characteristics of HPP Maurik are provided later in this chapter.

For a fixed rotation speed $N = 78rpm$ and discharge coefficient C :

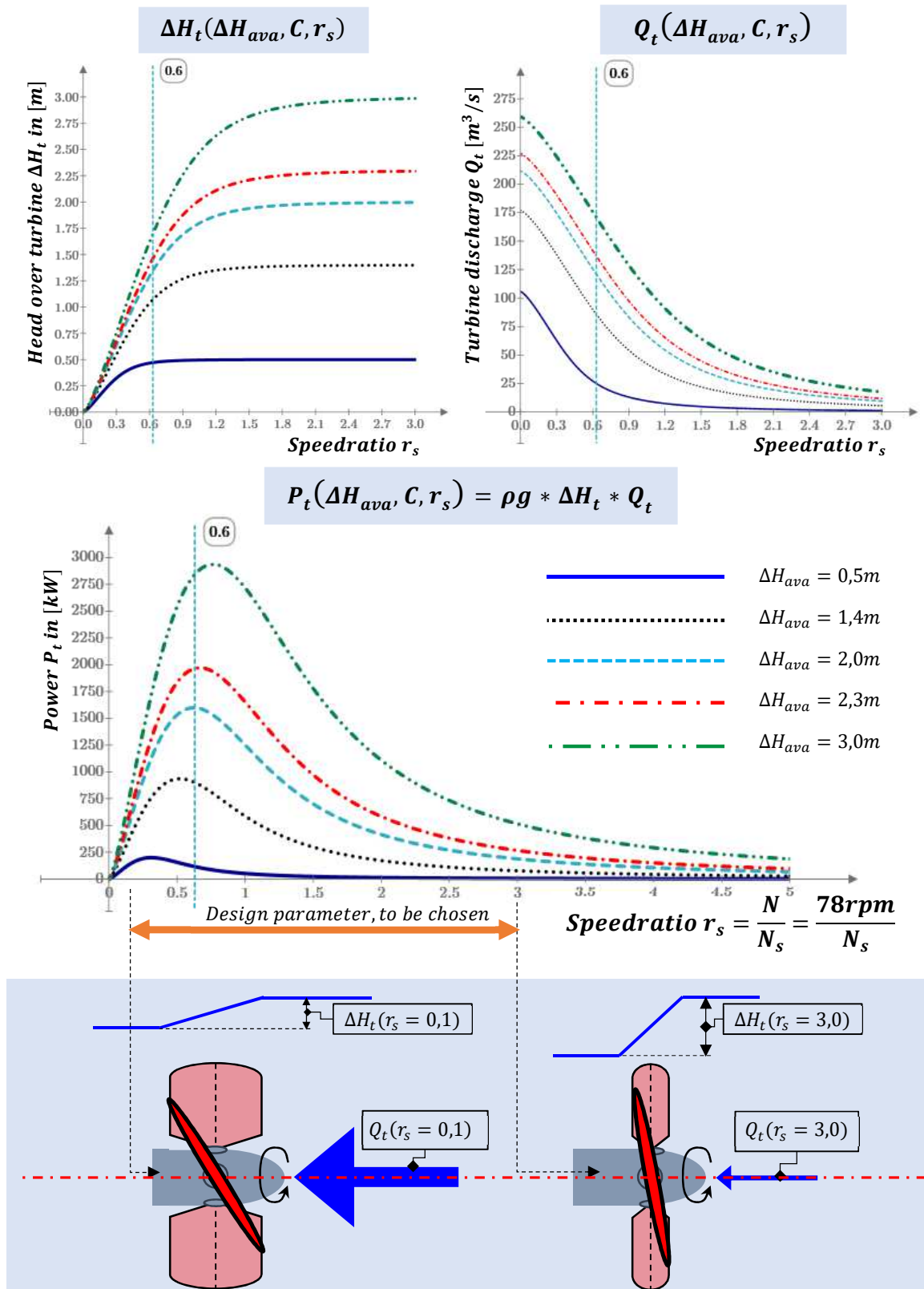


Figure 16 - Plot of head, discharge and power ratio against speed ratio $r_s = \frac{N}{N_s}$. See Appendix 3

Important note 1

Assuming a **fixed rotation speed of the turbine "N"** (often also required for network frequency stability), the speed ratio functions as a measure for resistance of the turbine where a zero speed ratio equals no resistance of from the turbine:

$$r_s = 0 \rightarrow \Delta H_t(r_s = 0) = 0$$

For a given Kaplan turbine this means that when the rotor blade angle and guide vane angle is set to fully open as well as the generator resistance set to zero, the specific speed of the turbine theoretically goes to infinity. Thus:

$$\text{as } r_s \rightarrow 0 \text{ then } N_s \rightarrow \infty \text{ and } \Delta H_t(r_s) \rightarrow 0$$

When r_s is exactly equal to 0 one can imagine the rotation speed N is also 0 and N_s is undefined at such a moment.

When speed ratio r_s increases, then so does the resistance of the turbine to the flow. Consequently N_s must decrease. For a given Kaplan turbine, a low specific speed corresponds with angles for the rotor blades and guide-vanes that are closed as much as possible without fully blocking flow and the generator also giving maximum resistance. Therefore:

$$\text{as } r_s \rightarrow \infty \text{ then } N_s \rightarrow 0 \text{ and } \Delta H_t(r_s) \rightarrow \Delta H_{ava}$$

Technically the specific speed cannot really reach zero ($N_s \neq 0$), nor can the head losses be completely zero when there is flow. In practise it is:

$$\text{as } r_s \rightarrow r_{s,max} \text{ then } N_s \rightarrow N_{s,min} \text{ and } \Delta H_t(r_s) \rightarrow \Delta H_{t,max}$$

Where:

$$\Delta H_{t,max} = \Delta H_{ava} - C \cdot (Q_t(r_{s,max}))^2$$

$$r_{s,max} = \frac{g \cdot (\Delta H_{t,max})^{3/4}}{Q^{1/2}} = \frac{g \cdot [\Delta H_{sys} - C \cdot (Q_t(r_{s,max}))^2]^{3/4}}{(Q_t(r_{s,max}))^{1/2}}$$

$$N_{s,min} = \frac{N}{r_{s,max}} = \frac{N \cdot (Q_t(r_{s,max}))^{1/2}}{g \cdot [\Delta H_{sys} - C \cdot (Q_t(r_{s,max}))^2]^{3/4}}$$

The head-difference over the turbine ΔH_t can be normalised by the available head difference over the structure ΔH_{ava} (see **(4 - 19)** below). The discharge through the turbine when loaded $Q_t(r_s > 0)$ can be normalised with the discharge that goes through the system when no load is applied (see also **Important note 1** and formula **(4 - 20)**).

The power can be normalised by the product of the available head ΔH_{ava} and the unloaded discharge Q_{NoLoad} , which is equal to the total the energy flux when no load is applied or equivalently is the sum of the power taken by the turbine and the energy flux of the losses (i.e. $\frac{dE}{dt}_{NoLoad} = \rho \cdot g \cdot Q_{NoLoad} \cdot \Delta H_{ava} = \frac{dE_t}{dt} + \frac{dE_{loss}}{dt}$, see formula **(4 - 21)** below).

All of these normalised values are shown in the relations below:

$$r_H(\Delta H_{ava}, C, r_s) = \frac{\Delta H_t(\Delta H_{ava}, C, r_s)}{\Delta H_{ava}} \quad (4 - 19)$$

$$r_Q(\Delta H_{ava}, C, r_s) = \frac{Q(\Delta H_{ava}, C, r_s)}{Q(\Delta H_{ava}, C, 0)} = \frac{Q_t}{Q_{NoLoad}} \quad (4 - 20)$$

$$r_P(\Delta H_{ava}, C, r_s) = \frac{P_t}{\max\left(\frac{d}{dt} E_{flow}\right)} = \frac{\rho \cdot g \cdot Q_t \cdot \Delta H_t(\Delta H_{ava}, C, r_s)}{\rho \cdot g \cdot Q_{NoLoad} \cdot \Delta H_{ava}} = r_H \cdot r_Q \quad (4 - 21)$$

Where:

- $r_H(\Delta H_{ava}, C, r_s) =$ The dimensionless head ratio as function of available system head, quadratic resistance coefficient and speed ratio.
- $r_Q(\Delta H_{ava}, C, r_s) =$ The dimensionless discharge ratio as function of available system head, quadratic resistance coefficient and speed ratio.
- $Q_t =$ the loaded discharge (where the turbine gives resistance to the flow) in $[m^3/s]$
- $Q_{NoLoad} =$ the unloaded discharge in $[m^3/s]$

In **Figure 17** these factors are combined with **Figure 16** resulting in a plot of the normalised head, discharge and power:

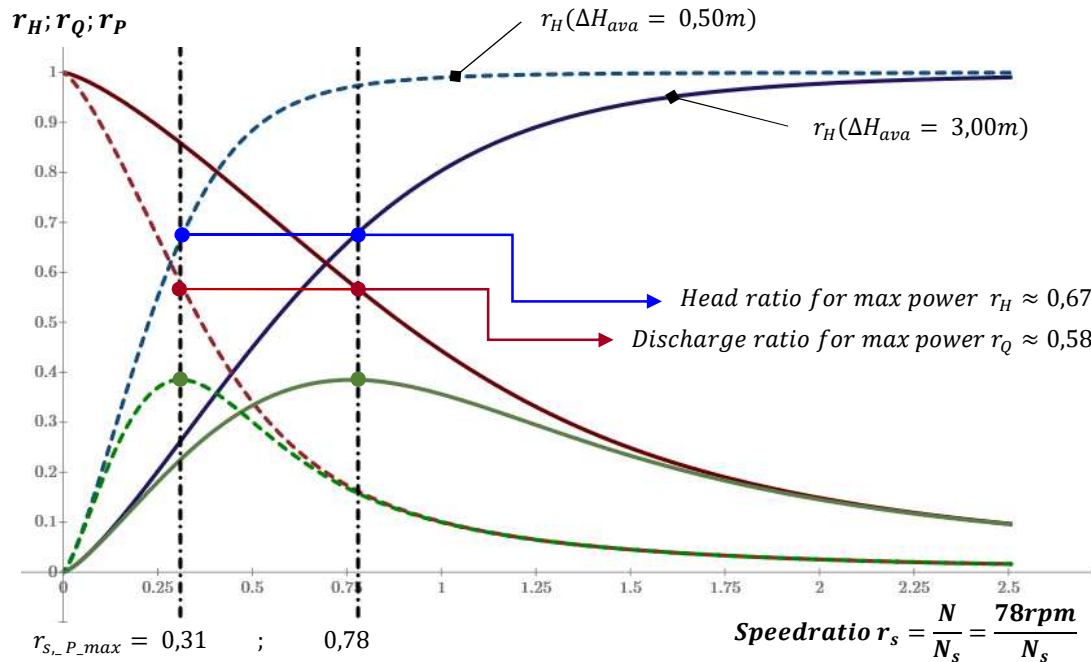
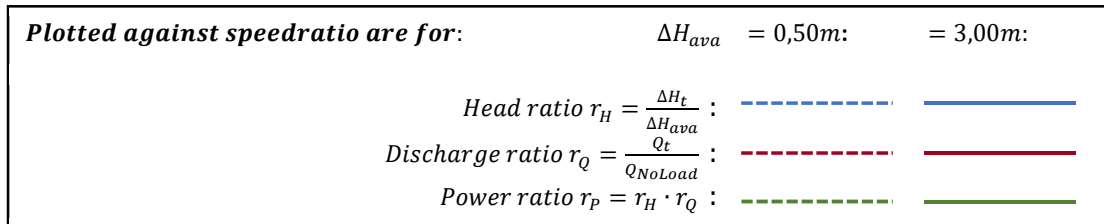


Figure 17 - Plot of head, discharge and power ratio against speed ratio $r_s = \frac{N}{N_s}$. See **Appendix 3**

Interestingly, the power output peaks at a certain value of r_s . This is because Q_t and ΔH_t have a more or less reciprocal relationship, where the discharge decreases with increasing turbine head. The maximum of the power P_t is P_{max} , consistently occurs when the turbine head is around $0,667 \approx 2/3$ of ΔH_{ava} . The speed ratio where this happens however, is different for each combination of system head and discharge coefficient C (see also **Figure 17** above).

Important note 2

This head-ratio of $r_H = 2/3$ is only relevant when enough flow is available for the chosen diameter. If the available discharge is less than Q_{NoLoad} of the turbine, then the discharge curve has a point where it reaches its maximum and doesn't increase more if the speed ratio is reduced further. In other words r_Q will not reach 1,0 when r_s goes below the point where $Q_{ava} \leq Q_t(r_s)$. This has the effect of the location of maximum power in the graph is shifted to the right and no longer coincides with $r_H = 2/3$.

The maximum power output and related head ratio is therefore very much dependent on the available discharge and the size of the turbine. There is not one fixed head ratio that gives maximum power for all situations.

Examples

To illustrate the statement in the **Important note 2** two examples have been worked out in **Appendix 2**. First one uses a head ratio of 95% and the second one a head ratio of 2/3 for a situation where there is an available system head of 1,4m. The turbines are designed such that both generate the same amount of power of 130,4 kW.

Summarizing the calculation results in the table below:

Quantity	Unit	Case 1: Minimal loss	Case 2: Minimal size
r_h	—	95%	67%
ΔH_{ava}	m	1,40	1,40
ΔH_t	m	1,33	0,93
ΔH_{loss}	m	0,07	0,47
Q_t	m^3/s	10,00	14,25
Q_{NoLoad}	m^3/s	44,65	24,71
r_Q	—	0,224	0,577
η	—	100%	100%
P_t	kW	130,4	130,4
D_d	m	2,24	1,67
A_t	m^2	3,92	2,18
r_s	rpm/rpm	2,17	1,39
ξ_{eq}	—	0,212	0,212
C_d	s^2/m^5	$7,02 \cdot 10^{-04}$	$2,29 \cdot 10^{-03}$

Table 1 - Summarizing results of example calculations for two different head-ratios r_h

A downside of the system in case 2 is that the turbine will stop working when the system head is low, due to the fact that:

$$\Delta H_{ava_thres} = r_H^{-1} \cdot \Delta H_{t_thres} \quad (4 - 22)$$

Where:

ΔH_{t_thres} = The minimum required (threshold value) head over the turbine for it to (start) work(ing) in [m]

ΔH_{ava_thres} = The derived minimum available head for which the turbine still works in [m].

So for the case 2:

$$\Delta H_{ava_thres} = 1,5 \cdot \Delta H_{t_thres}$$

Where the other system from the first example will work up till:

$$\Delta H_{ava_thres} = 1,053 \cdot \Delta H_{t_thres}$$

On the other hand, the diameter of the turbine with the 2/3 head-ratio is a factor 74,5% smaller and the discharge area even a factor 55,6% smaller. Therefore it depends very much on the location and the hydraulic resources what is the most optimal choice of head-ratio.

If there is enough space, the hydraulic efficiency is highest when the highest head-ratio is chosen. This means that the largest possible diameter needs to be chosen, because then the quadratic resistance coefficient C is lowest and the head-losses smallest.

4.2.6 Annual energy production

The annual energy production is a time integral of the power, as shown in **(4 - 23)**.

$$E_{annual} = \int_0^{t_{year}} P(t) dt \quad (4 - 23)$$

Where:

$P(t) =$ The instantaneous power output of the considered system at time t in $[kW]$

The resource supply (discharge and head) for a hydro-power turbine is not always present and thus a turbine can often not run at full capacity the entire year. They have a considerable time of "down-time" or times where the turbine runs at reduced efficiency. In the energy production industry a common way to express the percentage of "uptime" is by the Capacity Factor.

$$CF = \frac{E_{annual}}{t_{year} \cdot P_{rated}} = \frac{t_{full-load}}{t_{year}} \quad (4 - 24)$$

Where:

$CF =$ Capacity factor in [%]

$E_{annual} =$ The amount of energy produced in a year by the considered system in Joules $[J]$ or more commonly in kilo-Watt-hours $[kWh]$

$t_{year} =$ Amount of time in a year in $[s]$ or more commonly in $[hours]$, which is about 8760 hours.

$t_{full-load} =$ The equivalent amount of time in $[hours]$ the turbine runs at full capacity in a year. $\left(t_{full-load} = \frac{E_{annual}}{P_{rated}}\right)$

$P_{rated} =$ The rated (maximum) power-output of the considered system in Joules per second $[J/s]$ or more commonly in kilo-Watts $[kW]$

As noted in the problem analysis on page 5 global average capacity factor for hydro power, according to IPCC report on hydro-power of 2015, is 44% [10], which was based on a combined capacity of 926 GW (gigawatt) and combined annual energy production of $3,551 \cdot 10^6$ GWh/year (Gigawatt hours per year).

4.3 CAVITATION LIMITS

Cavitation is quite a complex phenomenon and will not be examined in too much detail. However, it has an influence on the design as it determines the depth at which the turbine needs to be installed.

In simple terms cavitation happens when the static pressure of the fluid is reduced to the vapour pressure for a certain temperature. In practise it is a more complex phenomenon and dependent on the physical state of the liquid. [17, p. 13]

Gasses dissolved come out of the solution when pressure goes down and create gas cavities. Interestingly, when no particles have been dissolved, a liquid can actually sustain negative pressures (tensile stresses), however this has only been achieved in laboratories and is not working practise for turbo-machinery.

From the hydro-power theory the admissible head formula is used:

$$h_{s,adm} = h_{at} - h_{vap} - \sigma_{Ts} \cdot h_f \tag{4 - 25}$$

Where:

- $h_{s,adm}$ = The admissible draft head in [m]. This is the minimal depth below the operational tailwater level.
- h_f = The usable fall head in [m]
- h_{at} = The atmospheric pressure head in [m] $h_{at} = \frac{p_{atm}}{\rho g}$
(at sea-level about 10m)
- h_{vap} = The vapour pressure head in [m] $h_v = \frac{p_v}{\rho g}$
- σ_{Ts} = Thoma's cavitation coefficient.

For Kaplan turbines a graph is available based on specific speed N_q . Also important to note is that the vapour pressure is temperature dependent. The vapour pressure head h_{vap} is larger with higher temperature (see **Table 2**).

Temperature in [°C]	Vapour pressure head h_{vap} in [m]
0	0,062
10	0,125
20	0,238
30	0,433
40	0,752

Table 2 - Vapour pressure head for different temperatures. - Source: Lecture slides Hydro-power engineering

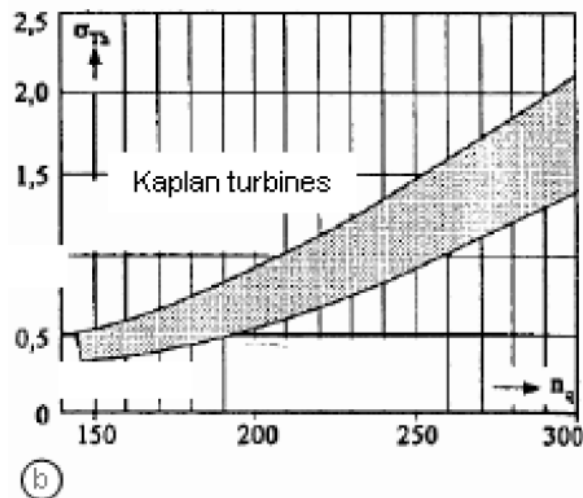


Figure 18 - Thoma's cavitation coefficient σ_{Ts} per specific speed N_q

4.4 EXISTING LOW-HEAD-HYDRO-POWER-TECHNOLOGIES

Various low head turbine technologies exist and each source has different tables of operational ranges of these techniques. Some of these and their operation ranges are listed below:

Turbine name	Head	Flow velocity	Discharge	Efficiency	Fish passage mortality rate
	m	m/s	m³/s	%	%
Kaplan in general	2,0-15,0	-	1-100	82-95	13,0
Kaplan fishfriendly Pentair	(0,3-) 1,0-15,0	-	1-150	82-95	2,0
Archimedes screw	0,5-10,0	-	0,01-10,0	80-88	5,0
Zuppinger wheel	0,5-2,5	-	0,5-0,95	71-77	
Overshot wheel	2,5-10,0	-	0,1-0,2	85-90	
Breast-shot wheel	1,5-4,0		0,35-0,65	79-85	
Stream-wheel	-	>1,0	-	29,5-36,3%	
Oryon watermill	-	>1,0	-	ytbd	ytbd
Tocado	-	>1,0	-	30-40%	no evidence of fish mortality

Table 3 - existing/considered low head hydropower technologies

4.4.1 Reference project HPP Maurik

The hydropower-plant near Maurik is the one that comes most close to the situation of Driel and is therefore one of the most interesting Hydro-power stations for to this research. Maurik is downstream of Driel and was built in 1988. A cross-section of the station is shown below.

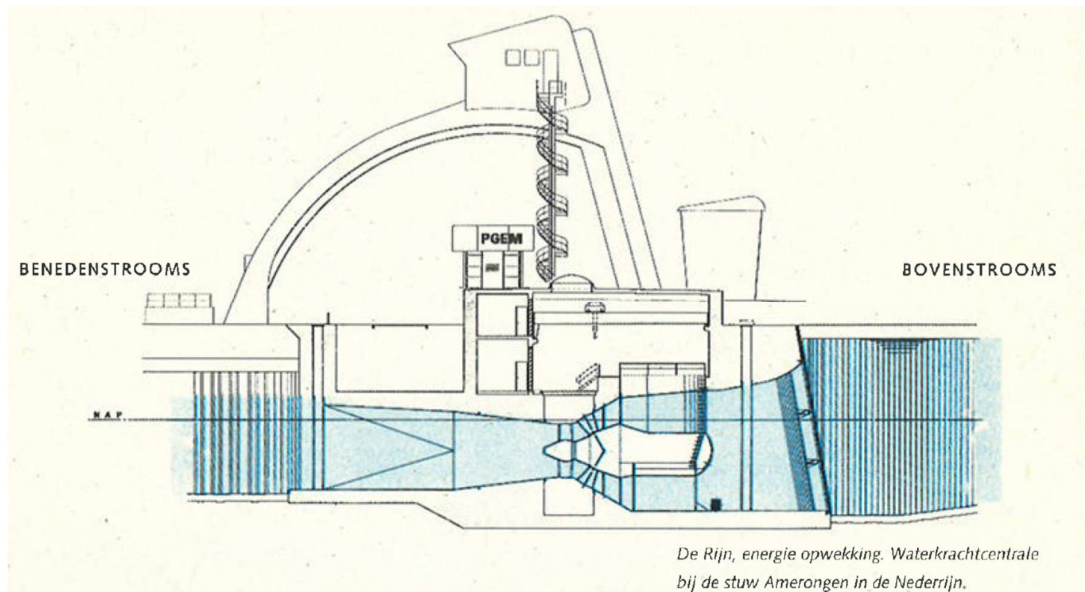


Figure 19 - Cross-section Power-house Maurik. At the time owned and operated by PGEM, now NUON/Vattenfal - source: [19, p. 8]

As can be seen, Maurik has horizontal axis Kaplan bulb turbines. In **Appendix 12** more information is given about the Maurik power plant. Most important information is that Maurik HPP is shown in the table below:

Technical data:			
Description	Quantity	Unit	Value
Number of turbines	n_t	-	4
Turbine rotor diameter	D_t	m	4,0
Discharge per turbine	Q_t	m ³ /s	100
Average system discharge	Q_{sys_avg}	m ³ /s	250
Largest head-difference	ΔH_{max}	m	4,0
Average head-difference	ΔH_{avg}	m	3,5
Rated power of turbine	P_{t_rated}	kW	2.500
Turbine rotation speed	N_{rotor}	rpm	78,0
Output rotation speed gearbox	N_{gear_out}	rpm	750,0

Table 4 - Performance data HPP Maurik - Source information: NUON

Also important to note is that the maximum head difference noted in **Table 4** doesn't coincide with the maximum discharge, but rather the opposite (maximum head with minimal discharge and vice versa).

Quite notable is that the capacity factor for Maurik lies much lower than the global average of 44%, as can be seen in **Table 5**. This may be due to the shared function with the weir (shipping and power production).

Below performance data gathered from NUON is shown.

Description	Quantity	Unit	Value
Initial investment	$Cost_{init}(1988)$	Mln. fl.	66,0
Current value of initial investment	$Cost_{init}(now)$	Mln. €	54,0 (120 mln. fl.)
Rated power Plant	$P_{rated,sys}$	kW	10.000
Average annual energy production	E_{ann}	GWh	20,0-25,0
High average full-load-hours per year	$t_{full-load}$	hr	2.000-2.500
Capacity factor (high production)	CF	%	22,8%-28,5%

Table 5 - Performance data HPP Maurik - Source: NUON. Guilder (fl.) in 1988 have been converted to current day (2019) value and currency using this source [20] and rounded to millions.

Some screenshots from NUON showing the operator’s screens were received, included in **Appendix 12** which were compared with flow data from Rijkswaterstaat. From that a resistance value can be estimated and also a head-ratio for this moment in time. The head-ratio is quite high, namely on average 96% the losses being on average 3,85%.

The specific speed is on average 44,1 rpm and with that the quadratic resistance coefficient for the turbine at this time is:

$$C_{Maurik} = \frac{(2,92m - 2,83m)}{(46,6m^3/s)^2} = 4,47 \cdot 10^{-5} \cdot \frac{s^2}{m^5}$$

However, this value can change, because it being a double regulable Kaplan turbine (as established in theory section before (**paragraph 4.2.5**). In **Figure 20**:

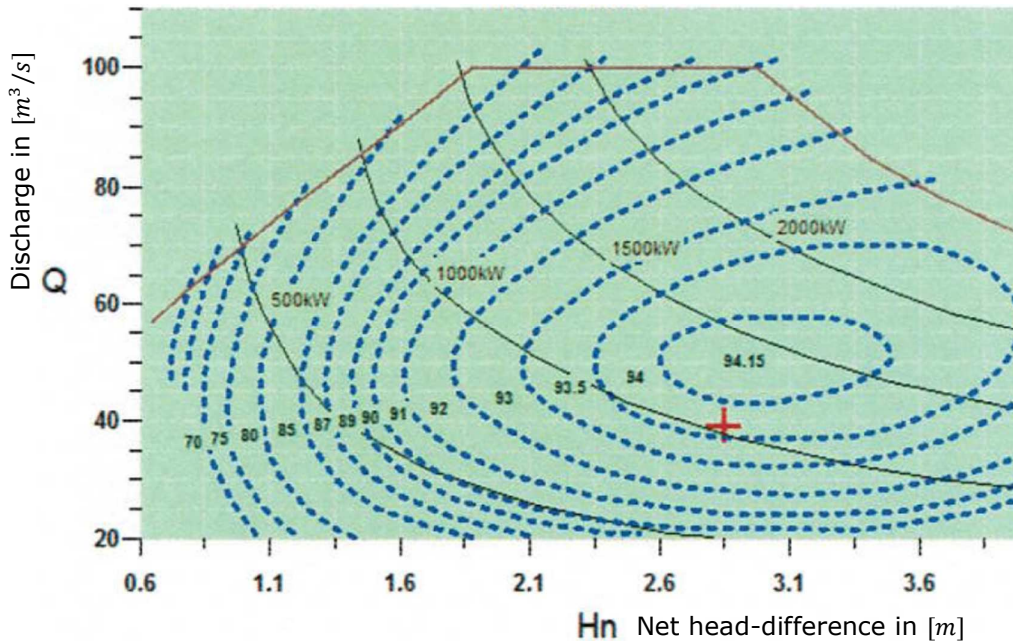


Figure 20 - Hill-chart indicating power-output (black solid lines) and efficiency (blue dotted lines) of the Kaplan Bulb turbine in Maurik HPP. (Red cross indicating the position of the moment the screenshot was taken (6th of June 2019 around 11:25) - Source: NUON

Using the turbine theory from **paragraph “Turbine theory”** the graph from **Figure 20** was reconstructed with a simplified efficiency curves shown in **Figure 101** and **Figure 102** in **Appendix 12**. The Isobars of power-output match quite well at the extremes of the curve and only lag behind the actual curve slightly in the middle. This in a way also

proves that the theory is indeed applicable for the situation in Maurik and similar situations.

4.4.2 Reference project Dommelstroom

For the Archimedes screw as reference is used the project "Dommelstroom" in Sint Michielsgestel. The turbine there is an Archimedes screw fitted with a frequency regulator, so it can change its rotations speed to optimise output. It is operational since October 2016 and has had 2 full years to produce energy as of now.

Quantity	unit	value
Head difference	m	1,8
Diameter	m	4,0
Number of blades	-	4
Pitch length (estimated)	m	5,5
Distance between the blades (estimated)	m	1,25
Length	m	6,0
Axis length	m	8,0
Inclination angle	°	22
Discharge	m ³ /s	8,0 to 10,0
Rotation rate	rpm	20 to 25
Weight screw	kg	13.000

Table 6 – Dommelstroom turbine dimensions - Source: [21]

Interestingly, the height difference that can be found by taking the screw length and the sine of 22° is 2,25m, which is larger than the stated head-difference. Apparently the screw can take more than the indicated 1,8m. This means that the Dommelstroom turbine is equipped to also handle the ranges of interest for Driel, so this existing design can be used for an estimate.

Recreating this turbine from theory:

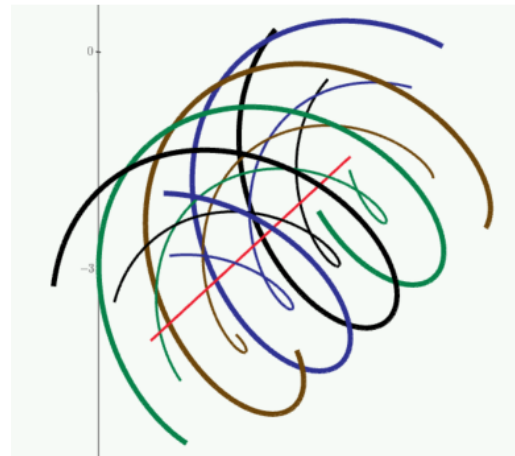


Figure 21 – 3D image of reconstructed geometry of the blade edge and connection to central axis of the Dommelstroom turbine and a picture for reference

The discharge that is found with Lubitz and Kozyn's method [22] by determining the bucket volume and then multiplying with the rotation rate as follows:

$$Q_{buc} = n_b * V_{buc} * \frac{\omega_{screw}}{2\pi} \quad (4 - 26)$$

Where:

n_b = The amount of blades (4 in Dommelstroom turbine)
 V_{buc} = The bucket volume in [m^3/s]
 ω_{screw} = The rotation rate of the screw in [rpm]

For the stated 20 rpm the discharge is with a full bucket (i.e. fill level is 100%) is 12,8m³/s. With a rotation speed of 25rpm the discharge is 16,0m³/s. This is of course without flow losses (leakage) or considering the fill level. The actual discharge is less, as is also given in the reference figures in **Table 6**.

The performance of the Dommelstroom turbine is shown below:

Quantity	unit	value
Rated power output	kW	120
Estimated efficiency	%	68 to 85
Average annual energy (claimed)	kWh/year	600.000
Production 2017	kWh/year	365.070
Production 2018	kWh/year	371.276
Capacity factor (claimed; historical)	%	57%; 35%
Costs (2016)	€	1.000.000 (750.000 crowd funded)

Table 7 - Performance figures Dommelstroom turbine - Source: [21]

Looking at some actual production values, the claimed 600 MWh per year seems a bit optimistic. At least this value is not really reached the last 2 years.

5 LOCATION ANALYSIS

Every location has specific parameters and challenges. Therefore an analysis of the location is required. The requirements for the designs are derived from this analysis and given in **5.8 "Requirements and design goals"**.

5.1 LOCATION IN DELTA

As shown in **Figure 9** in the problem analysis, Driel is one of the first hydraulic structure the flow from the river rhine encounters in the Dutch river delta. The weir determines the discharge going into the IJssel river and the Nederrijn river. In **Appendix 13** a drawing with the location with respect to other topographical locations can be found. Also an overview of the weir-complex can be found in this same drawing.

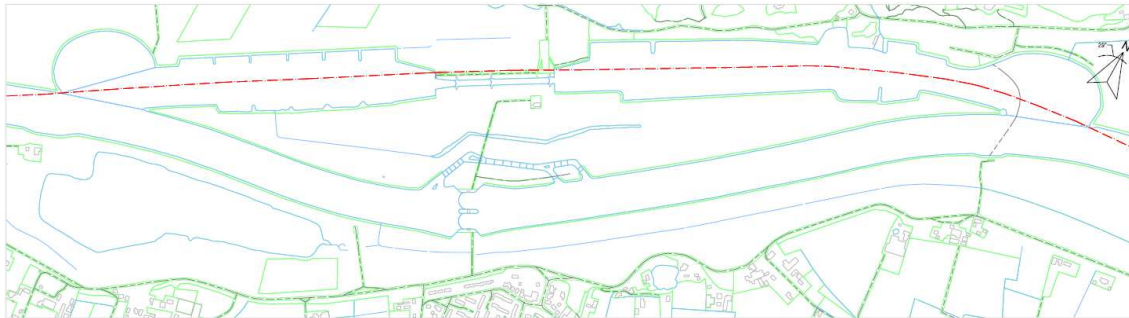


Figure 22 - Overview of weir-complex aligned to weir-river-axis (29 degrees anti-clockwise from North). See also **Appendix 13** for full-scale drawing with annotations. – Source: topography from Kadaster [23]

5.2 STAKEHOLDERS AROUND WEIR-COMPLEX DRIEL

Most important stakeholders are:

- Hevea initiative
- Dutch National Government
- Rijkswaterstaat (ministry of infrastructure and water protection)
- Energy companies;
- Shipping and inland waterway transportation professionals and community
- Sport fishing community;
- Local and provincial governments;
- Neighbours and locals;
- KNHM and Arcadis.

Their relation and interests in the project are explained in further detail in **Appendix 5**.

5.3 FLOW DATA ANALYSIS

For any hydro-power project arguably one of the most important knowledge to have is how the river behaves. The discharge and water-levels in the past is analysed, to be able to make a prediction for the future energy production. Fortunately a long record of flow and water-level data is available for the Nederrijn river.

5.3.1 Discharge data analysis

Data has been obtained containing the daily average discharge measurements from the Dutch Ministry of infrastructure [24] (called "Rijkswaterstaat – Ministerie van infrastructuur en waterstaat"). This data has been collected for just under 60 years, from 1961 up to and including 2018 (decision was made to stop updating the database for this research at 1st of January 2019, to have only "full years" of data. That means that the discharge measurements have been taken even almost 9 years before the weir was actually completed (which is in 1970, [25]). The measuring location for discharge is just upstream of the weir of Driel, as indicated at **Figure 23**.

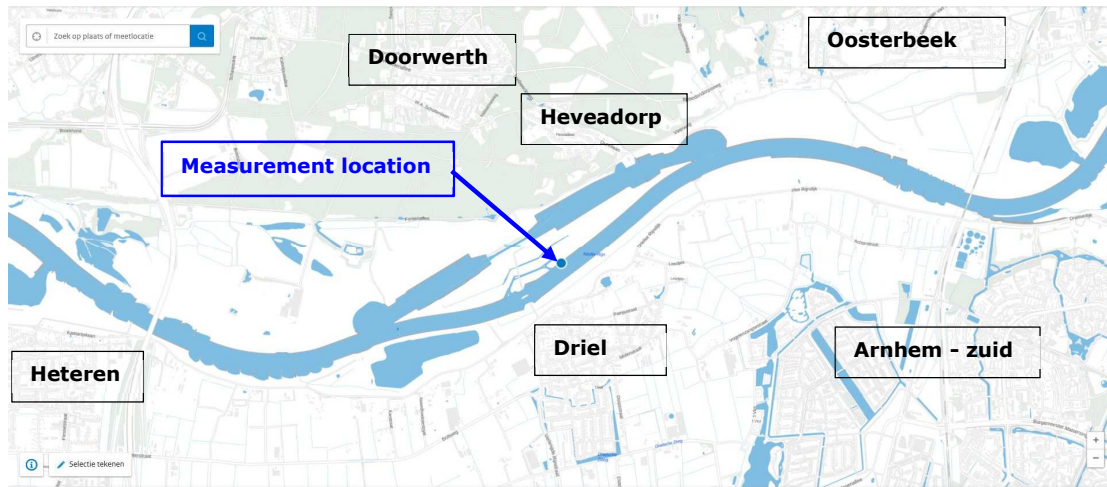


Figure 23 - Discharge measurement location with respect to weir-complex and nearby towns and villages – source: <https://waterinfo.rws.nl/#!#/bulkdownload/kaart/>

Erroneous or irrelevant data was filtered out. Some information on erroneous or missing data is given in **Table 38** of **Appendix 6**.

Negative discharges sometimes occurred when the water level near the weir of Driel is higher than that of the IJssel river in very low discharge situations. This flow is usually not more than a couple of cubic meters per second, an order of magnitude 5-25m³/s and doesn't occur very often. Therefore, the choice was made to not take this into account and instead make these values a 0-discharge. This effectively means that the turbine being designed will not work two-ways.

When the weir is fully closed with only the minimum discharge going through, the inclination of the water between Driel and the "IJssel-kop" at Arnhem is nearly zero, like a reservoir lake.

5.3.2 Discharge analysis results

Peak-discharges are measured in the years 1995, 1993 and 1988 mostly, all in the months December till March as can be seen in **Table 8**. These are of course discharges that the weir-complex must be able to let through to prevent flooding of the areas protected by the levees.

Looking at all the discharges over time it can be seen large peaks and intermediate periods with low discharges (see **Figure 24**). Both from knowledge of the river and from the histogram on the next page (see **Figure 27**)

2525	m ³ /s	1 Feb 1995
2515	m ³ /s	31 Jan 1995
2390	m ³ /s	2 Feb 1995
2350	m ³ /s	30 Jan 1995
2320	m ³ /s	25 Dec 1993
2255	m ³ /s	26 Dec 1993
2193	m ³ /s	30 Mar 1988
2155	m ³ /s	31 Mar 1988
2131	m ³ /s	29 Jan 1995
2085	m ³ /s	3 Feb 1995

it can be concluded that there are 3 distinct flow regimes happening that can be schematised as shown in **Figure 25** on the next page.

Table 8 - Peak discharges and date of occurrence at the weir of Driel

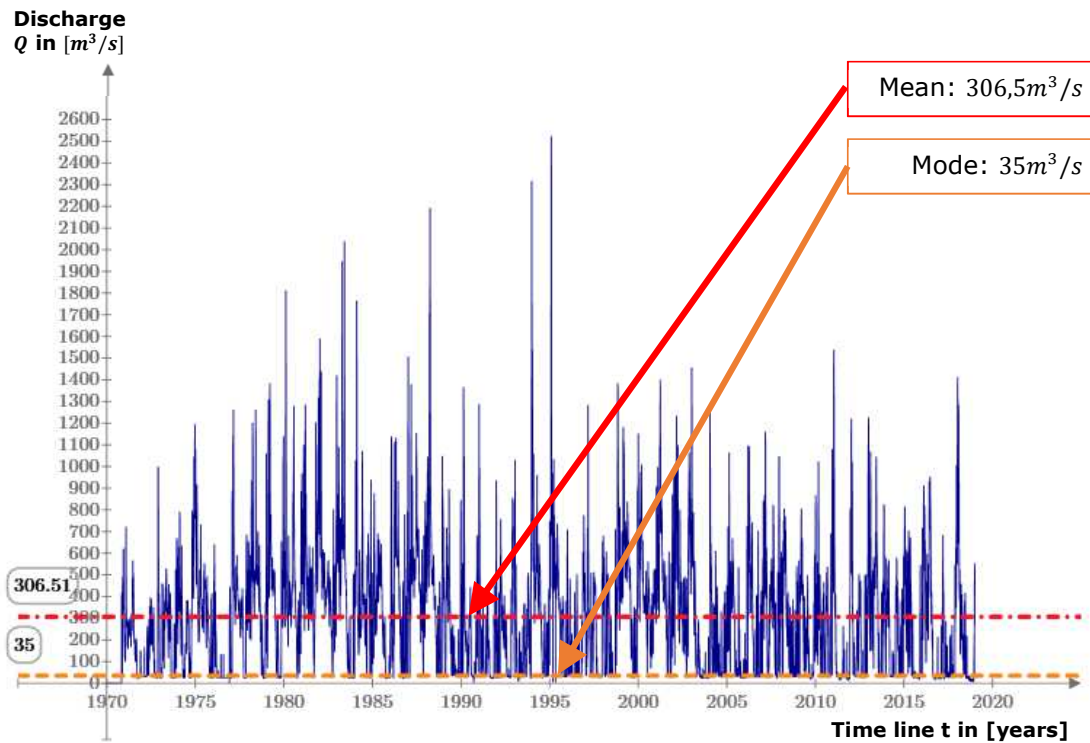


Figure 24 - Discharge time-series of Nederrijn near Driel. - see Appendix 7

Regime **c**) where flow is free to behave more or less naturally and thus having a lot variation depending on what is provided from upstream. This situation is associated with high flow and a wide spread of discharges. Regime **a**) where the flow is restricted to only the ecological minimum (officially $25\text{m}^3/\text{s}$, but in practise lies around $35\text{m}^3/\text{s}$), having a very narrow spread.

Regime **b**) is where it gets interesting, because it is associated with having both discharge and head-difference. The gates are then only partially closed. Diverting the flow through the gates to a turbine can result in production of electrical power.

Flow regimes **a)**, **b)** and **c)** are all shown on the next page in **Figure 25** and **Figure 26**.

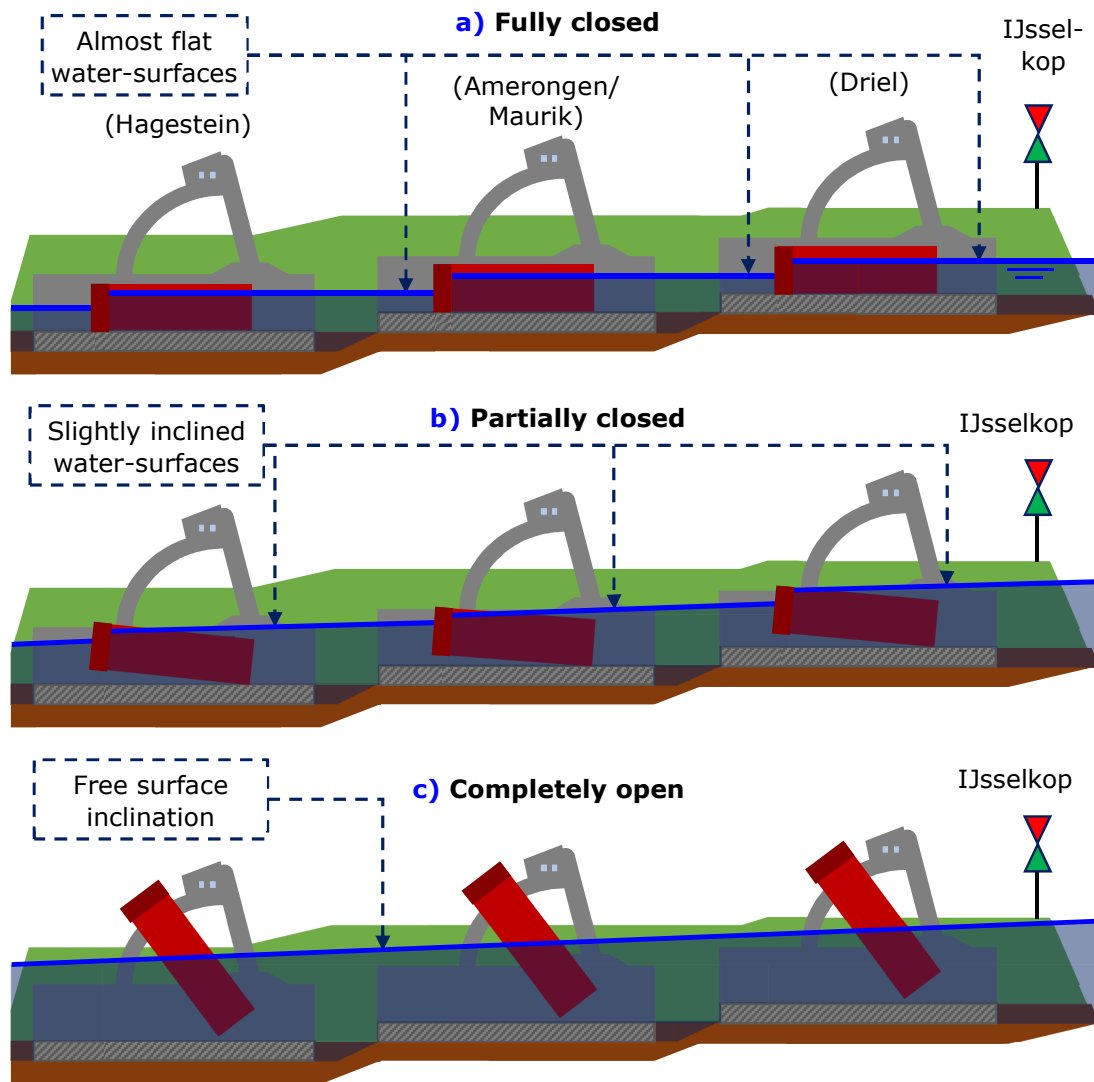


Figure 25 – Flow regimes in the Nederrijn. Combinations of gate settings are also possible where for example Driel is open, but Amerongen and Hagestein are partially closed.



a) Fully closed

b) Partially closed

c) Completely open

Figure 26 - Three stages of the weir gates corresponding with river situations from **Figure 25** - Sources: a): RWS [26] b): Techniek & Wetenschap [27] c):Photo by Hans Behrens [28]

Combining the discharge data with the water-level difference gives a clear image of when the gate is opened and closed and also gives an idea of the energy content of the river. See also paragraph **5.3.6**.

Looking at the frequency of occurrence it can be seen that the median value is biased due to the two flow-regimes. To get an idea of the distribution for un-obstructed flow regime a distribution is shown in the cut out section in **Figure 27**(top right) where the lowest 6 bins have been removed (cut at $60\text{m}^3/\text{s}$).

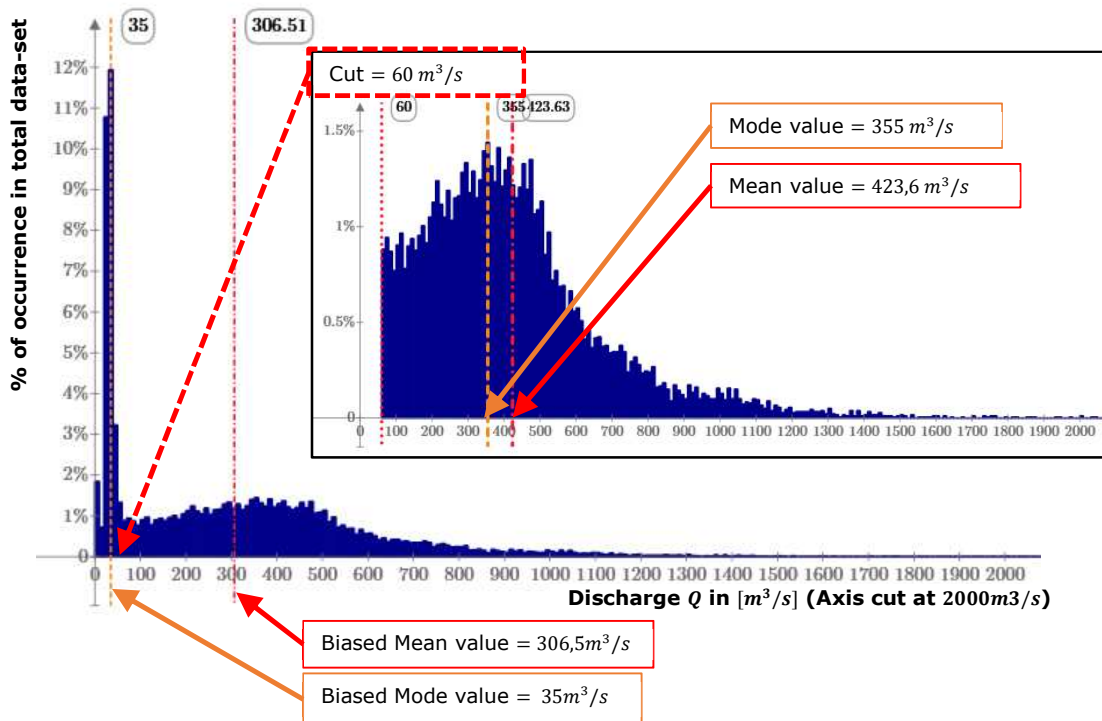


Figure 27 - Histogram from discharge time-series of the Nederrijn near Driel. - see Appendix 7

Immediate observation is that the mean is higher and the most occurring value for this distribution is $355\text{m}^3/\text{s}$. However, just removing the lowest 6 bins still doesn't remove the entire effect of the weir as it can let through a considerable discharge (till about $440\text{m}^3/\text{s}$).

Figure 27 shows the difficulty with separating the different flow regimes. From discharge alone the power cannot be determined. This data needs to be combined with water level differences.

5.3.3 Average values over time

As can be observed in the 48 year daily average in **Appendix 7**, over the year the discharge feed from upstream is highest in the months December up till about April. In the months July to November often a period of low-discharge is occurring. June seems to have a small peak as well, in contrast with its preceding month May. In general late summer has low discharges and spring sees the highest discharges.

Looking over multiple years, especially from 1980 till now the discharges seem to slowly decline, namely with about $-1,76\%$ per year with respect to the average value. In **Figure 28** the trend line for the data later than 1980 tangents the 30-year averages and appears to be a good average for 10-year and 1-year average discharges from 1980 up to and including 2018.

If the trend-line is taken over the entire measurement period then the decline is only about $-0,6\%$ per year with respect to the average value.

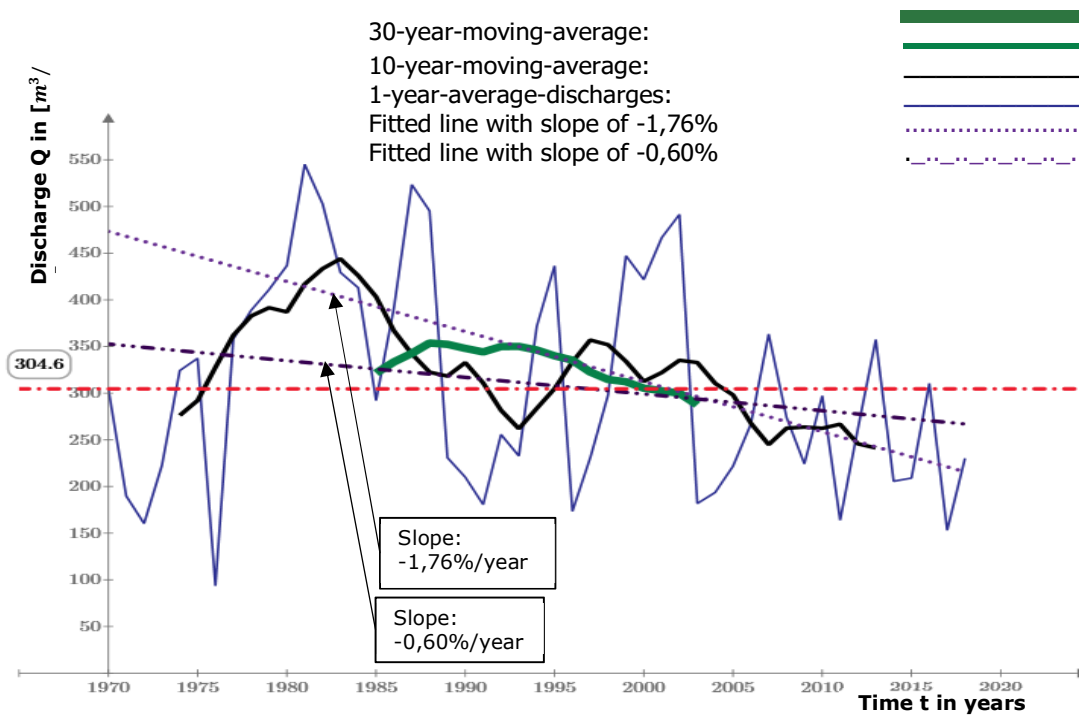


Figure 28 – Moving averages over the measurement years - see Appendix 7

5.3.4 Water level data analysis

Besides the discharge data, at the same time water level data has been obtained from the same source [24]. This data has been collected for 50 years, from 1968 up to and including 2018. That means that the water level measurements have started to be taken 2 years before the weir was actually completed [25]. There are two water-level measuring stations, one downstream and one upstream of the weir of Driel, as indicated at Figure 29.

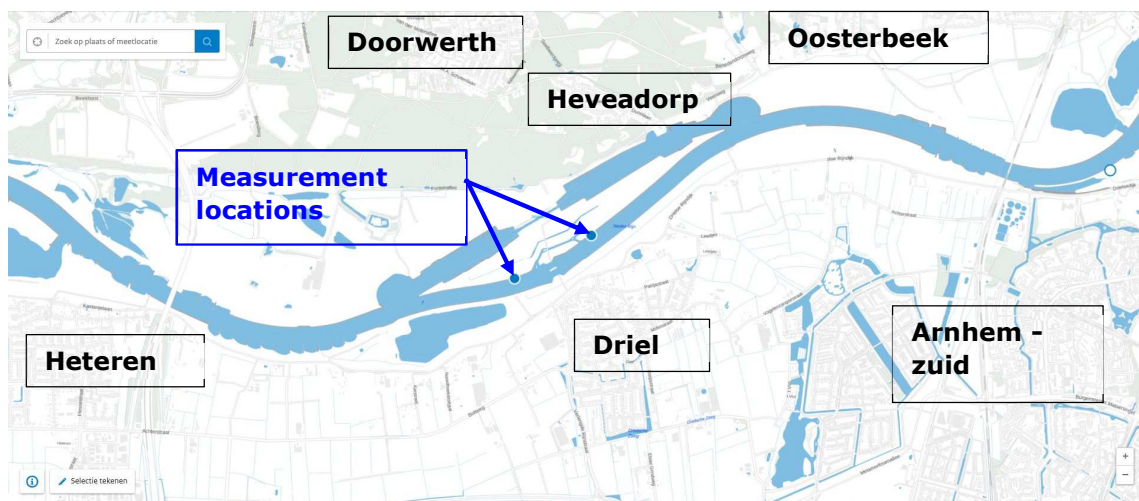


Figure 29 - Location of water-level-measuring devices in relation to the nearby towns and villages – from: <https://waterinfo.rws.nl/#!#/bulkdownload/kaart/>

However, the data from the downstream measurement station has 2 more years of data (starting in 1968), than the up-stream one (starting in 1970). Since the weir wasn't finished yet before 1970, any measurements before the completion of the weir are deemed irrelevant for hydro-power purposes and not taken into the analysis.

These water-level-measurement stations, "Driel boven" (upstream) and "Driel beneden" (downstream) are situated 580 m apart [29].

For the head difference data a correction has also been performed. Some information on this is given in **Table 39** in **Appendix 6**. The water level data has only a marginal amount of faulty data (0,02% versus the almost 5% for the discharge data).

5.3.5 Water-level-analysis results

In **Figure 30** the time-series is shown of the water-level-difference between the two measuring points from **Figure 29**. From the time series it is clear that there is a certain head-difference that is not exceeded, which although slowly changing over time, the last 20-30 years lies around 2,30m.

Head difference ΔH between the two measurement stations in [m]

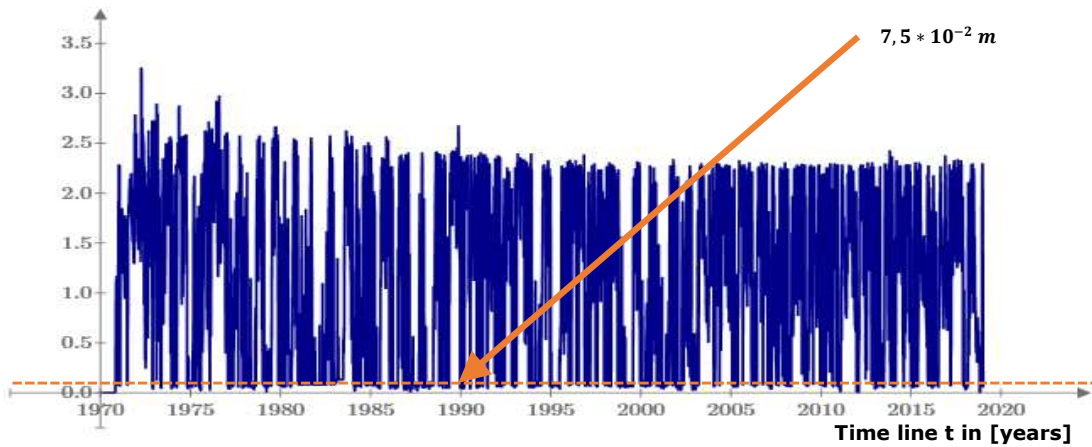


Figure 30 - Time-series of head-difference over weir complex Driel from 1970-2018 – Orange dashed line is mode value - see Appendix 7

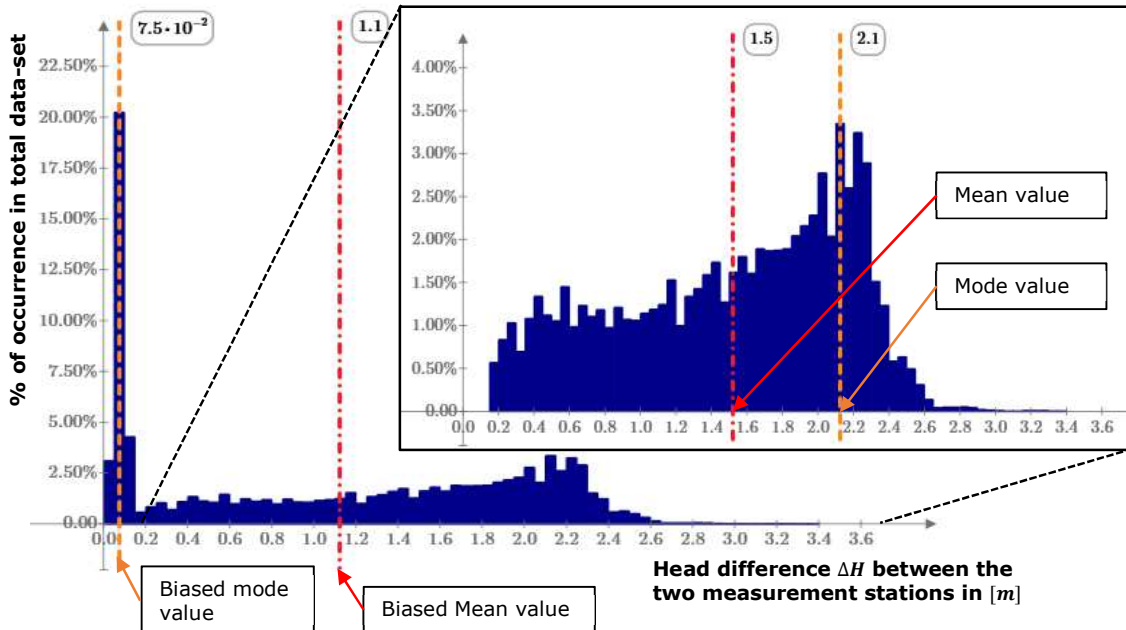


Figure 31 - Histogram of head-differences. 7,5cm head-difference occurs the most often (mode). Higher-head-differences have a larger spread. - see Appendix 7

In **Figure 31** the histogram is shown and there it can be clearly seen that there is a peak in percent of occurrence for low-head-difference around 0,075m, which corresponds with high discharges when the weir is opened. This means that on average the inclination of the water surface of the river in "free-flow-situation" is approximately:

$$i_{river} = \frac{\Delta H}{\Delta L} = \frac{7,50 \cdot 10^{-2} \text{ m}}{580 \text{ m}} = 1,293 \cdot 10^{-4}$$

It also shows that the weir is opened approximately 20-25% of the time.

Plotting only the bins that correspond to when the weir-gate is (semi-)closed gives the histogram shown in the top right corner in **Figure 31**.

5.3.6 Combining discharge and head-difference

To give an idea of how during a year the discharge and head-difference develops, the year of 2016 is shown in **Figure 32**. When the head-difference is more than 15cm the weir is assumed to be closed and opened otherwise.

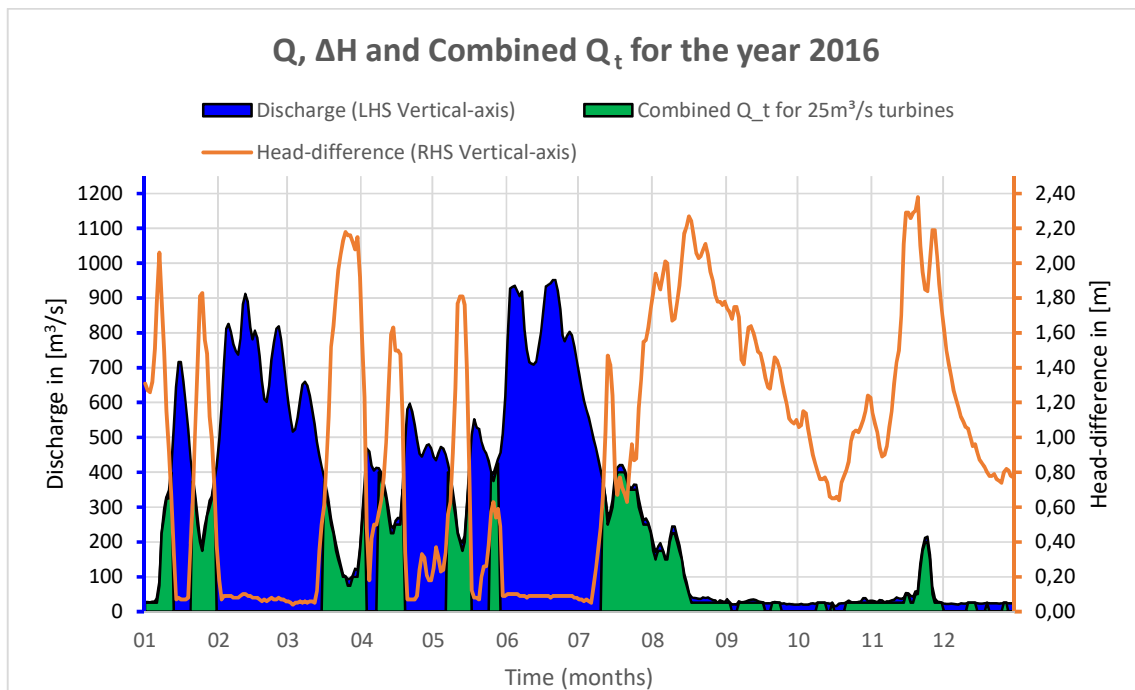


Figure 32 – Plotted over the year 2016 are time series of Driel for Discharge (left vertical axis), Head-difference (right vertical axis) and Combined turbine discharge for 25m³/s turbines - see Appendix 7

Looking at the entire dataset again, when ordering all the measured discharges in a descending fashion, the discharge-duration-curve is obtained and shown in **Figure 33**. Clear is that on average about 20% to 25% of the time the weir gates are opened due to high-discharge. Unfortunately that also means no useable head-difference.

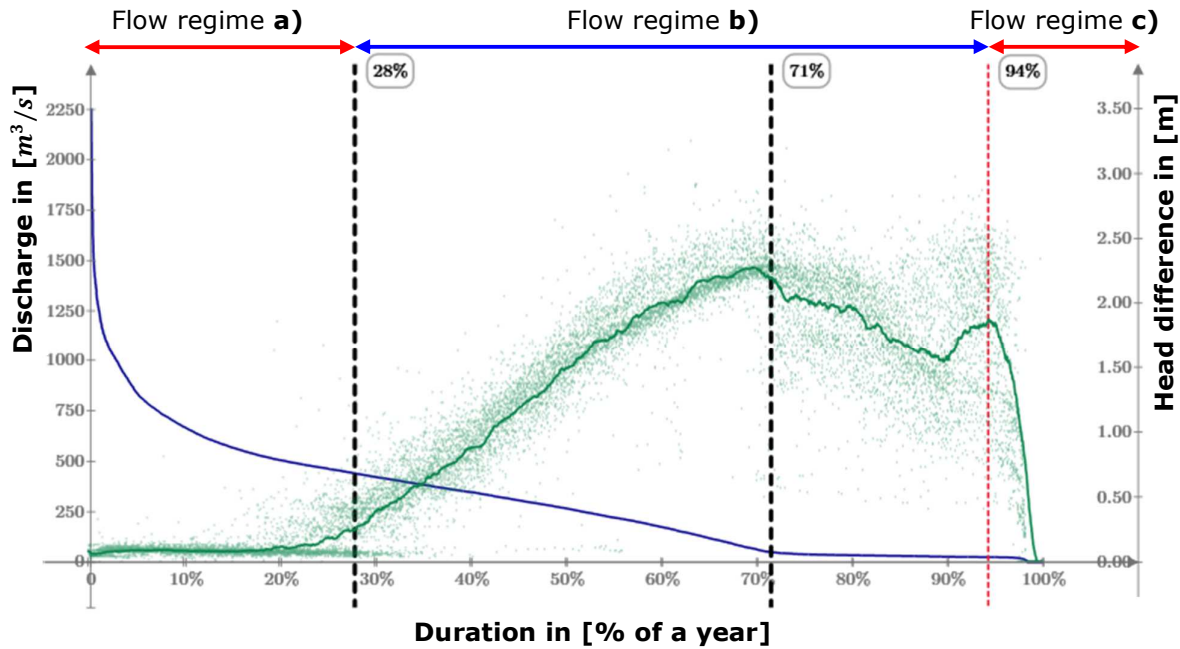


Figure 33 - Discharge duration curve and related water-level-differences. . - see Appendix 7
Left-hand-side-vertical-axis: Related to the discharge values (blue curve).
Right-hand-side-vertical-axis: Related to the head difference values (green dots)

Note that the discharges and head-differences have been ordered in pairs, where discharge was ordered in descending order and the head-difference moved along with it. A moving average is plotted of the head differences, using $4 \cdot 48 = 192$ data points for each average value.

This clearly shows that the highest discharge doesn't coincide with the highest head difference. Rather they have a reciprocal relationship.

It can be seen that from about $440 \text{ m}^3/\text{s}$ and upwards the water-level-difference becomes negligible, which corresponds to a water level at the weir of about $7,5 \text{ m} + \text{NAP}$ (upstream of the weir).

5.3.7 Operation of the weir

Assuming the requirement is to not change the water-level-regime, for the discharge to remain as it is before applying hydro-power with any given head-difference, the total hydraulic resistance of the complex needs to remain the same.

That is, the gates need to close more, as the turbine lets through more water than before. In terms of discharge the situation before can be described with **(1)**, and after with **(2)**:

$$Q_{\text{existing}} = Q_{\text{visorgates}} + Q_{\text{cylindergates}} + Q_{\text{fishladder}} + Q_{\text{nav-lock}} + Q_{\text{leakage}} \quad \text{(1)}$$

$$Q_{\text{design}} = Q_{\text{visorgates}} + Q_{\text{cylindergates}} + Q_{\text{fishladder}} + Q_{\text{nav-lock}} + Q_{\text{leakage}} + Q_{\text{powerhouse}} \quad \text{(2)}$$

Where Q_{design} must be equal to Q_{existing} .

This of course means diverting a part of the flow from the gates to the turbines, or an alternative way of thinking: that the resistance of the gates needs to be increased when the turbine are running.

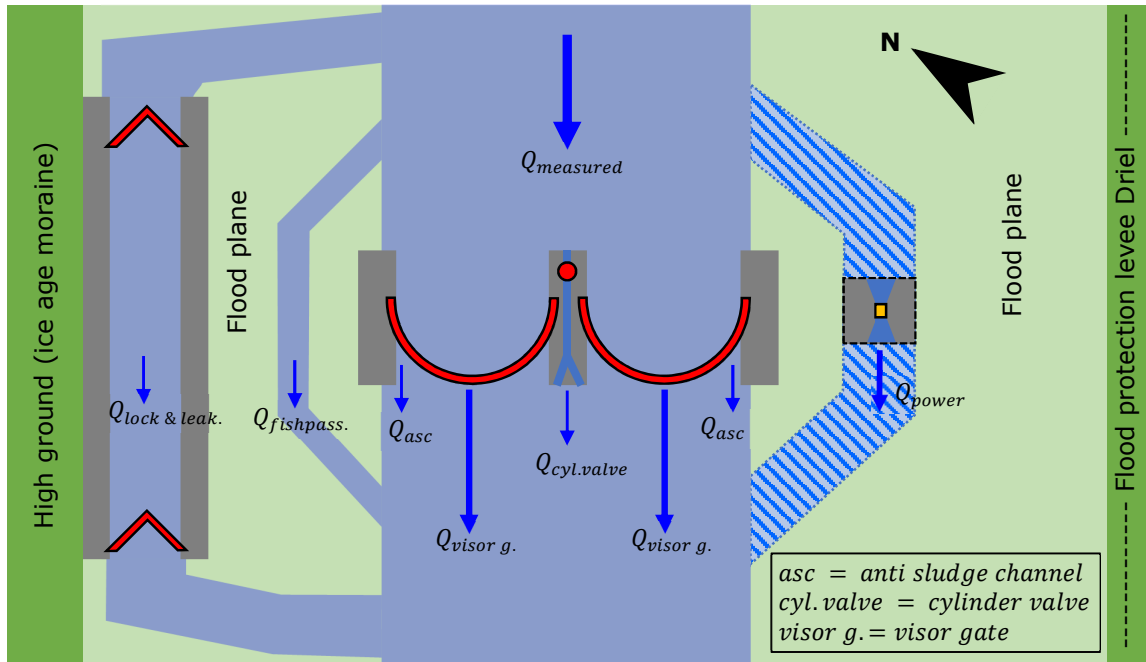


Figure 34 - Current (and future) contributors to discharge through the complex

Comparing with Maurik

As can be seen in **Figure 35** Maurik HPP is active more time of the year, as it has the gates closed for a longer time.

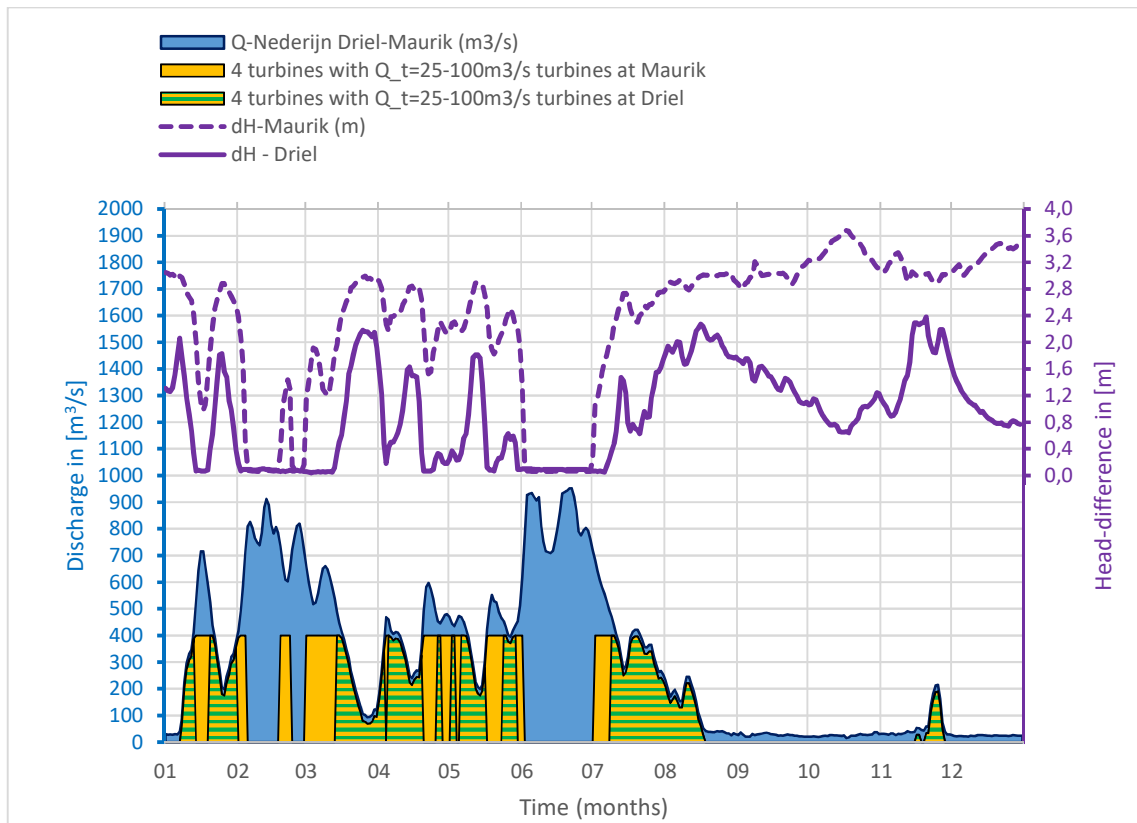


Figure 35 - Discharge, head-difference and turbine discharge for the year 2016 comparing Maurik with Driel. Ecological minimum (and unusable) discharge is 25m³/s - data from: [24]

If the decision was taken to increase the time Driel was closed the future power plant can produce for longer. This will change the weir regime of

This scheme will however affect shipping and in that shipping will have 30min extra travel time on each one-way trip for 50 days in a year more. This because the Weir of Driel opens on average 75 days per year and Amerongen only 25 days.

Operation of weirs in series

The weirs are placed in series, Driel being the most upstream, and Maurik and Hagestein the consecutive downstream weirs. However, they don't all open at the same time.

Nowadays a water-level-discharge relation has been determined for Lobith and for that reason the operation of the weir is now regulated based on a SOBEK model which looks mostly at the water-level of Lobith [30]. The modern day water-levels are shown in

Figure 36.

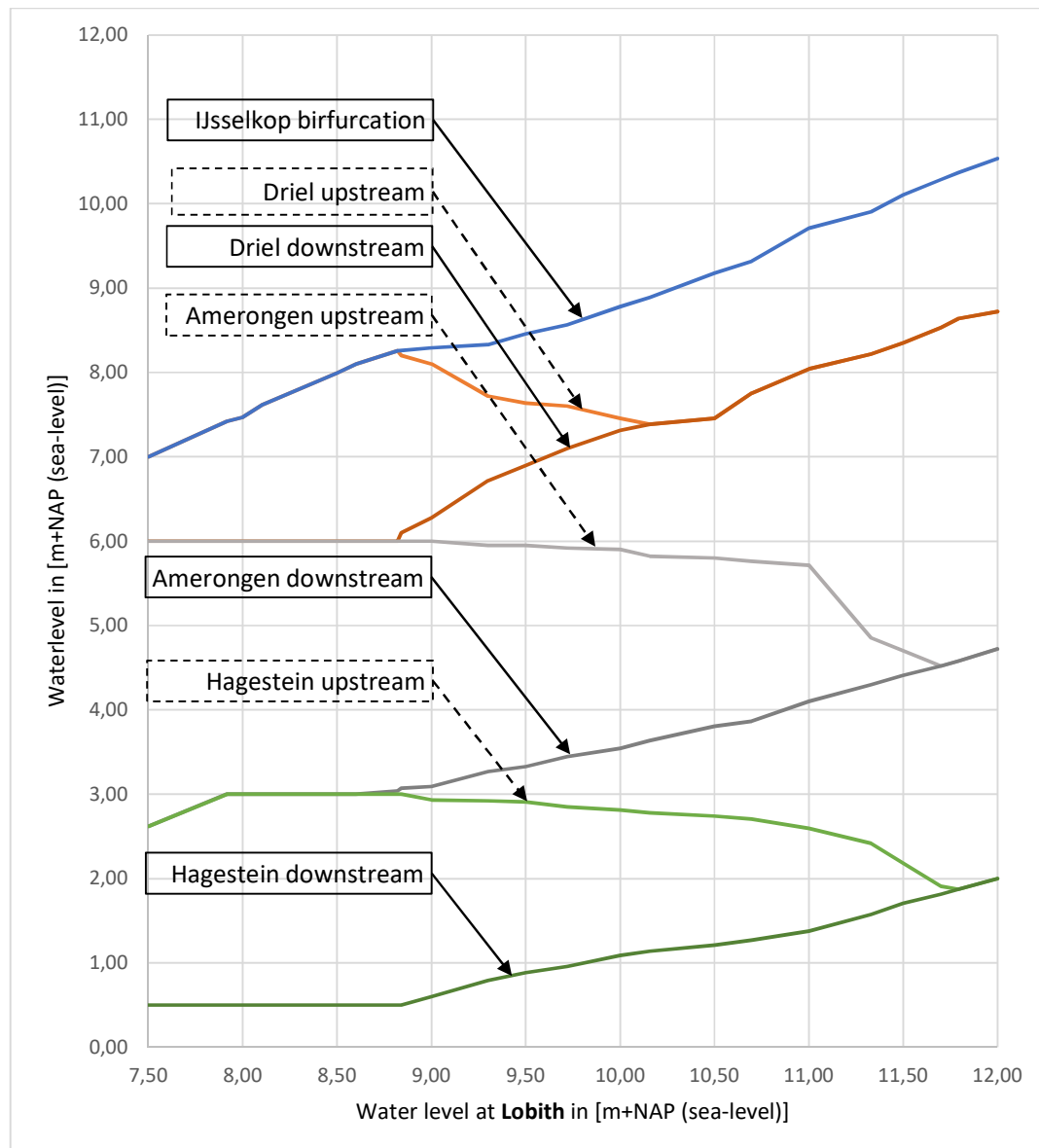


Figure 36 – Modern day water-level-management of the Nederrijn. Waterlevels as function of waterlevel at Lobith in [m+NAP]. - source: Henry Tuin [30, p. 33]

5.4 ELEVATION AND SUBSOIL ANALYSIS

5.4.1 Elevations

Figure 37 gives the height map of the location. Below in **Figure 38** a cross-section perpendicular to the river axis is taken across the weir and lock. Here it can be seen that the current flood-protection levee near Driel has an elevation of almost 14m above NAP (sea-level).

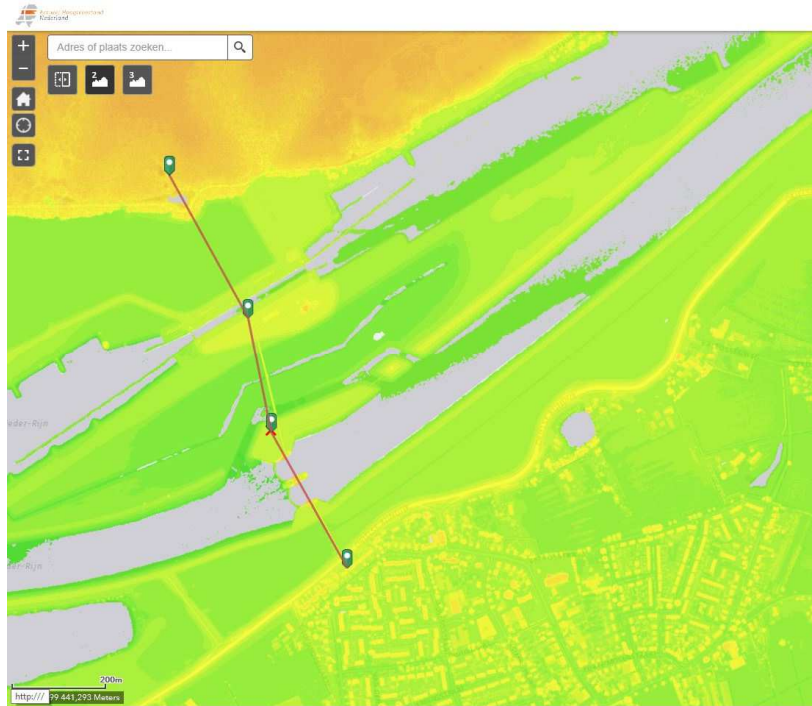


Figure 37 - Elevation map and path of cross-section - source: AHN [31]

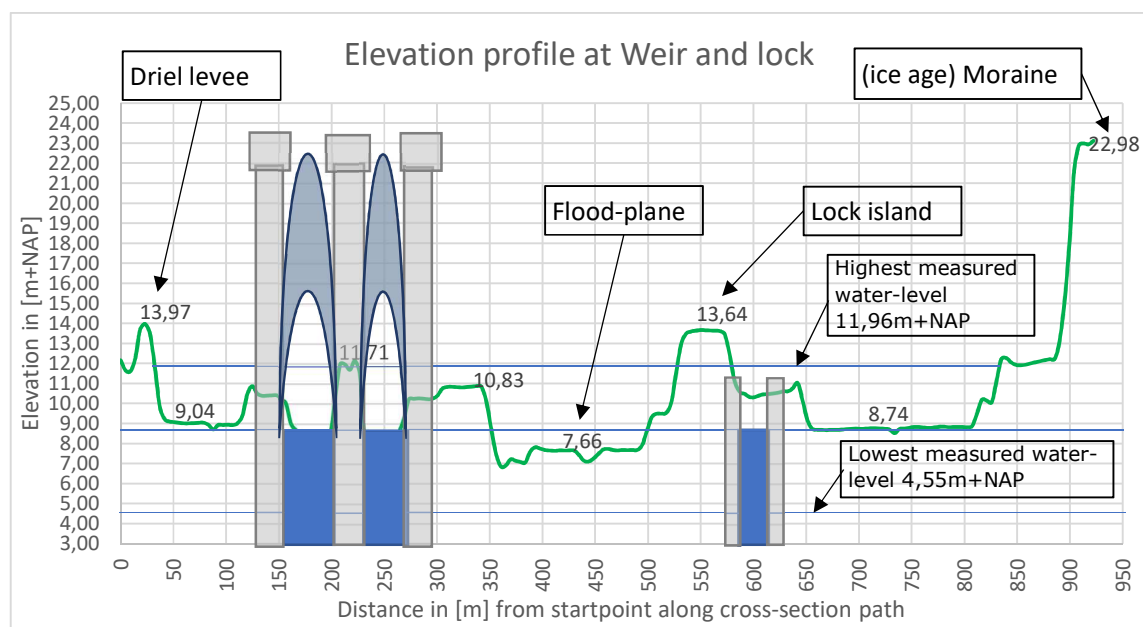


Figure 38 - Elevation profile across weir and lock - source: AHN [31]

5.4.2 Subsoil

See also **Appendix 10**. The subsoil is mostly sand and some deeper clay layers. Also layers of Loam are present. At a depth of -1m below NAP a fairly solid layer of sand can give 14-15 MPa of cone penetration pressure, indicating this is a solid layer to build a foundation on.

5.5 SHIPPING MOVEMENTS

From the monthly figures of 2005 it's clear that professional shipping for transport is quite constant throughout the year and is likely dependent on the state of the economy. Recreational shipping is mostly in the summer and in these months even larger than professional shipping.

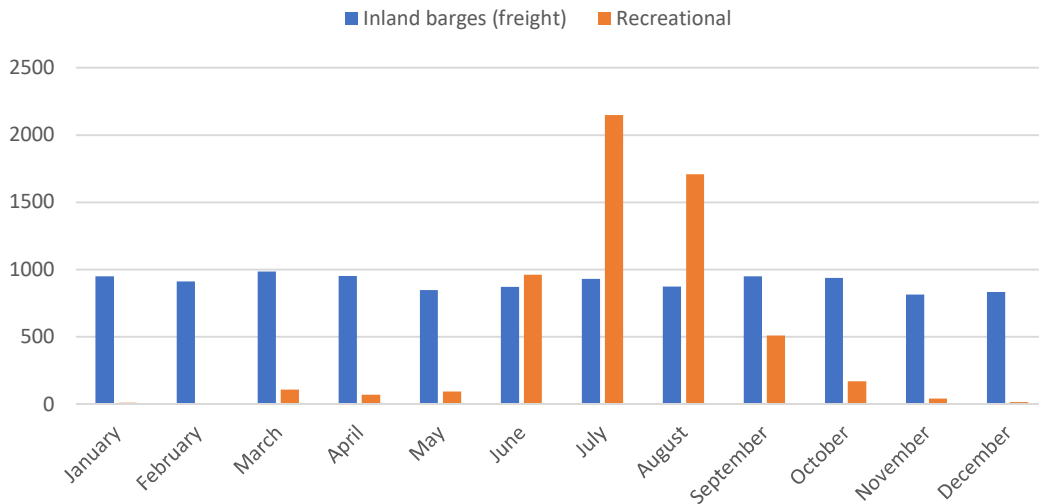


Figure 39 - Shipping traffic at lock/weir complex of Driel in 2005 - Source: [32]

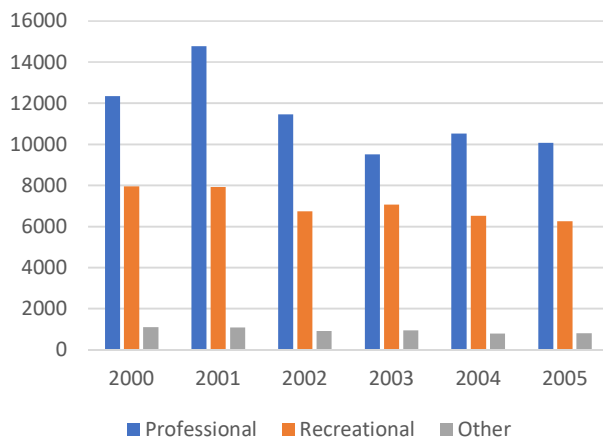


Figure 40 - Yearly total of ship passages per category - Source: [32]

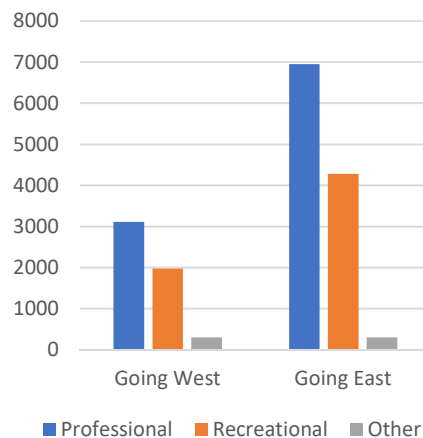


Figure 41 - Direction of shipping in 2005. Dominant seems to be going east. - Source: [32]

Apparently more shipping is going East than is going West. Shipping is a relevant factor at Driel, but for flow regime b shipping will go through the lock and interaction with a potential powerhouse near the weir will be minimal this way.

5.6 POWER GRID CONNECTIONS

The local medium-voltage cable location is indicated in

Figure 42. The cable runs through the tunnel under weir to cross the river.

3.1 Stuw - Driel



In case head-based turbine is chosen near the weir, the connection to the grid, given medium voltage cable will be enough, costs for connecting to the grid will be low. Then again, this also means that any excavation next to the weir will encounter this cable.

Figure 42 - Location of power-cables to which any hydro-power near the weir can be connected. Medium Voltage cable runs, through the weir. From Liandon: [33]

5.7 PROTECTED AREAS AND NATURE RESERVES

There are Natura2000 areas close the navigation lock and a few smaller areas downstream of the weir. This is indicated in **Figure 95** of **Appendix 11**.

Besides the Natura2000 areas, there is also an organisation called "Geldersch Landschap" that has property near the weir and lock as can be seen in **Figure 96** of **Appendix 11**. In **Figure 97** of **Appendix 11** it can be seen what the organisation does with the property. Parts of it are leased, likely to farmers that use it to produce hay. This however also gives an opportunity, because then the land might also be leased for hydro-power-purposes, if the organisation allows it.

The goals of the organisation has with these areas are shown in **Figure 98** of **Appendix 11**, where it becomes clear that they want to use it for nature (see also [34]). Should the area north of the lock be desired to use for hydro-power in some way, then careful consideration and communication with this organisation is required.

5.8 REQUIREMENTS AND DESIGN GOALS

From the relations and interests of the stakeholders and the gathered knowledge thus far the requirements and design goals are formulated.

5.8.1 Requirements

A short program of requirements is shown in . Most important is of course to maintain the desired safety level. Any changes done must not increase risk to loss of lives or (economic) damage.

Program of requirements		
Req. nr.	Linked to	Description
1		Discharge is only allowed through the weir-complex (including any new discharging structures) for maintaining water-levels at IJssel and Nederrijn rivers, according to the regime that RWS maintains.
2	1	Passage for shipping through the weir may not be delayed more than in the current situation by operating the hydro-electric plant. To be precise, the threshold for opening and closing the weir such that shipping can pass the weir must be maintained, meaning if the threshold water-level at Lobith is reached, the visor gates must be opened.
3	1	Only when there is a head-difference created by normal gate operation of the weir as described in requirement 1, can a part of the flow be diverted to the turbines for power production.
4	3	The combined discharge through the weir's visor-gates, cylinder-gates and the yet to be designed and build valves for regulating the flow through the turbines, must equal the total discharge through the weir-complex according to requirement 1.
5		Any alterations or structural connection with the existing weir-structure may not reduce its strength, stability or resistance to loads. Any such alterations to the structure required for the design, must provide sufficient proof that this is the case.
6		The current function of the weir-structure may not be obstructed or hindered by operation of the hydro-power-plant.
7		Any structure placed within the reach of river floods, may not reduce the discharge capacity during high discharge. Any obstructions placed, must be compensated for by additional discharge capacity within the weir-complex area.

Table 9 - Most important requirements for the project

Due to the complexity of changing the flow situation on a national level as well as the sensitivity of the topic of hydro-power at Driel for RWS, the choice is made to make the primary requirement that the flow-regime (the water level and discharge management) stays the same.

This means that an upstream observer (1) of the weir and a downstream observer (2) should not notice that there is a hydro-electric-powerplant at Driel. See also **Figure 43**.

Therefore, only when there is a head-difference due to normal gate operation of the weir can a part of the flow be redirected to the turbines.

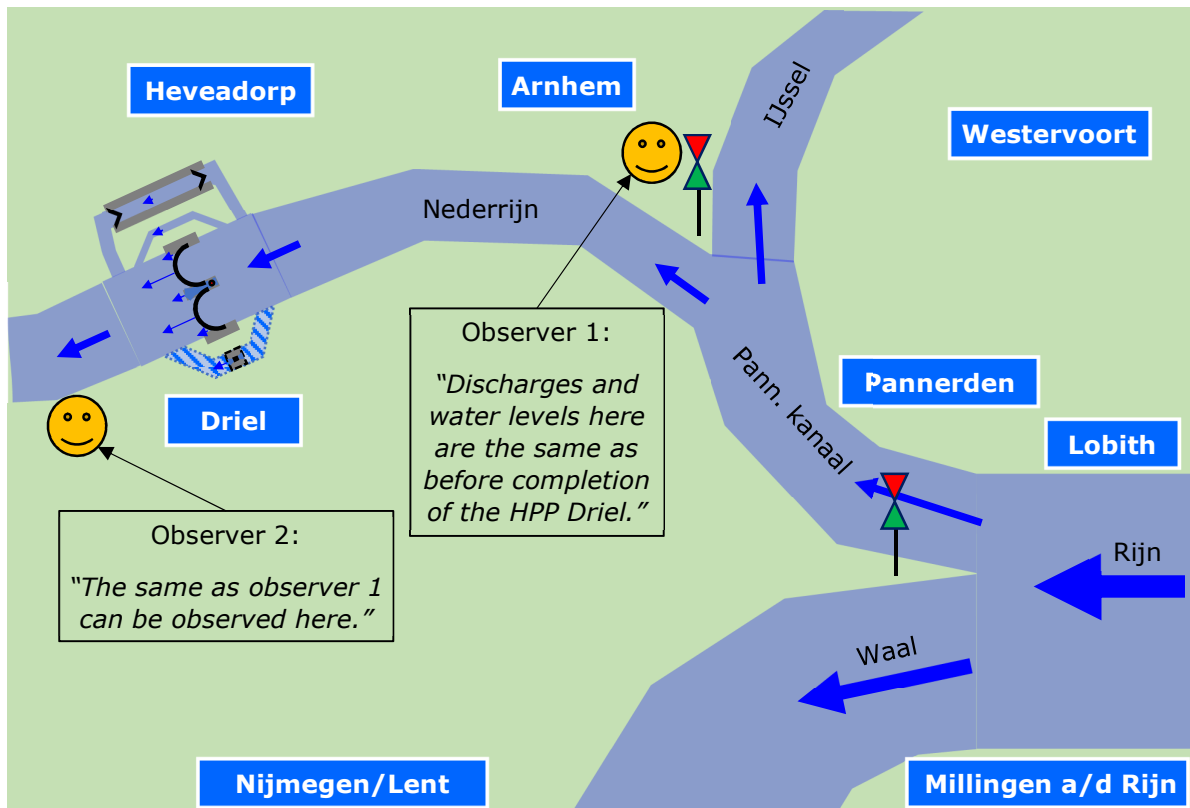


Figure 43 - Schematisation of discharge distribution of the weir-complex with two observers: nr. 1 upstream at IJssel-kop and nr. 2 just downstream of the weir.

5.8.2 Economic design goals

Besides requirements that have to be met, also design goals can be determined. These goals portray the wishes of various stakeholders. Economic reasons have always been a dominant factor in deciding whether to proceed with a project or not, and thus the economic design goals are mentioned first.

The goals to find the alternatives that have the "most economically feasible" design, meaning that the aim is to find the design(s) that have:

- The lowest Levelized Cost of Electricity (LCOE)
- The highest internal rate of return (IRR);
- The lowest initial investment, as getting the required starting capital may be a challenge for those interested in realising this project;

The IRR is somewhat similar to LCOE, but instead of energy price, uses the rate of return (interest rate) " r " as variable to get to zero NPV at the end of the considered lifetime.

In **Appendix 9** an explanation and short example is given for the LCOE (see **Figure 44**), IRR and related Net Present Value NPV. Should these terms be unfamiliar to the reader, it is advised to read this appendix.

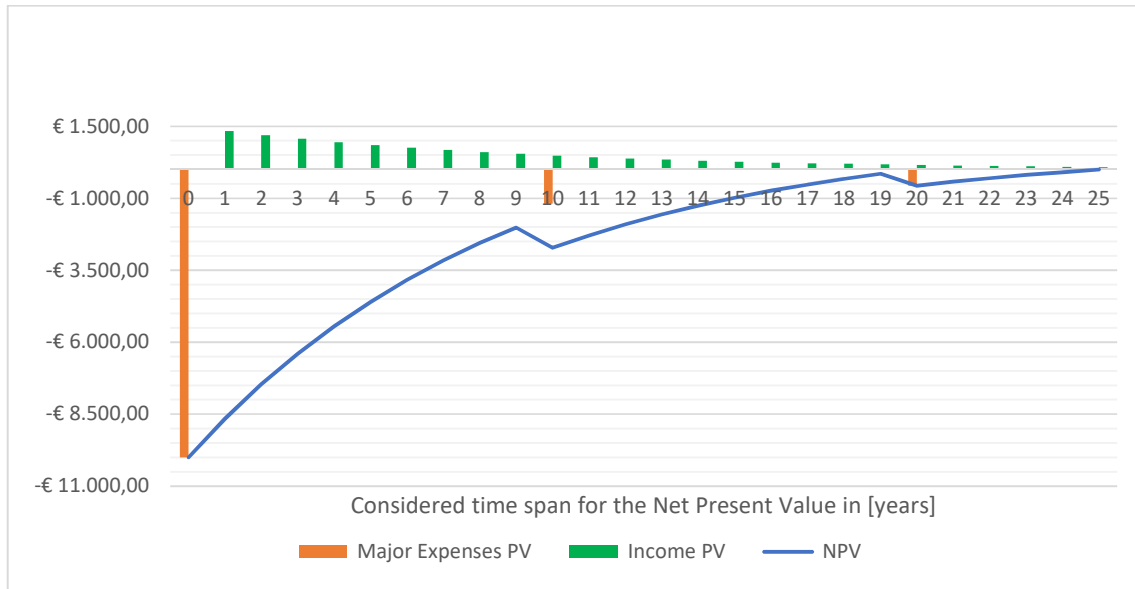


Figure 44 - Example of LCOE curve

Per example, in **Figure 44** inflation is accounted for with a rate of 0,04 (4%). After 10 years a replacement investment is taken into account as €2500 at year 0, so PV of investment at year 10: €1.191,5 and at year 20: €567,9. Cash-flow has been solved and found to be a value of: €1499,3 (year 0) such that NPV of total project after 25 years is €0,00. Assuming running costs of €1000,- which makes the required revenue = €2499,3/year at year 0. With an energy production of 30.000 kWh/year, the energy price needs to $LCOE=0,08331$ €/kWh.

5.8.3 Technical and secondary design goals

Although technical performance doesn't need to be a goal in and of itself, it is an indication for economic performance. Therefore at early stages in the design the goals concerning technical performance are in descending order of importance finding the design(s) that have:

- The highest amount of annual energy production;
- The highest capacity factor (CF, full-load-hours with respect to time in a year);
- The highest system efficiency (energy extracted from the water with respect to energy flowing through the system);

Goals towards public support of the project can be the following, but for now will be secondary objectives to the ones mentioned above:

- Keeping to a minimum the impact on local (surrounding) ecology;
 - o Minimize the fish-mortality of the turbine;
 - o Minimizing land-usage (small surface area);
- Minimizing global impact;
 - o Reducing use of materials and thus pollution related to their production;
 - o Creating positive life-time energy balance (energy produced versus energy required to build and maintain the powerplant);
- Minimizing negative effects on shipping
 - o Preventing (jet-like) flows re-entering the shipping lane being in use at disruptive angles;

6 CONCEPTUAL DESIGN

In the conceptual design various turbine types are being considered and worked out at a minimal level to determine their potential. A few of these concepts are worked out to preliminary design.

6.1 POTENTIAL LOCATIONS

Around the weir only a limited amount of locations are possible for implementing hydro-power. Especially for pressurised flow, a head-difference is needed for it to work. Ideally the pipe-system leading to the turbine needs to be as short as possible to reduce friction losses.

For free-flow hydro-power any location with high flow-velocity is ideal. However, also shipping needs to be taken into account. Putting a turbine in the middle of the shipping lane is not an option. Any locations within the shipping lane are ruled out as the turbines cannot be fit inside without obstructing navigation.

6.1.1 Potential locations for head-based turbines

South of the weir between the main flood-protection levee and the structure a bay-type hydro-power scheme is a possibility. This design would essentially be a copy of what is done in Maurik. A conceptual-drawing of this hydro-power-scheme variant is **Appendix 14** and is shown without annotations in **Figure 46** below.



Figure 45 - **Left:** Map overview of Bay-powerplant Maurik. – Source: OpenStreetMap: [35]
Right: weir and hydro-power-plan Maurik – Source: photo from visit.

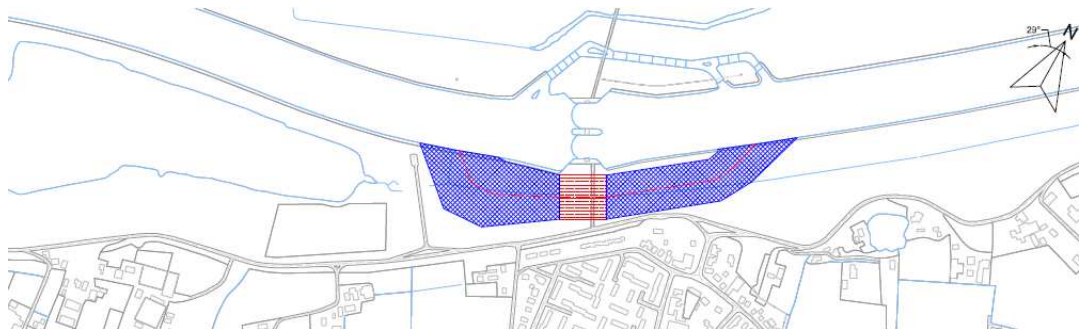


Figure 46 - Hydro-power-scheme-variant 1 - Sketch of bay power-plant south of the weir at Driel – see **Appendix 14**.

The advantage of this design is that shipping is not hindered and it uses space effectively. The downside is that, depending on how large the powerhouse will be and

how many turbines will be placed in it, the structure and related construction works is close to the main flood-defence levee of Driel.

Another option is to make a channel or to lay a pipe from the upstream side of the lock to the downstream-side of the weir (see **Figure 47**). Advantage of this design is that more space is available to place the power house. Less favourable is that more energy is lost due to a friction in the relatively long pipe or channel.

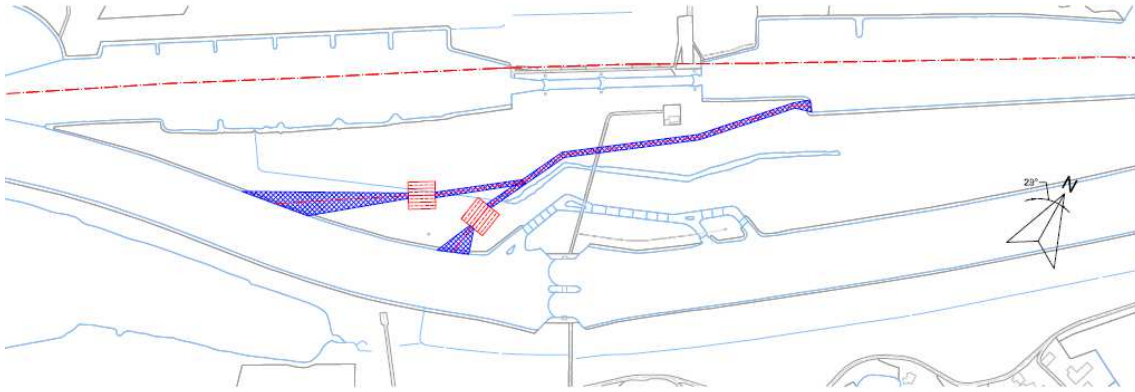


Figure 47 - Hydro-power-scheme-variant 2 - diagonal channel or pipe through the flood-plane. Note: there are multiple options for the outflow. - see **Appendix 14**.

Third and last option is to make a pipe North of the lock (see **Figure 48**). An interesting proposition here is that a reservoir could be made (with cooperation of the land-owner, that is) to store water during high river discharge and use this to run the turbine at an opportune moment.

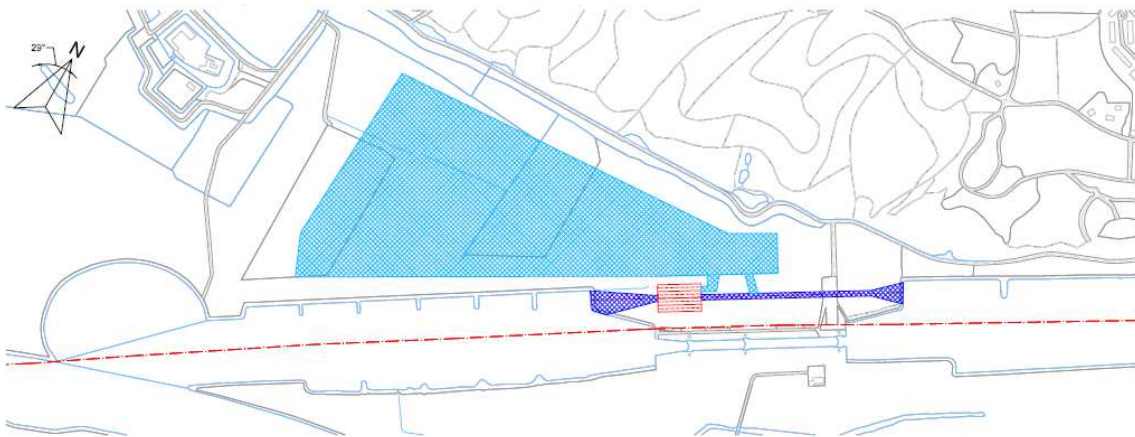


Figure 48 - Hydro-power-scheme-variant 3 - pipe north of the navigation lock with possible reservoir (indicated with light-blue). - see **Appendix 14**

The area indicated in **Figure 48** is 185.295 m², so while not giving it a volume like any of the reservoirs that can be found in mountain regions, it does give some volume to work with.

6.1.2 Free flow hydro-power schemes

For free-flow turbines there are only two real options without getting in the way of shipping, namely:

- At the groynes (see **Figure 49**)
- Behind the weir's outflow point (see **Figure 50**).

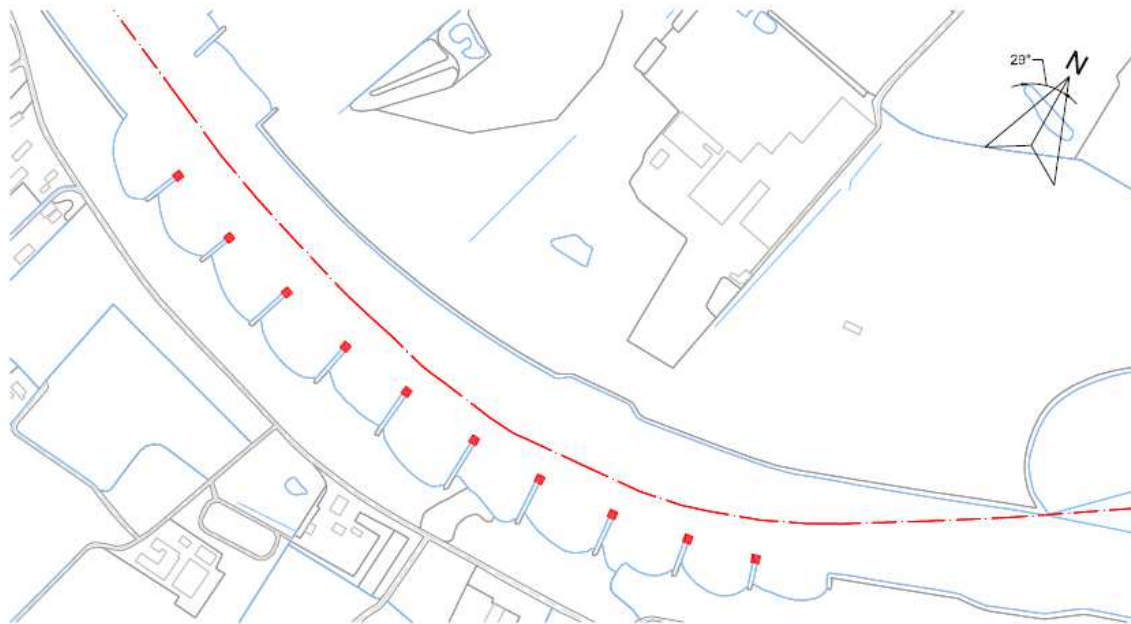


Figure 49 - HPS variant 4 - free-flow-turbines at the spur dam ends

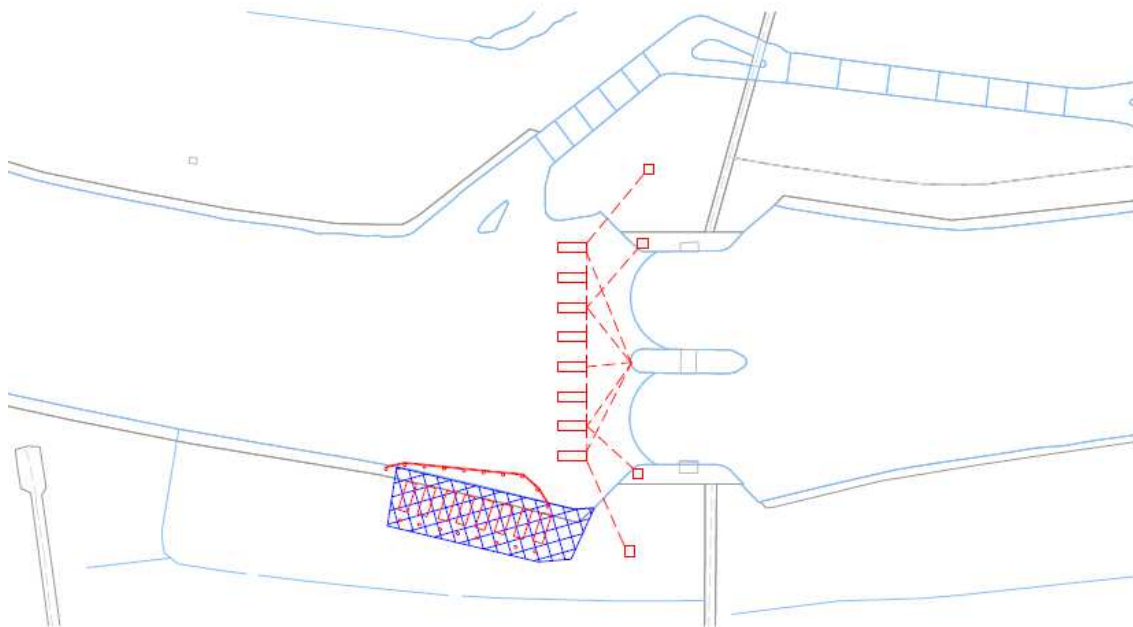


Figure 50 - HPS variant 4 - free-flow-turbines behind the weir opening with harbour for storage when the weir gate is opened completely

This last variant however requires a lot of maintenance and relocation during operation, to prevent being in the shipping lane when the weir opens. Also making the anchors is a serious technical challenge and will be costly. For these reasons, investigation into this variant is not further pursued.

6.2 VARIANT GENERATION

Now that the possible locations have been sighted, the type, size and number of the turbines are the next logical points to determine. Below the longlist of turbine types that fit in the locations is shown. Below that a short description is given of the related ideas.

Longlist

- 0. Group 0 Generic turbine (to get an idea of nr. Of turbines)**
- 1. Group A (head-based)**
 - 1.1 Null-variant: copy of Maurik (Vöst Alpine company, "Old" Kaplan technology)
 - 1.2 Regular Kaplan turbine (PFN's "New" Kaplan turbines)
 - 1.3 Venturi Enhanced Kaplan (VETT)
 - 1.4 Archimedes Screw Turbine (AST. Manufacturers: Landustries, Spaans Babcock)
 - 1.5 Pump enhanced AST (with pump to keep stable intake level)
 - 1.6 Variable inclination Enhanced AST (with adjustable inclination/intake height)
 - 1.7 Waterwheel
 - 1.7.1 Breastshot
 - 1.7.2 Overshot
 - 1.7.3 Undershot
- 2. Group B (velocity based)**
 - 2.1 Oryon watermill
 - 2.2 Smart Hydro Power (underwater windmill)
 - 2.3 Underflow waterwheel on floats (without pumping function)
- 3. Group C (Hybrid)**
 - 3.1 Underflow waterwheel on floats (with pumping function)
 - 3.2 Oryon watermill (Floating variant)

Shortlist

Only a few of these have been worked out. The variants that were expected to be the most interesting or promising have been chosen to asses.

- 1. Generic turbine (to get an idea of nr. Of turbines)
- 2. Null-variant: copy of Maurik
- 3. Regular Kaplan turbine
- 4. Venturi Enhanced Kaplan (VETT)
- 5. Archimedes Screw Turbine
- 6. Pump Enhanced AST

The Kaplan turbines are chosen because they have the most efficient power production and way of extracting the energy from the water for low head situations. The Venturi enhanced Kaplan is an interesting concept to prolong time of use in a year and is therefore also included. It can have higher energy gain for the high flow, low head situation.

The Archimedes screw is chosen because in the reference project it was quite cheap compared to Kaplan turbines, although it is a more simple turbine with lower efficiency, albeit still reasonable. This one could be more feasible due to the low costs.

The waterwheels were not considered due their small discharge capacity compared to the large available flow. In **paragraph 6.4** it is explained why free flow turbines are not developed into conceptual designs.

6.3 GENERIC TURBINE

The goal of analysing the "Generic turbine" is to assess the available energy, to find the cross-sectional area c.q. size and number of turbines as well as the discharge that goes through it. To do this, the discharge duration curve is assessed further. With this turbine a number of assumptions are done:

- Only 1 size turbine is considered at a time, no combinations of different size turbines;
- the efficiency is fixed to one value (90%), which it will have when active;
- the type of turbine is being left open for now, a turbine type will be considered in the next paragraphs.
- The minimum head to run a turbine is 0,3m;
- The ecological minimum of 25m³/s is not useable for power production.

6.3.1 Discharge duration curve

In practise, it is advised to design the hydro-power-plant for a discharge that is exceeded between 60 and 120 days in a year. Considering the discharge-duration-curve from **Figure 51**, the head-differences hardly exceed 0,3m around the 60 days exceedance. At around 101 day exceeded discharge the 0,3m minimum is exceeded most of the times and chosen as design point.

In **Figure 51** the right vertical axis shows Head-difference that are 0,3m or higher. The left vertical axis shows the discharges that are between a minimum of 25m³/s and a maximum of 550m³/s. Higher discharges don't fall within the range of interest and are therefore not shown here.

In **Table 10** on the below values related to important parts of the graph are shown.

Relevant points in graph of Figure 51	days Q-exceed.	% of a year	Related Q In m ³ /s	Difference (%points)	Differ. (days)
Advised design point minimum	60	16,4%	550	16,5%p	60
Advised design point maximum	120	32,9%	400		
Head-difference $\Delta H > 0,3m$	101	27,7%	440	66,5%p	243
Discharge $Q > 25m^3/s$	344	94,2%	25		
Discharge $Q > 50m^3/s$	261	71,4%	50	43,7%p (w.r.t. 27,7%)	160
$50 > Q > 25 \text{ m}^3/s$	-	-	-	22,8%p	84

Table 10 - Table with relevant points in graph of Figure 51

Assuming the minimal head-difference required to run a turbine is 0,3m and that the 25m³/s ecological minimum discharge cannot go through the turbine, but instead goes through the fish passage, then the operational range of discharges for the hydro-power-plant is between 28% and 94% (or 101 and 344 days) exceedance discharges. Of these 243 days per year, 84 days the discharge doesn't exceed 50m³/s as shown in the last row of **Table 10**.

Below in **Figure 52** an approximated graph is shown that is used to give an estimate of the potential power that can be produced.

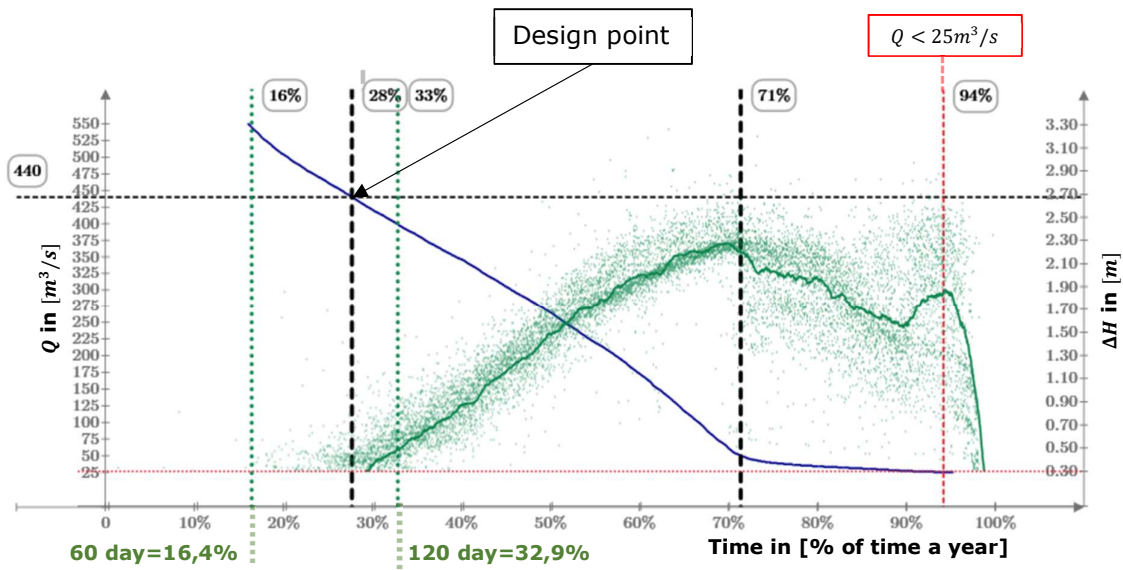


Figure 51 - Sub-section of the discharge duration curve with related head-differences that shows the relevant values for Hydro-power purposes. NOTE: ΔH related to Q on that point, not to x -axis!

Linearized discharge duration and related head-differences

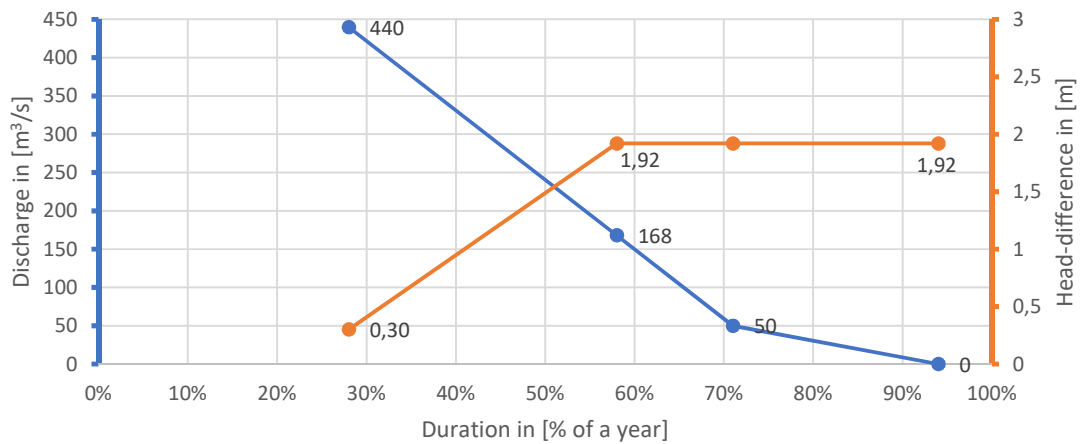


Figure 52 - Linearized discharge duration and related head-difference curve

Duration of Q in % of year	28%	58%	71%	94%
Q (m ³ /s)	440	168	50	0
ΔH (m)	0,30	1,92	1,92	1,92

Table 11 – Key points in the graph with linearized head-difference and discharge **Figure 52** (Based on **Figure 51**)

The way the turbines in an array are operated, is such that when enough discharge is available for another turbine, the new total discharge is equally distributed over each active turbine. This is shown in **Figure 53** for a powerhouse that has 6 turbines and the same maximum and minimum discharge per turbine as the Maurik HPP. This to show the progression of the discharge per turbine in relation to the total going through the plant.

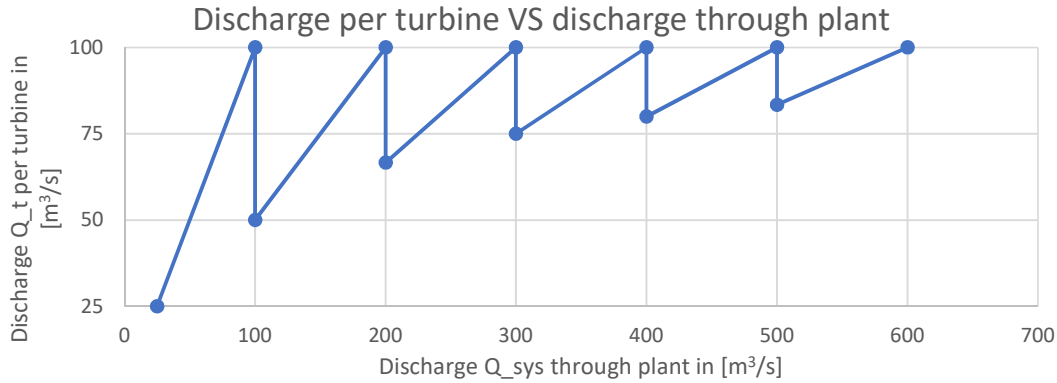


Figure 53 - Discharge Operation of hydro-power-plant (maximum discharge per turbine $Q_{t,max} = 100m^3/s$, minimum is $Q_{t,min} = 25m^3/s$, nr of turbines shown $n_t = 6$)

Note that the discharge of the powerplant can channel any flow-rate as long as they are within the limits of minimum flow of one turbine or the maximum flow of the set.

6.3.2 Discharge area

The effective cross-sectional area needs to remain the same to the current situation to fulfil the functional requirements of the weir-complex, as was mentioned in **paragraph 5.3.7**. It was found that a μA of about 200m² is available. In effect the discharge is divided between the weir and the power-plant unless all discharge can go through the turbines.

Using a simplified approach where the head over the turbine is assumed to be a fixed percentage of the head over the system. Working under the assumption that the turbine can change its resistance such that this head-ratio and discharge is achieved. So for the moment the assumptions is:

One given turbine design is capable of being configured such that:

$$\Delta H_t = \Delta H_{ava} * r_h \tag{3}$$

And:

$$Q_t(Q_{ava}, \Delta H_{ava}, r_h, A_t) = \min \left[Q_{ava}, \sqrt{\frac{1-r_h}{\xi_{eq}}} * A_t * \sqrt{2g * \Delta H_{ava}} \right] \tag{4}$$

Where:

Q_{ava} = The Available discharge of the river in [m³/s]

ΔH_{ava} = The available head-difference in [m] measured between the measuring points.

A_t = The physical discharge area in [m²]

$\xi_{eq} = A_t * \sum_{i=1}^N \frac{\xi_i}{A_i}$ The equivalent loss-coefficient.

For a Kaplan turbine this assumption isn't such a farfetched assumption, as the guide-vane and rotor-blade angles can be changed, thus changing the geometry and with that the specific speed of the turbine (within certain geometrical/physical limits).

The discharge is therefore the minimum of the two values, either the discharge that the pipe-system lets through or the discharge that is at that moment available.

The discharge that is lost, i.e. that goes through the weir is then:

$$Q_{weir}(Q_{ava}, \Delta H_{ava}, r_H, A_t) = Q_{ava} - Q_t(Q_{ava}, \Delta H_{ava}, r_H, A_t) \tag{5}$$

Using the $\xi_{eq} = 0.102$ found for Maurik it is possible to plot the following graphs showing that with different head ratios it's possible to reach the same discharge, as long as a sufficient discharge area is chosen (see **Figure 54** below).

Discharge - at design point: $\Delta H_{ava} = 1,92m$; $Q_{ava} = 50m^3/s$

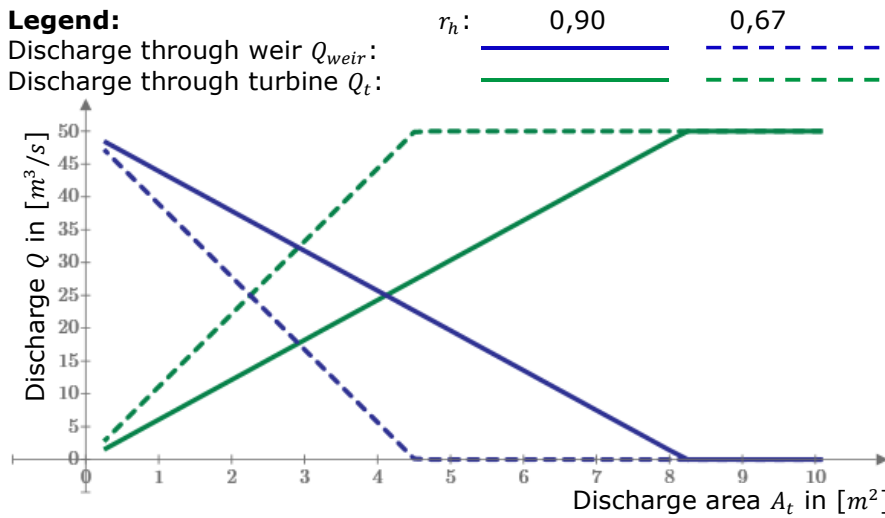


Figure 54 - Discharge through weir (descending) and through turbine (ascending) per discharge area for 2 different head-ratios.

6.3.3 Power and energy production

This results in the maximum attainable power increases with a larger head ratio, because of the product of head and discharge (see **Figure 55** on the next page). Note that the efficiency of the turbine is assumed to be a constant 90%. See also **Appendix 15**.

Power - at design point: $\Delta H_{ava} = 1,92m$; $Q_{ava} = 50m^3/s$; $\eta = 90\%$

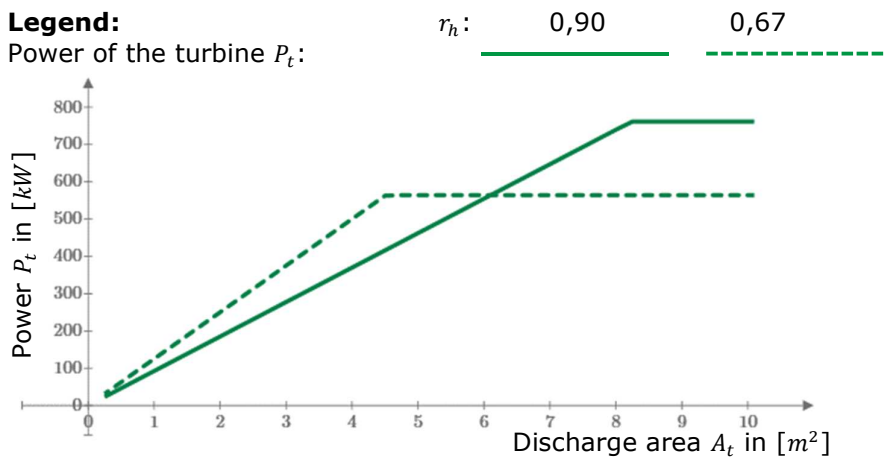


Figure 55 - Power of the turbine per discharge area for 2 different head-ratios.

To get to energy per year the power and discharge duration curve need to be combined. The following integral leads to the energy production:

$$E_{annual}(A_t, r_h) = \int_{t_1}^{t_2} P_t(Q_t(t), \Delta H_t(t), r_H, A_t) * dt \tag{6}$$

Where, per previous definition:

$$Q_t(t) = Q_t(Q_{ava}(t), \Delta H_{ava}(t), r_H, A_t)$$

$$\Delta H_t = \Delta H_{ava}(t) * r_h$$

Numerically integrating this per day, the yearly energy production per discharge area is shown in **Figure 56** below. This graph shows that the higher the discharge ratio is, the higher is the maximum amount of energy that can be reached. However, also that this amount of energy is achieved at a larger diameter. For instance taking a 99% head-ratio means that the amount of energy reaches it's more or less maximum value at 250m² or higher, where with a head ratio of 0,67 reaches its maximum already at about 90m².

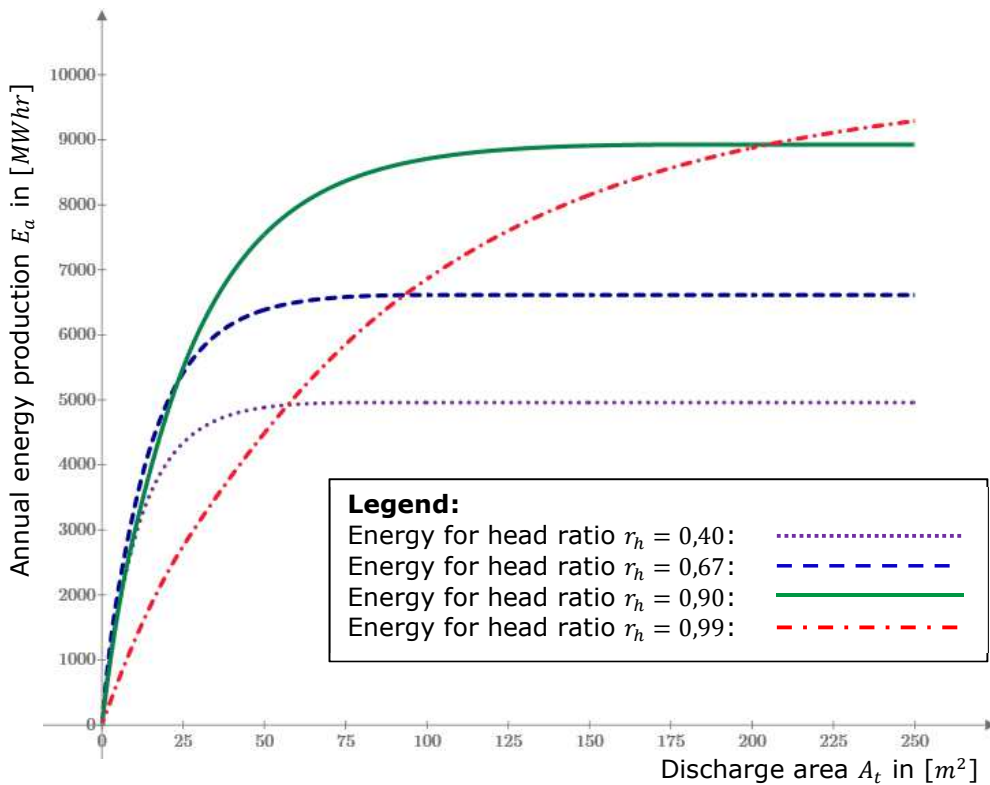


Figure 56 – Annual energy production estimate per discharge area based on linearized discharge duration curve of for 4 different head-ratios.

Driel hydro-power station is expected to be smaller than Maurik, so going over the amount of discharge area of Maurik ($A_{maurik} = 4 * 10,8m^2 = 43,2m^2$, perhaps rounding it up to 50m² as there may be differences), seems illogical. Having more discharge area and thus larger turbines than Maurik means it will also be more expensive than Maurik Hydro-power plant, while having less than half of the production.

6.3.4 Design variants

Therefore, taking a closer look at **Figure 63**, 5 areas have been chosen for closer inspection. Namely, at:

Design variant name	Discharge area in [m ²]	Annual energy production in [MWh]
Nr. 1	10,0	3336
Nr. 2 (head ratio intersect)	23,4	5281
Nr. 3	35,0	6549
Copy of Maurik (CoM)	43,2	7162
Nr. 4	50,0	7546
Total available energy:	∞	11022

Table 12 - Discharge area and annual production of chosen design variants. Energy is the largest values at chosen A_t 's from **Figure 57** (see black dots).

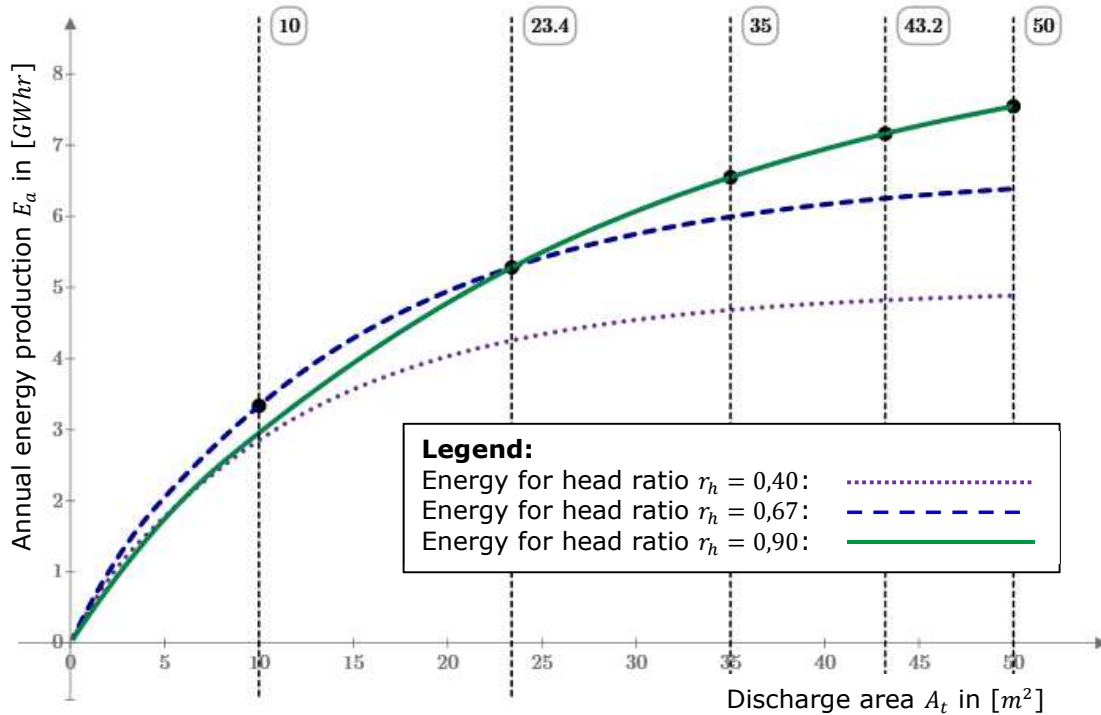


Figure 57 – Annual energy production estimate per discharge area based on linearized discharge duration curve of **Figure 52** within the applicable range of Driel.

From the graph above it seems that there is a head ratio that is most optimal for each design discharge. However, this optimal head ratio is dependent on the available head, available discharge and the discharge that the turbines can effectively let through.

To illustrate this, for an available head of 1,92m and a discharge of 168m³/s the power curve per head-ratio looks as follows:

Legend:	Design variant:		For design p.:
1	($A_t = 10m^2$)	:	$\Delta H_{ava} = 1,92m$
2	($A_t = 23,4m^2$)	:	$Q_{ava} = 168m^3/s$
3	($A_t = 35m^2$)	:	
CoM	($A_t = 43,2m^2$)	:	
4	($A_t = 50m^2$)	:	

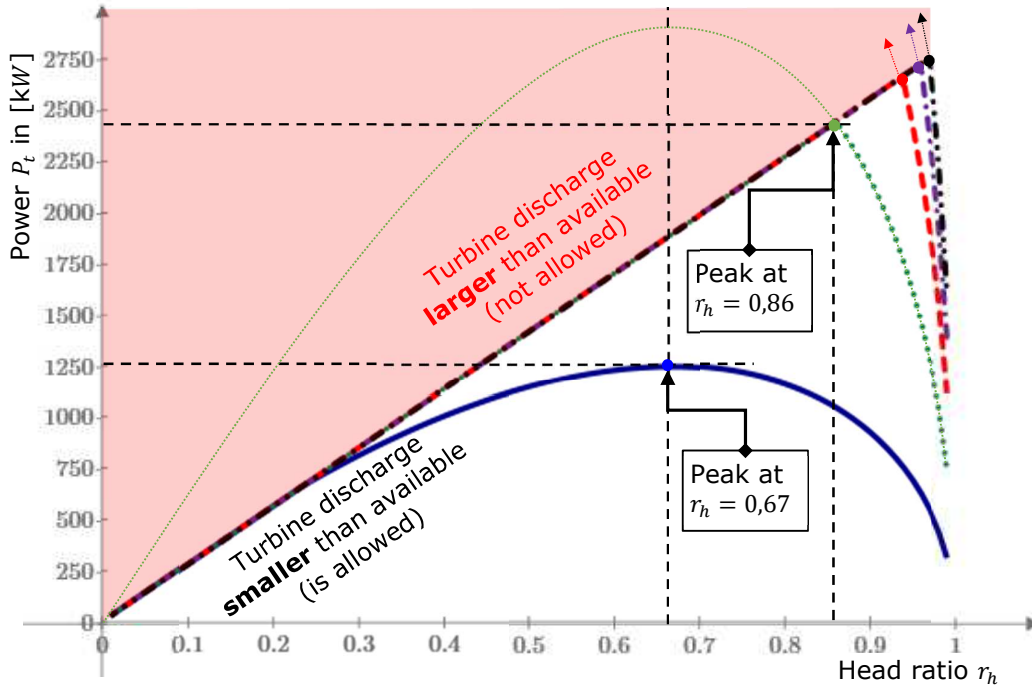


Figure 58 – Power per head ratio for each design variants with an available discharge of 168m3/s and a head of 1,92m

The image above (**Figure 58**) shows that, for this discharge-head-situation and for the smallest discharge area variant (blue line), the optimal head ratio is still at 67%, but for the other variants it is around 86 to 97%. The value is limited by the losses in the pipe system until the point where, if the available discharge would be used, the losses would exceed 1/3 of the available head.

Rewriting the discharge formula for when the flow through the turbine is equal to the available flow:

$$Q_t = Q_{ava} = \sqrt{\frac{1 - r_h}{\xi_{eq}}} * A_t * \sqrt{2g * \Delta H_{ava}}$$

Rewrite:

$$r_h = 1 - \xi_{eq} * \left(\frac{Q_{ava}}{A_t * \sqrt{2g * \Delta H_{ava}}} \right)^2 = 1 - \frac{\xi_{eq} * Q_{ava}^2}{A_t^2 * 2g * \Delta H_{ava}} = 1 - \frac{\Delta H_{loss}}{\Delta H_{ava}} \quad (7)$$

This head ratio is plotted with the orange dashed line in **Figure 59**. If, when the head-ratio goes below 2/3 the resistance is increased to remain at 2/3 the most power is generated for each available discharge.

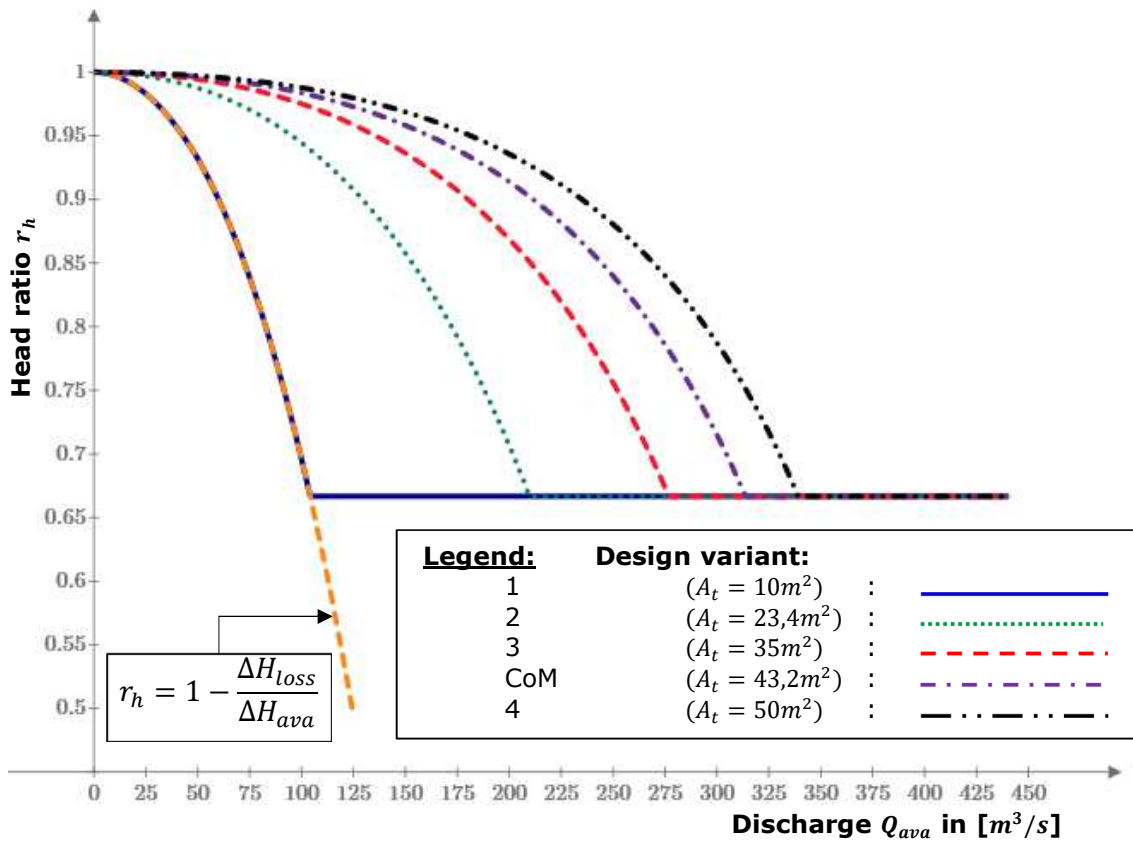


Figure 59 – Optimal head ratio per available discharge for each variant.

It can be seen that for larger turbines the point of transition is at a larger discharge. Using these head ratios gives an average 12% increase to annual production:

Design variant	New energy value [MWh]	Percentual increase adjustable r_h in [%]	Energy per discharge area [MWh/m²]	Rated power in [kW]	Capacity factor In [%]
CoM	7926	10,7	183,5	3000	30,2
1	3685	10,5	368,5	1400	30,0
2	6158	16,6	263,1	2400	29,3
3	7360	12,4	210,3	2800	30,0
4	8280	9,7	165,6	3100	30,5

Table 13 - Improvement with variable head-ratio

Interestingly, the increase is largest for design variant nr. 2, which has an area that in Figure 57 gave the same annual energy for both head ratios 0,9 and 0,67.

The energy per discharge area is highest for the smallest turbine. This could be an indication for a higher rate of return. i.e. Largest gain per investment.

Again considering the flow duration curve, but now taking into account variations in the years, three curves have been selected as being a wet, dry and average year in terms of discharge. The head difference is very much related to the discharge, so this is not considered separately. In Figure 60 below the flow duration curves of these years have been plotted.

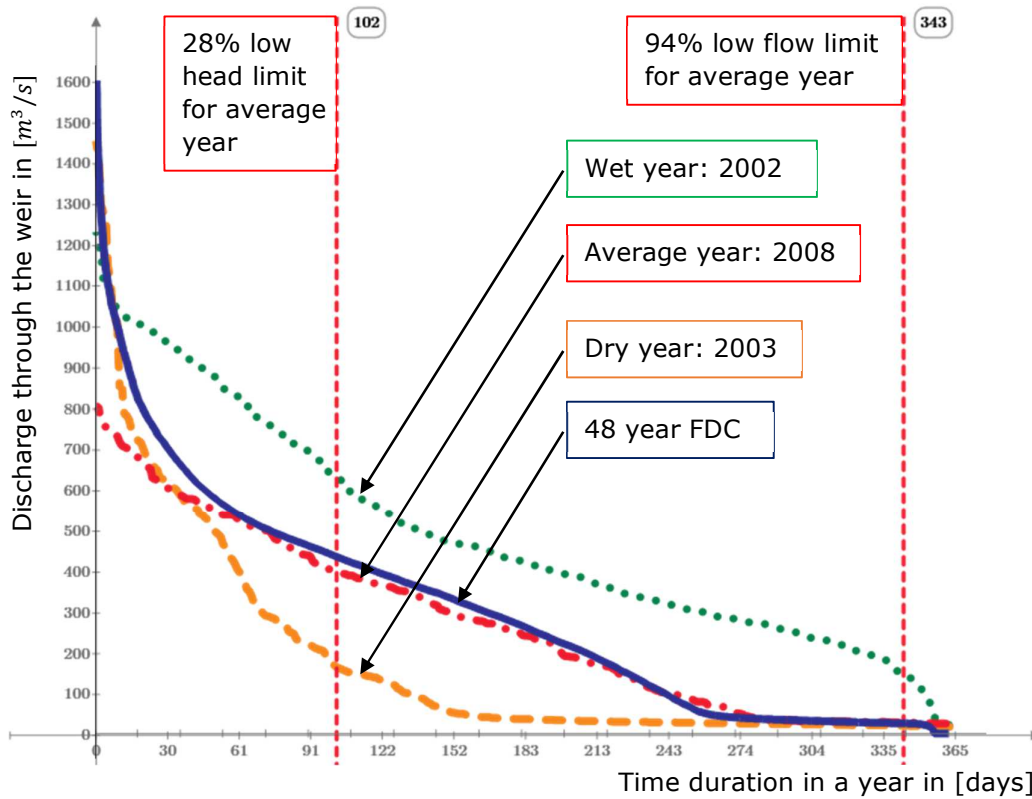


Figure 60 - Flow duration curves for a wet year, an average year and a dry year compared to the 48 year data (All time) flow duration curve

On the next page the production time series of these years are shown.

Design variant	Annual production Wet year in [MWh]	Annual production Dry year in [MWh]	Annual production Average year in [MWh]
CoM	9814	4866	8524
1	3416	2705	3926
2	6951	4123	6612
3	8874	4640	7886
4	10389	4994	8892

Table 14 - Annual production for chosen reference years

The table above shows that in wet years more power is produced than in dry years. Having more discharge has apparently not lead to too low head-differences or increase in situations where the turbine cannot be operated.

This can also be seen in the **Figure 61** in that the amount of down-time for the dry year is larger than for the wet year. Interesting to note is that for a dry year the production actually lies more in the months that normally have too higher a discharge for the weir to be closed. They utilise the “floods” of such a year as it were.

Looking at a the reference yearly time series for an average, wet and dry year the energy production looks like:

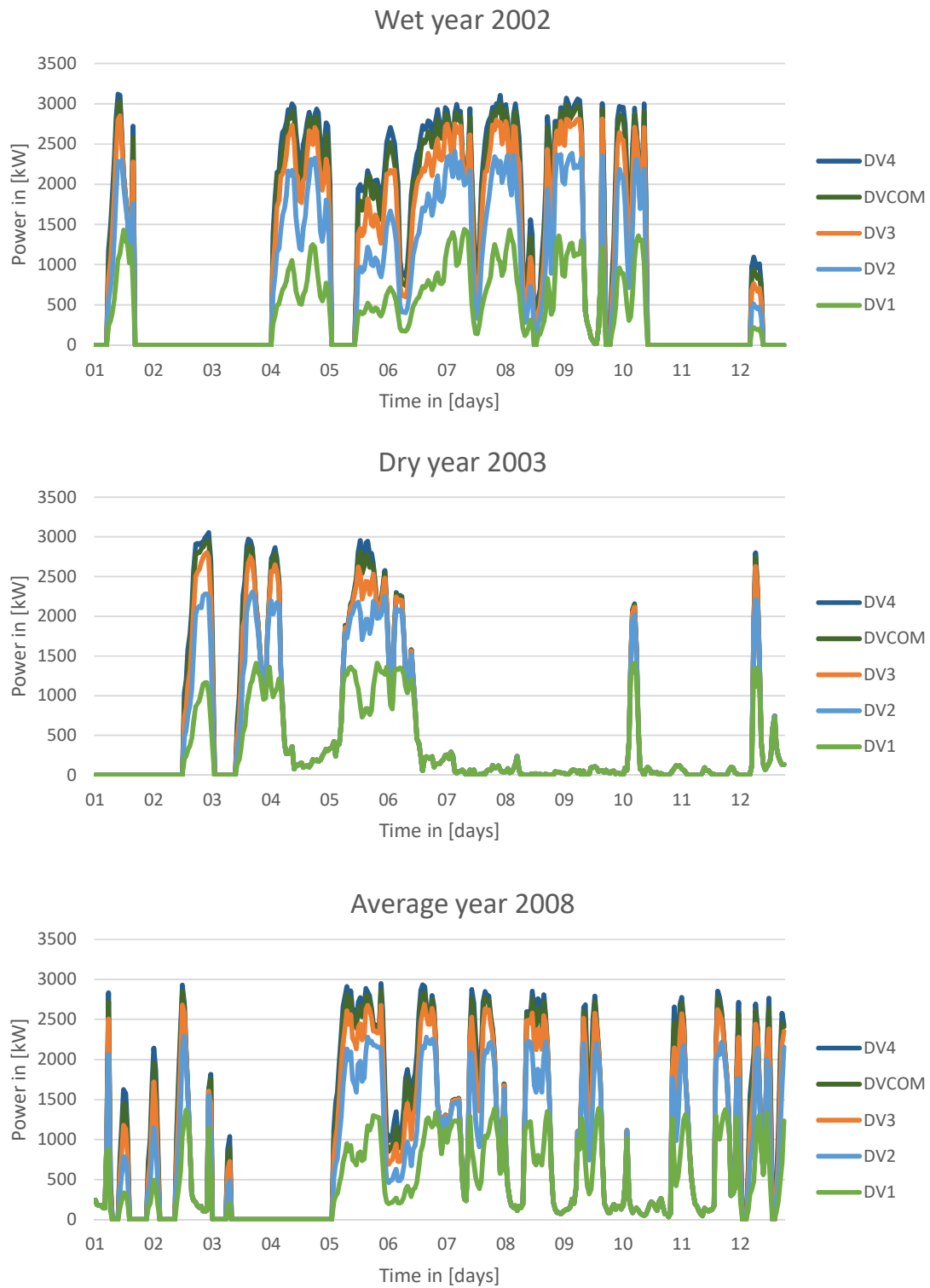


Figure 61 - Time series of power production for the 5 design variants. Assumed minimum head is 0,3m.

Discharge and efficiency range of low-head-turbines

A turbine has a fixed discharge for which efficiency peaks at each head-difference. This means that, when there’s a lot of fluctuation in the flow, one turbine is not likely to run at high efficiency for long periods of time. A set of multiple turbines gives more options to tune the discharge to attain a higher average efficiency (both over time and instantaneous).

In **Figure 62** below it can be seen that *Kaplan turbines* are reduced to less than 40% efficiency when the discharge going through them is nearing about 15% of their design maximum flow-rate Q_{max} (Kardi and Pandey [36]). Also, Kaplan turbines reach peak efficiency at around 60 to 80% of Q_{max} .

The *Archimedes Screw* retains its efficiency longer, down till 8-12% of maximum flow, and stays above 70-75% efficiency for most of its range, peaking at 85% efficiency at around 80% of maximum discharge. However, this turbine type is more sensitive to inflow water-level. **Figure 62** is presumably only valid for constant water-level and head.

Water-wheels perform even more consistently over the discharge axis, but at a lower efficiency, below 75%. Overflow water-wheels are also dependent on relatively constant upstream and downstream water-levels.

Turbine	Lowest effective Q_{min}/Q_{max}	Peak efficiency Q/Q_{max}	Approximate Maximum efficiency
Kaplan	15-20%	60-85%	92%
AST	8-12%	80%	88%
Waterwheel	7,5-10%	100%	77%
Francis	20-30%	80%	88%
Cross-flow	20-30%	60%	83%

Table 15 - Efficiency effective discharge ranges for several turbine types. Derived from **Figure 62**

Ignoring the Cross-flow and regular propeller types, it would be a safe assumption that at 20% of the maximum flow, low head turbines lose their efficiency and will be switched off.

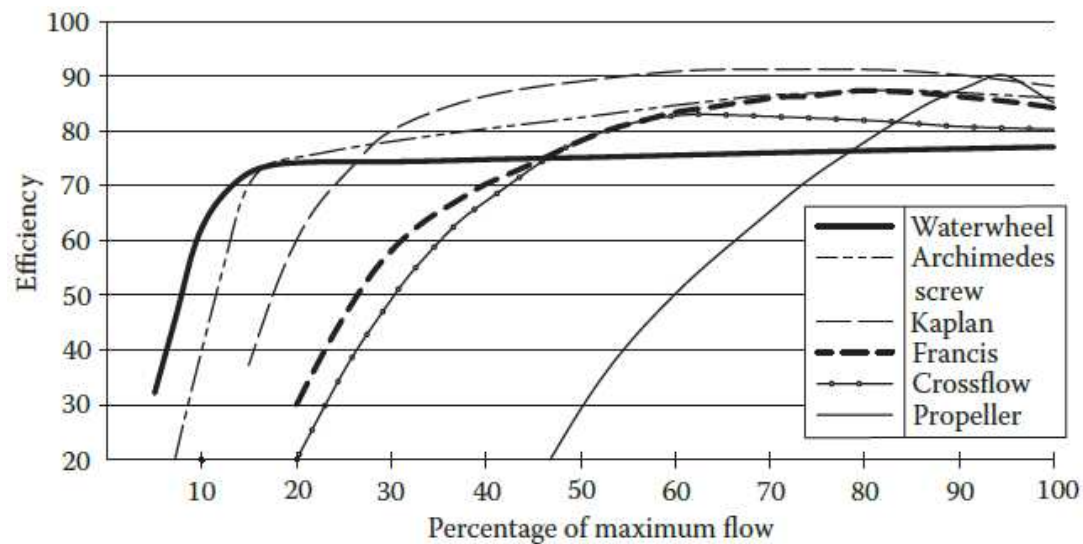


Figure 62 – General efficiency of various low-head-turbines for reduced flow - Source: Kardi and Pandey 2016 [36, pp. 312 - fig. 12.8]

Demonstrating the point made at the beginning in this paragraph, 1 turbine that has a discharge capacity of $400\text{m}^3/\text{s}$ and in accord with the efficiency loss at 20% of Q_{max} , consequently loses all energy that could be generated from $80\text{m}^3/\text{s}$ and down.

To make the calculation more simple at first a approximated efficiency function is used to calculate power as shown in **Figure 63**.

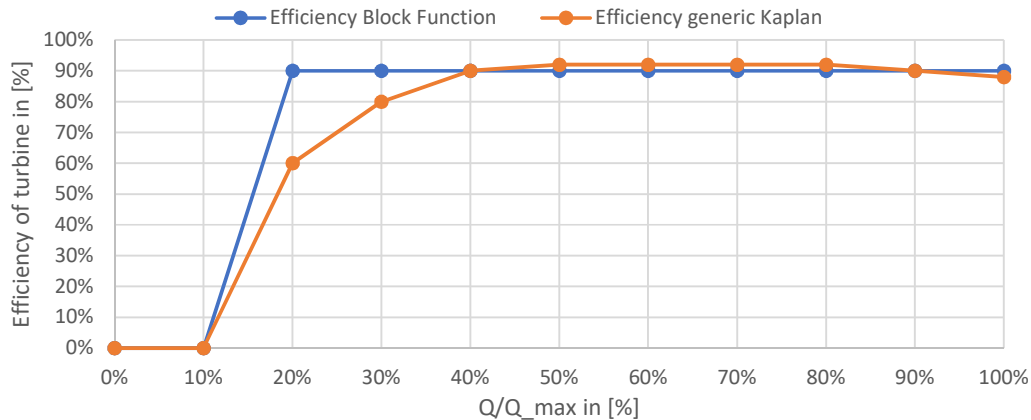


Figure 63 - Approximated discharge-efficiency-curve based on **Figure 62**.

Number of turbines

When less than or equal to $15\text{m}^3/\text{s}$ cannot be taken by the turbine, the amount of energy that is lost drops below 100 MW hours. Comparatively, if the same is done for $50\text{m}^3/\text{s}$, then almost 958 MW hours are lost. $15\text{m}^3/\text{s}$ therefore seems a good cut-in discharge. A minimum number of turbines can be determined this way.

Using the 5 previously defined design variants:

Design variant	Total discharge $Q_{max,total}$ in $[\text{m}^3/\text{s}]$	Number of turbines n_{min}	Discharge area A_t per turbine In $[\text{m}^2]$	Cut-in discharge $Q_{t,20\%}$ in $[\text{m}^3/\text{s}]$	Lost energy from discharges lower than cut-in in $[\text{MW} * \text{hr}]$
CoM	333,6	4	10,8	16,68	108,55
1	110,8	2	5,00	11,08	48,10
2	232,1	3	7,80	15,48	93,80
3	298,8	4	8,75	14,94	88,00
4	356,3	5	10,00	14,35	80,50

Table 16 - Minimum amount of turbines for cut-in discharge of $15\text{m}^3/\text{s}$

Conclusions Generic turbine

A theoretical maximum amount of energy has been established to be 11,02 GWh. This maximum is very unlikely to be exceeded as effects of efficiency, effective head and such have not been taken into account for that value.

5 variants have been determined. The one with a discharge area of 50m^2 (10m^2 per turbine) is estimated to produce the most energy, about 8,9GWh. However, the one with the smallest discharge area has the largest energy per discharge area, which could indicate a larger yield per invested amount of money. A cost analysis is required to determine this.

Also an amount of turbines per variant is determined. Generally, having larger turbines leads to less losses in the system, so it makes sense to stick to the minimum amount of turbines and keep the discharge area per turbine as large as possible.

6.4 FREE FLOW TURBINES

Considering the average flow in the Neder-rijn river, about 306m³/s and an a depth of 3m and width of about 100m the average flow velocity is about 1,02m/s. Considering that with high flow the water level rises and the discharge area increases, it is not expected that with larger discharge the flow velocity will increase substantially.

With that depth a reasonable rotor diameter would be 2m, so the flow area is then $A_t = 12,5m^2$.

For a free flow turbine the maximum power can be extracted is limited by the Betz limit [37], where only $\frac{16}{27} \approx 0,59\%$ of the energy in the flow can be absorbed by any turbine.

The energy in the flow is:

$$P_{flow}(A_t, u) = \frac{1}{2} * \rho * A_t * u^3 \quad (8)$$

Where:

$u =$ The flow velocity in [m/s]

$A_t =$ The cross-sectional area of the turbine rotor in [m²]

$P_{flow} =$ The available power or energy flux in the flow in [W]

So the theoretically extractable energy considering the Betz-limit is per turbine:

$$P_{free-flow}(A_t, u) = \frac{16}{27} * \frac{1}{2} * \rho * A_t * u^3 = \frac{16}{27} * \frac{1}{2} * \frac{1000kg}{m^3} * 12,5m^2 * (1,02)^3 = 3951 W = 3,9kW$$

Having discarded the variant where the turbines are suspended in front of the weir (see **Figure 50** in **paragraph 6.1.2**) due to practical reasons, only the variant where turbines are installed in the spur dams is left.

To get an equivalent amount of power as the generic turbines a lot of these free flow turbines are needed. For design variant 1 to get an equivalent amount of power and neglecting even the mechanical efficiency of the turbine 354 free flow turbines are needed to produce the same amount of power. For design variant 4 this 785.

Considering spur dams on only 1 side of the riverbank (which seems to be realistic looking at satellite images) with an inter distance of the spur dams of about 95m, a stretch of river of 33,6 km is needed to equal the power of design variant 1 and 74,5 km is needed for design variant number 4.

Within the spatial scope of this research variant 1 could perhaps fit (the stretch of river considered being about 43km). However, the distance over which the power needs to be transmitted is then much larger than for the head-based variants.

This also means that either electrical losses (long cables with low voltage) or costs for electrical equipment (transformers at many locations to increase the voltage to reduce transport costs) are quite substantial for free flow turbines.

This disadvantage is so large that free flow turbine manufacturers also indicate that the Nederrijn is not economically feasible (see also quote in **Appendix 4**). For this reason they have not been investigated further.

6.5 REGULAR KAPLAN TURBINE

The Kaplan turbine has the highest efficiency rating of all considered turbine types and therefore is a good place to start. Now that a type of turbine is chosen, the diameter can be determined. The diameter is estimated using the following approach:

Assume the ratio of the turbine outer diameter and inner rotor diameter is more or less constant. From the drawing of the Pentair fish-friendly turbine it was measured that the ratio is 1,6/4,0:

$$D_{in} = \frac{1,6}{4,0} * D_{out} \rightarrow A_t = \frac{\pi}{4} * (D_{out}^2 - D_{in}^2) = \frac{\pi}{4} * D_{out}^2 \left(1 - \left(\frac{1,6}{4,0}\right)^2\right)$$

Rewrite:

$$D_{out} = \sqrt{\frac{A_t * 4}{\pi * \left(1 - \left(\frac{1,6}{4,0}\right)^2\right)}}$$

(9)

For the 5 design variants that is:

Design variant	Number of turbines n_{min}	Discharge area A_t per turbine In [m ²]	Diameter - Outer rotor diameter in [m]	Diameter - Rounded to nearest multiple of 10cm:
CoM	4	10,80	4,04	4,00
1	2	5,00	2,75	2,80
2	3	7,80	3,44	3,40
3	4	8,75	3,64	3,60
4	5	10,00	3,89	3,90

Table 17 - Kaplan turbine diameters for each design variants

Interestingly the Maurik variant and the 3th variant result in the same rounded diameter. Only the number of turbines is still different. Entering this into the hydraulic model gives the following results.

6.5.1 First estimate of costs

Working from the Maurik case, which at the time was 66 million guilder, that translates to 54 million euros current day, the costs for the design variants can be determined. Design variant "Copy of Maurik" then serves as reference.

Driel is of not exactly the same situation as Maurik, so a 20% uncertainty margin is taken for all variants. It is customary to indicate investment cost to a per kilowatt price in hydro power engineering, so that is adopted here to. The price per kilowatt is then:

$$PoT = \frac{€54mln}{10.000kW} = €5.400 kW^{-1} \rightarrow PoT_d = 120\% * €5.400 kW^{-1} = €6.480 * kW^{-1}$$

This leads to the following costs estimation:

Design variant:	CoM	1	2	3	4	
Rated power	kW	2.975	1.475	2.642	3.031	3.160
Total costs	mIn €	19,3	9,6	17,1	19,6	20,5
Energy production	kWh	8.524.000	3.926.000	6.612.000	7.886.000	8.892.000
Price per kWh	€/kWh	2,26	2,43	2,59	2,49	2,30

Table 18 - Costs estimation based on Maurik

6.5.2 Hydraulic model Kaplan

In the hydraulic model of the Kaplan turbine, the turbine diameters are taken and used as input for rules of thumb for sizes of the system from hydro power engineering.

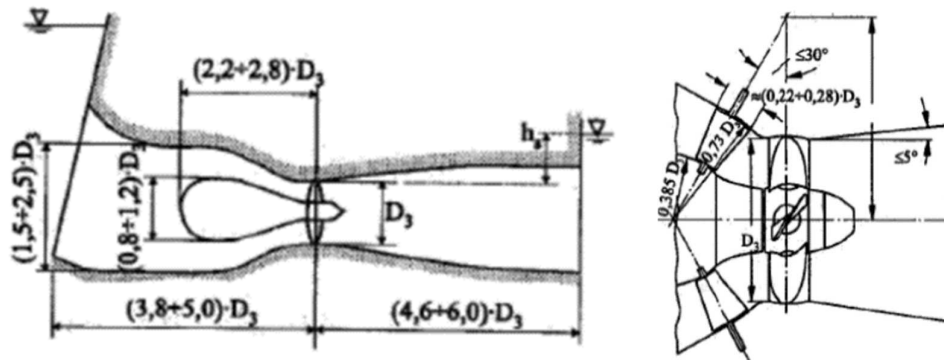


Figure 64 - Kaplan dimension rules of thumb. - Source: Marencé

In the generic turbine paragraph a simple approximation with a based on head-ratio has been done. In this paragraph a more refined calculation is done, where the geometry of the turbine is taken into account and the head-ratio and discharge were determined with the turbo-machinery theory as explained in **paragraph 4.2.4**.

The land use of the turbine is estimated by taking the largest diameter in the design, which is the inflow diameter and the pipe-system length. This gives an indication of how much space is needed to build the turbine.

Design variant	Number of turbines	Diameter of rotor	Inflow opening diameter	Length of pipe system	Width total	Area per turbine	Area total
DV	#	m	m	m	m	m ²	m ²
0	4	4,0	10,0	44,0	45,0	440	1.760
1	2	2,8	7,0	30,8	17,0	216	431
2	3	3,4	8,5	37,4	29,5	318	954
3	4	3,6	9,0	39,6	41,0	356	1.426
4	5	3,9	9,8	42,9	54,8	418	2.091

Table 19 - Relevant dimensions for regular Kaplan turbines

In the table above the dimensions of the regular Kaplan turbines are shown as well as their "land usage", the minimum space they occupy should they be built.

The head losses for all design variants with an available head are shown in

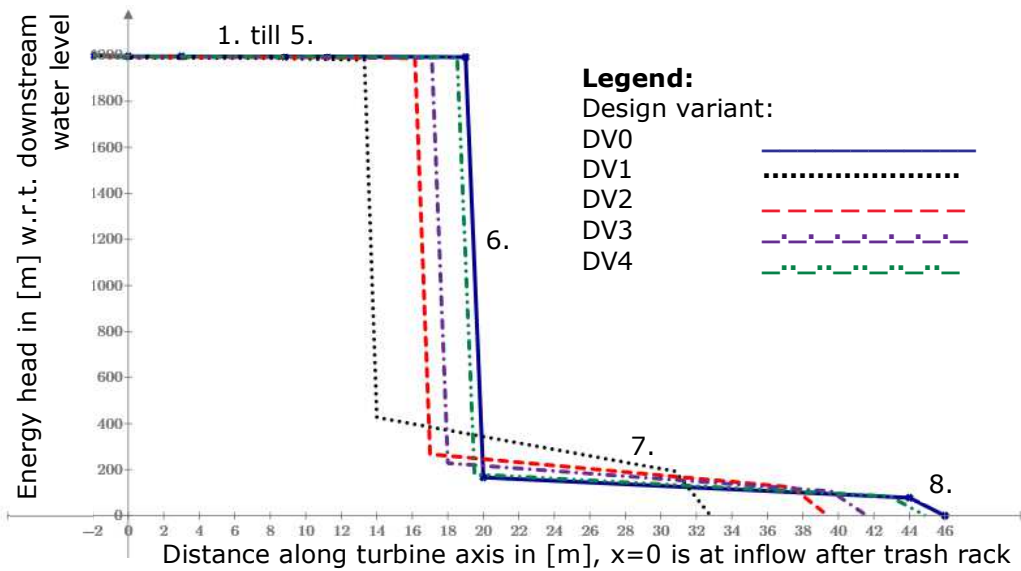


Figure 65 - Head levels for the 5 design variants for available head of 2m, speed ratio of 1,1 and efficiency of the turbine of 95%

Head loss at	Amount of head loss in [mm]	x-location in [m] w.r.t. inflow
1. trash rack	4,38	-2,0
2. inflow	0,20	0,0
3. friction inflow pipe	0,39	3,0 till 8,8
4. Bulb contraction	0,00	8,8
5. friction bulb	2,86	11,2 till 19,0
6. turbine	1814,93	19,0 till 20,0
7.1 expansion draft tube	10,92	20,0 till 44,0
7.2 friction draft tube	88,3	
8. outflow	78,03	46,0

Table 20 - Head losses and location for design variant 0 (copy of Maurik) for an available head of 2m, speed ratio of 1,1 and efficiency of the turbine of 95%

Kaplan turbine power

Two approaches have been taken:

1. Where the speed ratio is constant and the whole system has fixed geometry
2. Where the speed ratio is varied, assuming that varying the speed ratio is equivalent as changing the resistance given by the turbine, as in blade angle, generator resistance, etc.

The whole model is written in Mathcad and added as **Appendix 16** – Hydraulic model Kaplan-bulb.

For a fixed speed ratio, the error that the approximation has given compared to the theory, is such that head-differences lower than the design point the head over the turbine will be under-estimated. For head-differences that are larger than the design point the head over turbine will be over-estimated. This can also be seen in **Figure 66**.

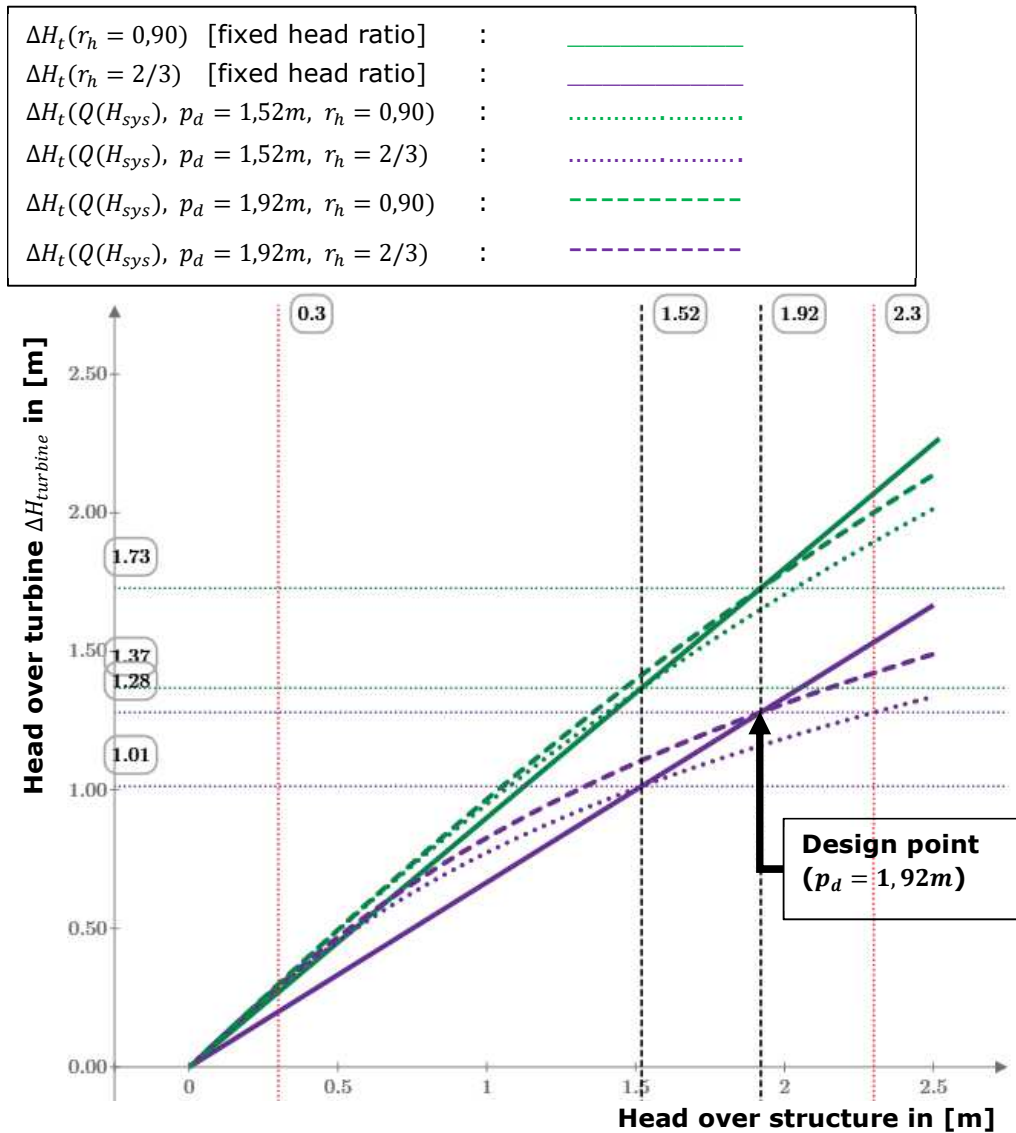


Figure 66 - Fixed head-ratio versus head-ratio conform turbo-machinery theory

What can also be seen in **Figure 66** is that for higher head-ratios, the error with the theory is smaller.

The efficiency curves have been estimated using a hill chart from Pentair (see **Appendix 16**). The algorithm for calculating the power for both with fixed and variable speed ratio were determined and data from the average year 2008 also used in the generic turbine paragraph gave the following result shown in **Figure 67**.

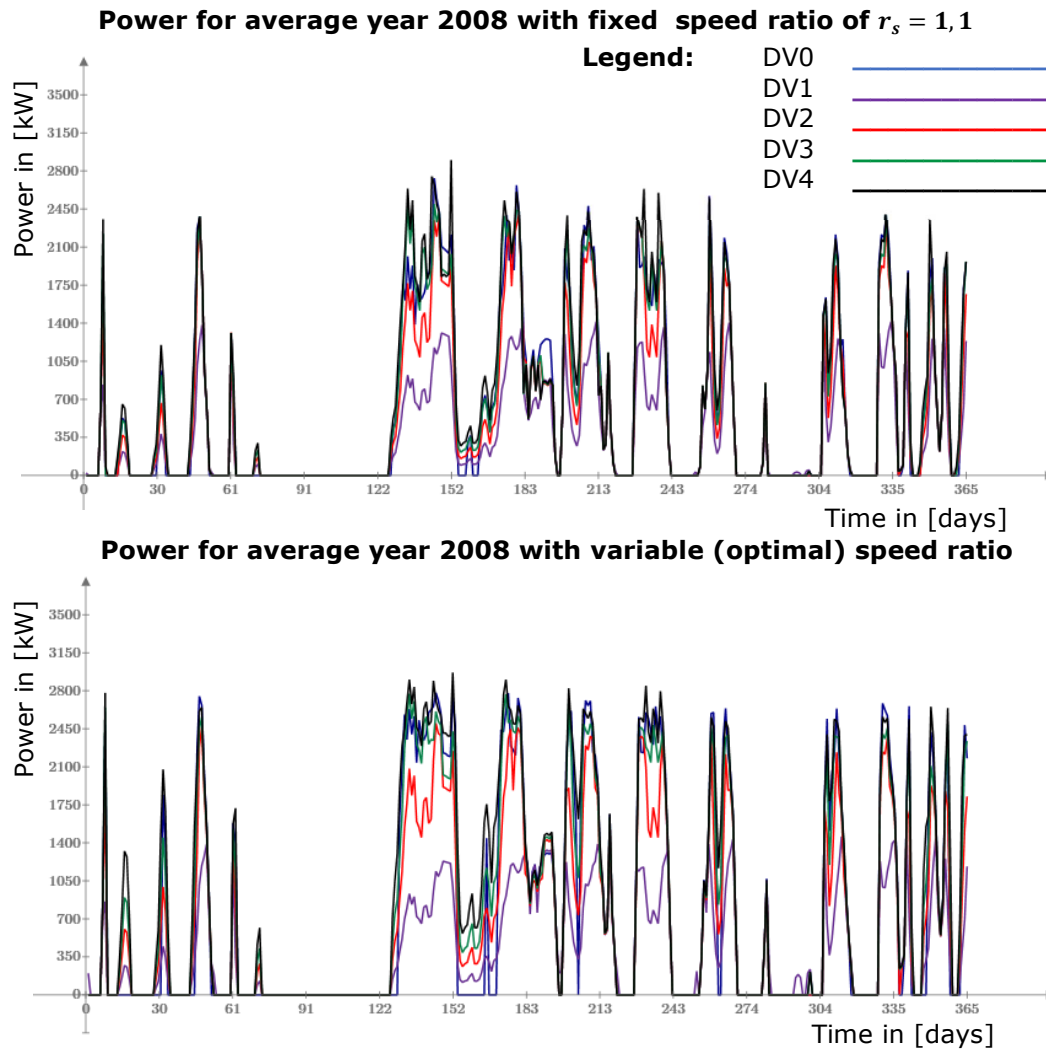


Figure 67 - Fixed versus variable speed ratio power production for data from 2008 – **Appendix 16**

Clearly having the variable speed ratio with the changing geometry (blade angle, etc.) produces more power, especially when head or flow is low.

Results from entering the design variants into the hydraulic model the power and energy produced are shown in **Table 21** below for variable speed ratio production:

Design variant	n_{min}	Diameters (rounded)	Rated Power in [kW]	Energy Production in [MWh]				
				Wet year 2002	Dry year 2003	Average year 2008	10 year average	30 year average
0	4	4,00	2975	8368	4156	6669	7180	5713
1	2	2,80	1470	3221	2439	3559	4499	2996
2	3	3,40	2550	6538	3634	5843	6453	4944
3	4	3,60	2800	8250	4124	7003	7356	5858
4	5	3,90	3000	9561	4422	7879	8118	6612

Table 21 – Hydraulic model Kaplan turbine results

Using the 2008 average as representative value the results from **Table 18** change to:

Design variant:		CoM	1	2	3	4
Installed capacity	kW	2975	1475	2642	3031	3160
Total costs	mIn €	19,3	9,6	17,1	19,6	20,5
Energie production	kWh	6.669.000	3.559.000	5.843.000	7.003.000	7.879.000
Price per kWh	€/kWh	2,89	2,69	2,93	2,80	2,60

Table 22 - Updated economic performance of regular Kaplan turbine

6.6 VENTURI ENHANCED KAPLAN

Venturi enhanced in this case means that the venturi effect, drop of pressure when flow-velocity increases, is used to increase the head-difference over the turbine. To achieve this, discharge is being employed to increase flow-velocity behind the outflow pipe of the turbine. This discharge (ideally) would otherwise not be used.

Basically, discharge is being used to increase the head-difference over the turbine, which makes it interesting for the location of Driel, because the head-difference is low and discharge can be relatively large as opposed to for instance hydro-power-dams in mountainous regions.

The test setup that was used in the research of 2014 [38] by "VerdErg Renewable Energy Ltd." is shown below in **Figure 68**. The tube or pipe with the turbine in it will from here on be called the "turbine tube". The main flow goes through what could be called a bypass from the turbine, so this is called the "bypass tube". In the mixing section the two flows come together and this pipe section till the outflow will be called the "common tube".

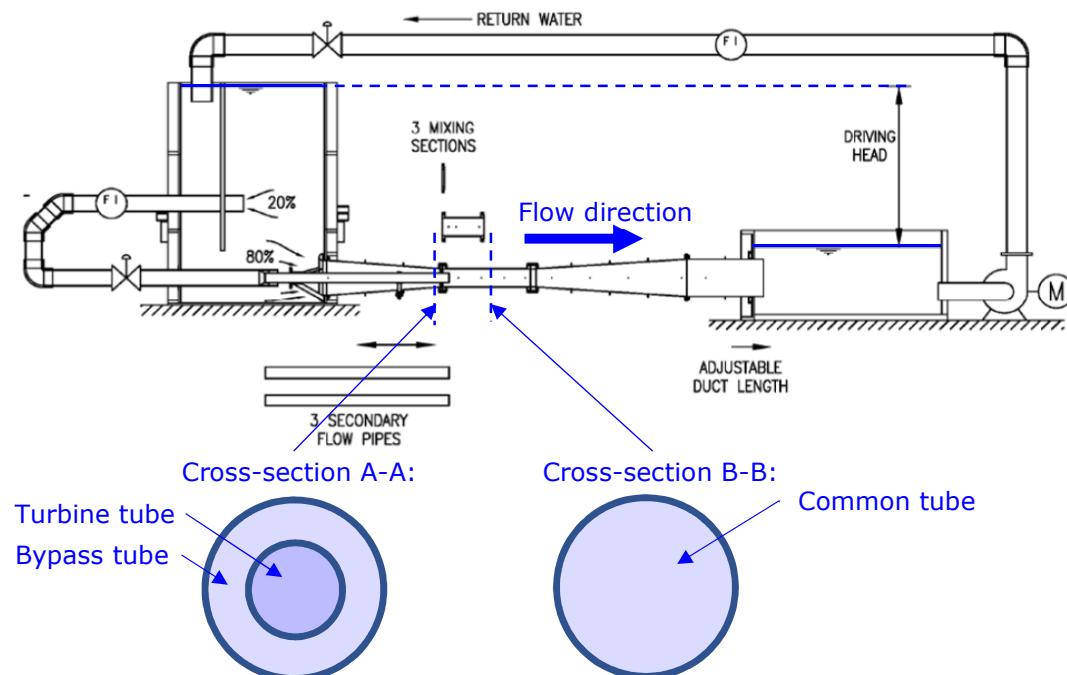


Figure 68 - Drawing of test setup for performance tests on Venturi Enhanced Turbine (top) and below cross-sections and flow velocities - Source: [38, p. 5]

6.6.1 Head discharge relation

The head gain is caused by the mixing zone, the “conflux zone”. The water going through the bypass tube just before the confluc zone has a higher flow velocity than the turbine flow and slows down in the common tube giving its momentum to the slower moving water particles from the turbine flow.

The turbine flow gets boosted by this bypass flow interaction and instead gains momentum when transitioning to the common flow. Eventually after some length (the mixing length) the flow velocity stabilises to the well-known velocity profile and the flows have mixed completely. This can also be seen in **Figure 69**.

In **Appendix 2** the “loss” coefficients related to this head gain are described and included in the hydraulic model of the VET included in **Appendix 17**.

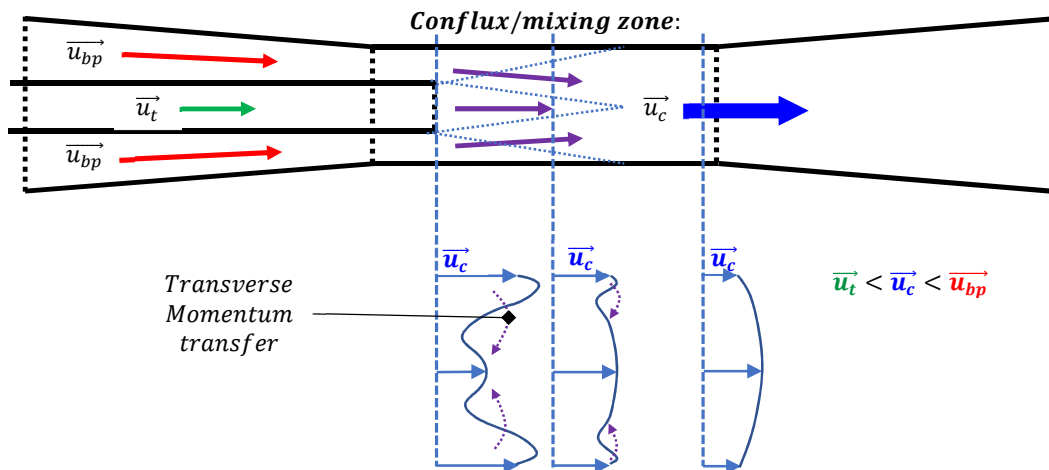


Figure 69 - Longitudinal cross-section with flow velocities and sketch of velocity field

This makes determining the discharge a bit more challenging. The company indicated that the ratios of discharge were 20% through the turbine and 80% through the bypass [38]. This distribution is a bit arbitrary, because it may change per head difference

From continuity the discharge through the turbine and through the bypass together need to be equal to the common flow. What discharge actually goes through each pipe is determined by its resistance which can be quantified with the quadratic resistance coefficient and for turbine tube also by the turbine head. Essentially the turbine tube is just a regular Kaplan pipe system except it has no draft tube.

What also needs to hold true is that the head over the two separate pipes is equal. The following can be stated:

Head over turbine and bypass:

$$\Delta H_{tt} = \Delta H_{bpt} \quad (10)$$

And:

$$\Delta H_{tt} = \Delta H_t + \Delta H_{tt_loss} = (Q_{tt})^2 * \frac{\eta^2}{g} \left(\frac{N}{N_s}\right)^4 + Q_{tt}^2 * C_{tt} \quad (11)$$

$$\Delta H_{bpt} = \Delta H_{bpt_loss} = Q_{bpt}^2 * C_{bpt} \quad (12)$$

$$\Delta H_{ct} = \Delta H_{ct_loss} = Q_{ct}^2 * C_{ct} \quad (13)$$

$$Q_{ct} = Q_{tt} + Q_{bpt} \quad (14)$$

Where the following subscripts correspond to these sections of the pipe system:

tt = the turbine tube section
 bpt = the bypass tube section
 ct = the common tube section

And where:

ΔH_t = The head over the turbine in [m]
 ΔH_{tt_loss} = The head-losses in the turbine tube in [m]

To get to the total head difference over the structure the head over the separated section and the common section are summed.

$$\Delta H_{ava} = \Delta H_{par} + \Delta H_{ct} \quad , \quad \text{where: } \Delta H_{par} = \Delta H_{tt} = \Delta H_{bpt} \quad (15)$$

The subscript "par" correspond to the section where the parallel tubes are present, indicating both turbine and bypass tube.

For a parallel system without a turbine load the equation could be rewritten to:

$$Q_{par} = Q_{tt} + Q_{bpt} \leftrightarrow Q_{ct} = \sqrt{\frac{\Delta H_{tt}}{C_{tt}} + \frac{\Delta H_{bpt}}{C_{bpt}}} \leftrightarrow \sqrt{\frac{\Delta H_{par}}{C_{pt}}} = \sqrt{\frac{\Delta H_{par}}{C_{tt}} + \frac{\Delta H_{par}}{C_{bpt}}}$$

Rewrite to C_{par} :

$$C_{par} = \frac{1}{\frac{1}{C_{bpt}} + \frac{1}{C_{tt}}} \quad (16)$$

Note: this is just like summing the resistances of parallel resistors in an electric circuit.

However, when also the turbine is taking a part of the head this doesn't work anymore.

Deduced is that two variables need to be solved, namely the discharge through the system Q_{sys} and the discharge through the bypass Q_{bpt} (or, alternatively the turbine, either one works).

Defining the following relations:

$$Q_{sys} = Q_{ct} \quad (17)$$

$$Q_{tt} = Q_{sys} - Q_{bpt} \quad (18)$$

Where:

Q_{sys} = The system discharge in [m^3/s] going through the entire pipe system. It is equal to the common tube discharge and also the combined discharge through the parallel part of the system.

The system of equations to solve Q_{bpt} and Q_{sys} with is then:

$$\begin{cases} \Delta H_{ava} = \Delta H_t + \Delta H_{t,loss} + \Delta H_{ct} \\ \Delta H_{bpt} = \Delta H_{tt} \end{cases}$$

Expanding/substituting previously defined relations:

$$\begin{cases} \Delta H_{ava} = \left(\frac{(\eta * (Q_{sys} - Q_{bpt}))^{\frac{2}{3}} \left(\frac{N}{N_s} \right)^{\frac{4}{3}}}{g} \right) + (Q_{sys} - Q_{bpt})^2 * C_{tt} + (Q_{sys})^2 * C_{ct} \\ C_{bpt} * (Q_{bpt})^2 = \left(\frac{(\eta * (Q_{sys} - Q_{bpt}))^{\frac{2}{3}} \left(\frac{N}{N_s} \right)^{\frac{4}{3}}}{g} \right) + C_{tt} * (Q_{sys} - Q_{bpt})^2 \end{cases} \quad (19)$$

All the variables in this set of equations, except for the system discharge Q_{sys} and the bypass discharge Q_{bpt} , are either given for a situation (the available head for instance), or part of the geometry and configuration of the system and thus known. Solving the system in **(19)** with Newtonian method, making use of the inverse Jacobian matrix, gives both the unknown discharge and enables calculation of all the discharges, head losses, etc. in the system. (See also **Appendix 17** with the hydraulic model of the VET)

6.6.2 Design variants

In the eye of time, the design variants will be based on the regular Kaplan designs (same discharge area). This in effect means that the existing design variants are fitted with a bypass. The VET design variants are determined with the same diameter ratio as well:

Design variant	Number of turbines n_{min}	Discharge area A_t per VET* in $[m^2]$	Diameter of VET (rounded to 5cm) in $[m]$
0 (CoM)	4	10,8	4,05
1	2	5,00	2,75
2	3	7,80	3,45
3	4	8,75	3,65
4	5	10,00	3,95

Table 23 – Design variants for Venturi Enhance turbine (VET) – See **Appendix 17**

All the parts of the VET have been designed with the rules of thumb for Kaplan turbines as shown in **paragraph 6.5 “Regular Kaplan Turbine”**.

Below a table with important dimensions:

Design variant	Nr. of turb.	D_{rotor}	Diameter Inflow opening of the bypass tube	Length total	Width total	Area per turbine	Area total
DV	#	m	m	m	m	m^2	m^2
0	4	4,0	10,4	86,3	46,8	901	3.603
1	2	2,8	7,1	58,6	17,2	416	831
2	3	3,4	8,9	73,5	30,7	654	1.961
3	4	3,6	9,4	77,7	42,7	732	2.926
4	5	3,9	10,1	83,1	56,3	835	4.176

Table 24 – Dimensions of power house for Venturi enhanced Kaplan turbine

6.6.3 Head gain

The discharge area ratio is defined as:

$$r_A = \frac{A_{tt}}{A_{ct}} \quad (20)$$

Where in this case the:

A_{tt} = The discharge area in [m^2] of the turbine tube at the cross section where it connects with the confluent zone

A_{ct} = The discharge area in [m^2] of the common tube/confluent zone

By trial and error changing this ratio it was found that the head gain is largest when the area ratio is 80% or higher. The related discharge ratio is actually lower than the claimed 80%/20% ratio. The claim that Verderg makes is also that with a 2,5m head ratio a 7,5m head ratio can be achieved. This seems unlikely, but was also not disproven here.

The higher the flow-velocity of the bypass tube with respect to the turbine tube is, the larger the head gain. Increasing the area ratio does this, although there is a point where the gap is so small that the flow is stopped completely. So r_A can for instance not be 99,9%. To prevent the flow velocities from getting unrealistic (in the order of 200m/s) a nice middle way was found at an area ratio of 94%.

For this ratio the discharge and head differences were calculated for 4 available head differences shown in **Table 25**. As can be seen the head differences over the turbine are higher than the available head. This goes at the cost of a discharge between 4 and 16 m^3/s , that is around 20% for available heads of 2,5 and 2,0m and near 50% of the total discharge for the lowest available head differences.

Available head in [m]	DV0	DV1	DV2	DV3	DV4
2,5	2,95	2,91	2,95	2,96	2,98
2,0	2,46	2,43	2,45	2,46	2,47
1,4	1,74	1,73	1,74	1,74	1,74
0,5	0,54	0,54	0,54	0,54	0,54
Speed ratio:	1,6	2,35	1,9	1,8	1,7

Table 25 – Head over turbine in [m] - Venturi effect quantified – Head over turbine for 3 available head-differences – See **Appendix 17**

The speed ratio also plays a role in the head gain. There is a certain optimal value, but the relation is not as clear as for the regular Kaplan. The optimal speed ratio is therefore determined iteratively.

When the bypass is opened there is also a small increase in discharge. Comparing power gained and power lost, for the area ratio of 94% is as follows:

Power in [kW] gained by opening bypass					
Available head in [m]	DV0	DV1	DV2	DV3	DV4
2,5	972	422	683	770	883
2,0	627	274	437	492	559
1,4	250	111	173	193	216
0,5	5,8	2,7	4,0	4,4	4,8
Power in [kW] Lost by opening bypass					
2,5	481	215	346	390	449
2,0	354	158	254	286	328
1,4	198	89	141	159	181
0,5	26,6	12,2	19,0	21,3	24,1

Table 26 – Power gained/lost by opening bypass for different available heads – See **Appendix 17**

As can be seen in the table above, whether more power is gained or lost by opening the bypass depends on its configuration (speed ratio), available head and geometry. However, with the speed ratio above it is possible to gain power till at least 1,4m.

6.6.4 Power output VET

In the model for the power production both open and closed bypass are calculated and the largest one is chosen. Instead of deriving the exact relation for the optimal speed ratio, an approximation is made here where the optimum was found for the available heads shown in **Table 26**. The speed ratio was then interpolated.

The same efficiency curves have been used for the VET as were used for the regular Kaplan turbines, only now scaled to the discharge of these turbines. The head-difference efficiency remains the same. The same range of head differences as for the Kaplan is expected for the VET.

Turbines switch on and off in the same way as regular Kaplan, except for the VET first the discharge with the bypass is checked. If not enough is available to run the bypass, then the remaining flow is used to power the turbines with switched of (meaning they closed the valve) the bypass.

Because the system of equations was a bit demanding computationally a series of discharges was calculated for a predefined series of available heads. A cubic spline function was then defined for faster lookup.

Design variant	n_{min}	Diameter of VET (rounded to 5cm) in [m]	Rated Power in [kW]	Energy Average year 2008 in [MWh]	10 year average - Energy	30 year average - Energy
CoM	4	4,05	3673	8087	6307	6565
1	2	2,75	1699	3994	3184	3312
2	3	3,45	2909	7105	5508	5741
3	4	3,65	3510	8097	6372	6654
4	5	3,95	3977	9256	7334	7603

Table 27 – Hydraulic model Venturi turbine results

The difference between the Regular Kaplan Turbine and Venturi Enhanced Kaplan are shown in **Figure 70** on the next page.

6.6.5 Cost estimation VET

The investment cost have been estimated in the same way as the Kaplan, being based on the cost per kW from HPP Maurik. The uncertainty for the VET has been taken to be 30%, because of the larger number of parts in the system, making the price €7.020,- per kW.

With those assumptions the following cost-breakdown can be made:

Design variant:		0 (CoM)	1	2	3	4
Turbine diameter	m	4,05	2,75	3,45	3,65	3,95
Rated Power	[kW]	3.673	1.699	2.909	3.510	3.977
Total costs	mIn €	25,8	11,9	20,4	24,6	27,9
Energy production	kWh	8.087.000	3.994.000	7.105.000	8.097.000	9.256.000
Price per kWh	€/kWh	3,2	3,0	2,9	3,0	3,0

Table 28 –Costs of VET design variants – See **Appendix 17**

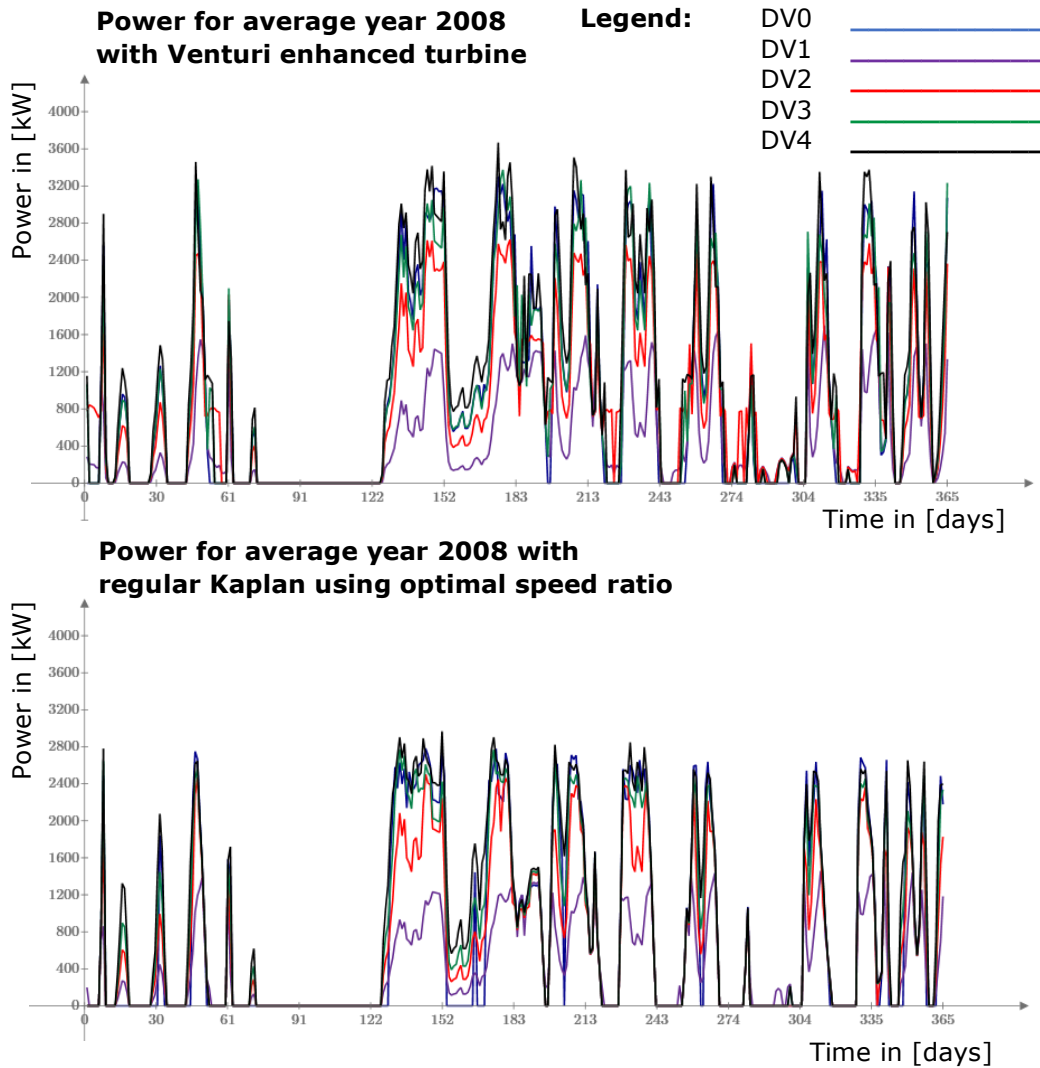


Figure 70 – Venturi versus Regular Kaplan power production for data from 2008 – **Appendix 17**

6.6.6 Conclusions VET

The Venturi Enhanced (Kaplan) turbine is an interesting concept and can be investigated further still. Many optimisations and design considerations can still be done. The current version of the design is expensive for the energy yield it has (€/kWh). But it was definitely proven that by sacrificing discharge the head can be increased till more than the available head-difference, which means that the turbine can be operated for longer than ones without a bypass enhancement.

The most cost effective design variant is design variant number 2. It is however clear that by basing the design variants directly of the Kaplan design the energy extraction is not ideal. Having larger and more turbines can be a solution to this.

Also the energy has been calculated with a fixed speed ratio (so basically it is a propeller instead of a double regulated Kaplan). This because calculating the optimal ratio proved challenging, especially within the used program (MathCad).

Recommended would be to do the calculation with a software package that is better suited to run extensive loops. Perhaps a Python script will work well.

6.7 ARCHIMEDES SCREW TURBINE (AST)

Taking a copy of the reference project (see **4.4.2 Reference project Dommelstroom**) "Dommelstroom" at Sint-Michielsgestel to the situation of Driel, for the design variants the amount of turbines can be estimated by taking the same total discharges from the Kaplan turbines (as discharge area for a Kaplan system is not really comparable with an AST).

Design variant	Total discharge $Q_{max,total}$ in $[m^3/s]$	Number of turbines $n_{Q=10}$	Discharge per turbine Q_t in $[m^3/s]$	Total power ($P_{rated} = 156kW$) [kW]
CoM	333,6	33	10,1	5137
1	110,8	11	10,0	1712
2	232,1	23	10,1	3580
3	298,8	30	10,0	4670
4	356,3	36	9,9	5604

Table 29 - Amount of AST's per design variant

A large amount of turbines are needed to get the same amount of power as the Kaplans due to the smaller discharge capacity of the AST's. The area south of the weir has about 87m available. The turbine in Sint Michielsgestel is 6m wide. Assuming some extra space is needed and each turbine needs 7m, then 12 AST's can be fit south of the weir. This is sufficient for design variant 1, but only gets to half or 1/3 of the required amount for the other design variants.

This makes the land usage as follows:

Design variant	Nr. of turb.	D_{rotor}	Width per turbine	Length total	Width total	Area per turbine	Area total
DV	#	m	m	m	m	m ²	m ²
0	33	4,0	7,0	8,0	231,0	56	1.848
1	11	4,0	7,0	8,0	77,0	56	616
2	23	4,0	7,0	8,0	161,0	56	1.288
3	30	4,0	7,0	8,0	210,0	56	1.680
4	36	4,0	7,0	8,0	252,0	56	2.016

Table 30 - Dimensions of power house for Archimedes Screw Turbine

Inflow water and fill level

AST's are most efficient when both downstream and upstream ends of the turbine are halfway in the water [39, p. 7]. The water level is therefore also of influence on the efficiency of the turbine. However, this goes beyond the scope of this research to exactly calculate this.

From geometry the minimum head can be calculated. Assuming for the moment the downstream level is constantly at turbine axis level, regulated by the downstream weir.

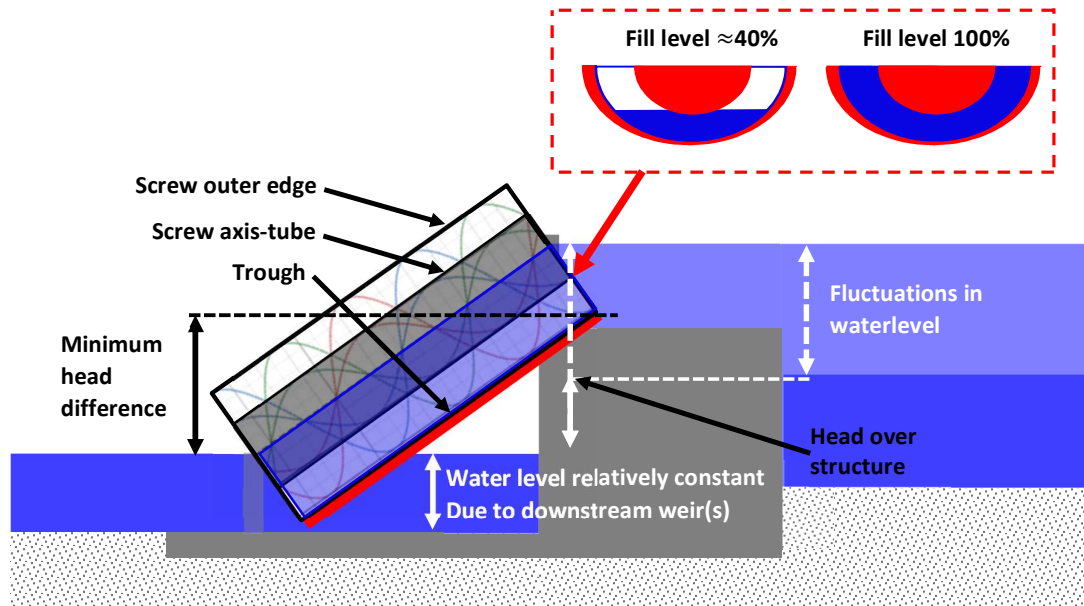


Figure 71 – Longitudinal schematic cross section of Archimedes screw to determine minimum head difference

The minimum head difference is clearly also dependent on where the through opens up stream. For the copy of Dommelstroom, the trough is assumed to be closed at the outside edge of the screw till the end of its length (like indicated in **Figure 71**). Thus the minimum head required to let water through the turbine is as follows:

$$\Delta H_{t,thres} = L_{screw} * \sin(\beta) - \frac{D_{out}}{2} * \cos(\beta) = 6,0 * 0,375 - 2,0 * 0,927 = 0,393m \approx 0,4m \quad (21)$$

Where:

L_{screw} = The length of the screw in [m]
 D_{out} = The outer diameter of the screw turbine in [m]
 β = The angle of inclination (with respect to horizontal) in [°]

The cross-section of the inlet looks somewhat like indicated in the top right of **Figure 71**. The effect of a head difference lower than design level will be taken into account by a percentage based on the fill level.

Approximated as shown in **Figure 72**. Here also the efficiency as function of discharge is shown. The total efficiency is assumed to be the product. The maximum efficiency is then at 80% of the discharge and 100% of the head-difference.

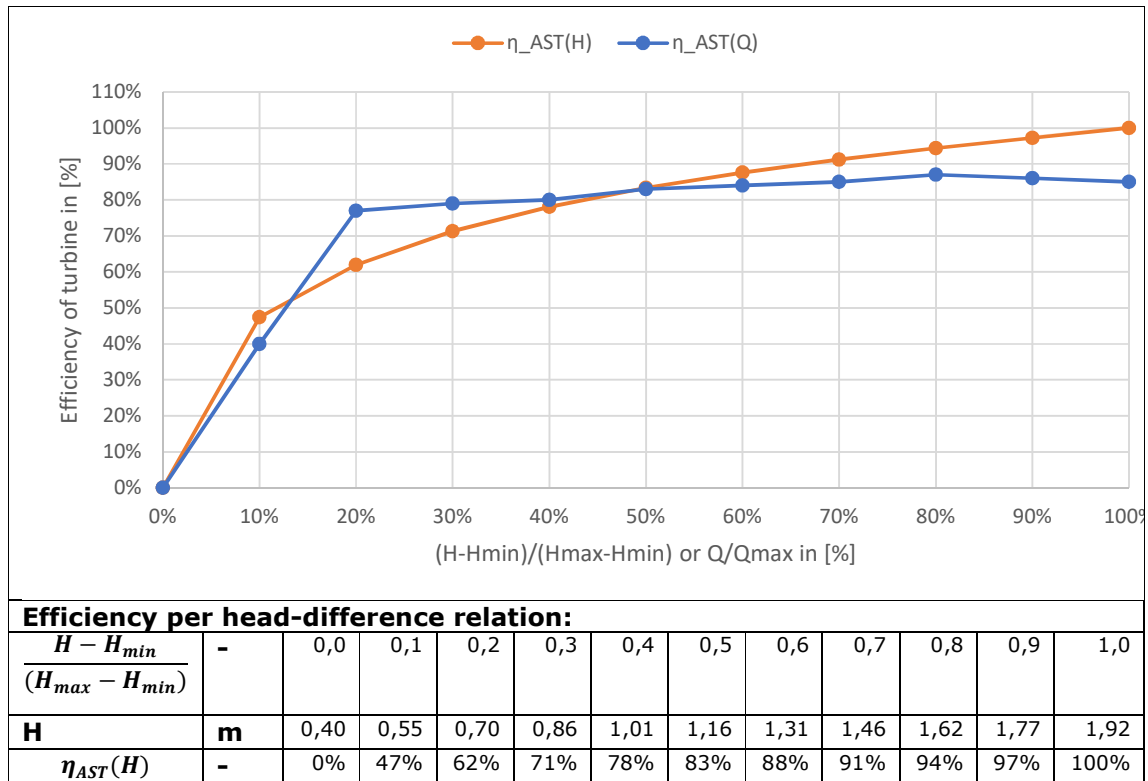
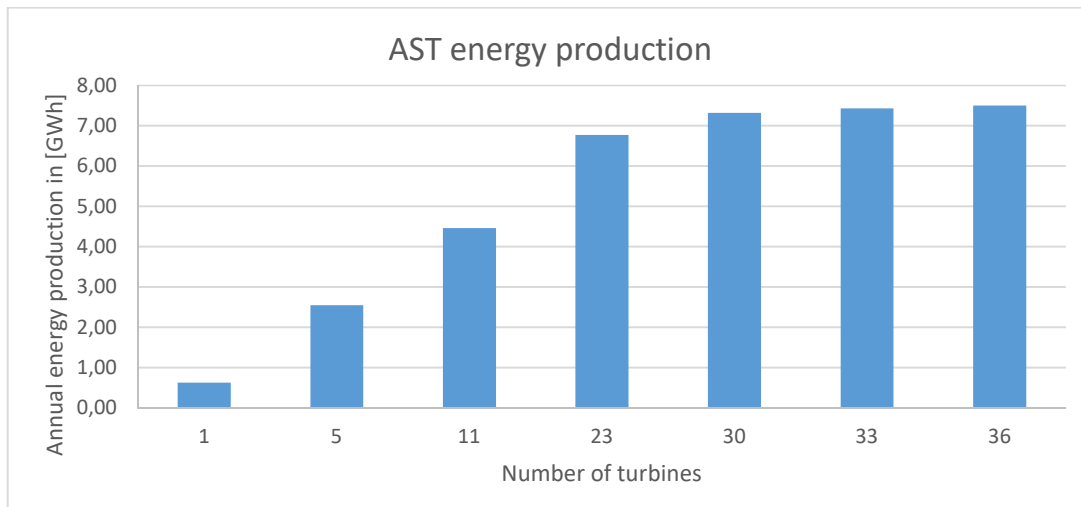


Figure 72 - Efficiency as function of fill level of AST inlet.

With that the production is:



Design variant	Nr. of turbines $n_{Q=10}$	Annual Energy in [GWh/year]	Capacity factor in %	Cost based on Dommelstroom in [mln €]	Investment per annual energy in [€/kWh/year]
CoM	33	7,44	16,5%	51,4	6,90
1	11	4,46	29,7%	17,1	3,84
2	23	6,77	21,6%	35,8	5,29
3	30	7,32	17,9%	46,7	6,38
4	36	7,50	15,3%	56,0	7,47

Table 31 - Performance AST's

Costs estimate made in **Table 31** is based on Dommelstroom, but with a uncertainty margin of 20% as the situation at Driel is different than at Sint Michielsgestel. They are estimated as being 1,2 million € per 120kW including all civil works, electrical equipment, etc. This makes the price €10.000,- per kW, much higher than the other turbine types.

Conclusions for AST

The Cost assessment in **Table 29** is perhaps a bit crude, as for Driel there will be much more civil engineering costs with dredging a channel and creating a sufficient spill way to cancel the obstruction that these number of turbines will form.

The AST performs best for low flow situations. The energy density is larger for Kaplan turbines as less turbines are needed to create the same amount of energy.

The variant with the lowest price per yearly estimated kWh is design variant number 1 of only 3,84 euros per kWh which is scoring the best and thus included in the scoring table in **chapter 7**.

The pump enhanced AST was looked into but quite quickly it became clear this is not interesting for the location at Driel.

6.8 CONSTRUCTION DEPTH

Concerning the rotation speed all the designs are based on Maurik. This means the rotor turns with a speed of about 78rpm and has a gearbox that increases the rotation speed to the generator to 750rpm. For cavitation the 78rpm is the relevant number.

The Thoma coefficient is largest when the specific speed is largest. With a constant rotation speed this happens at a low head and a large discharge, due to the specific speed relation.

For the regular Kaplan turbines the admissible depth of the central axis of the rotor is:

Setting depth for Kaplan turbines					$T = [^\circ]$	0	10	20	30
					$h_{vap} = [m]$	0,06	0,13	0,24	0,43
Design variant	h_f	N	N_{qmax}	σ_{Ts}	h_{atm}	$h_{s,adm}$	$h_{s,adm}$	$h_{s,adm}$	$h_{s,adm}$
	m	rpm	rpm	-	m	m	m	m	m
0	0,60	78	188	0,65	10	9,55	9,49	9,37	9,18
1	0,30	78	185	0,60	10	9,76	9,70	9,58	9,39
2	0,30	78	226	0,90	10	9,67	9,61	9,49	9,30
3	0,30	78	239	1,10	10	9,61	9,55	9,43	9,24
4	0,33	78	259	1,30	10	9,51	9,45	9,34	9,14

Table 32 - Setting depth of Kaplan turbines using Thoma's cavitation coefficient

The Regular Kaplan turbines need to be built quite deep, but this is quite comparable to the construction depth of the Maurik power plant, so not unexpected.

For the AST cavitation doesn't play a role and for the Venturi Enhanced turbine more research should be done into cavitation as it is not clear if it can be assumed that the method used for regular Kaplan turbines is also valid for the more complex hydraulic system of the Venturi turbine.

6.9 FINANCIAL ANALYSIS

6.9.1 Magnitude of investment

	Design variant	Investment costs in [mln €]	Cost per kW	Cost per kWh per year
Kaplan 1988 (copy of Maurik)	0	19,3	6.480	2,89
Kaplan Pentair Turbine	1	9,6	6.480	2,69
	2	17,1	6.480	2,93
	3	19,6	6.480	2,80
	4	20,5	6.480	2,60
Venturi Enhanced turbine	2	20,4	7.020	2,87
	4	27,9	7.020	3,02
Archimedes Screw turbine	1	17,1	10.000	3,84
	2	35,8	10.000	5,29

Table 33 - Magnitude of investment summarizing table

By sheer volume of money the Regular Kaplan turbine design variant 1 wins by quite a lot. The next cheapest variant is 7,5 million euros more expensive than that one. Of the selected design variants the most expensive is the Archimedes screw turbine variant number 2.

6.9.2 Levelized cost of electricity (LCOE)

For investments in renewable energy development projects Triodos bank uses a rate of interest of 3,3% [40]. For lending money they will probably take a margin above this, so a percentage 5,3% is also considered in the results table.

Costs have been subdivided based on the percentages shown in **Figure 73**

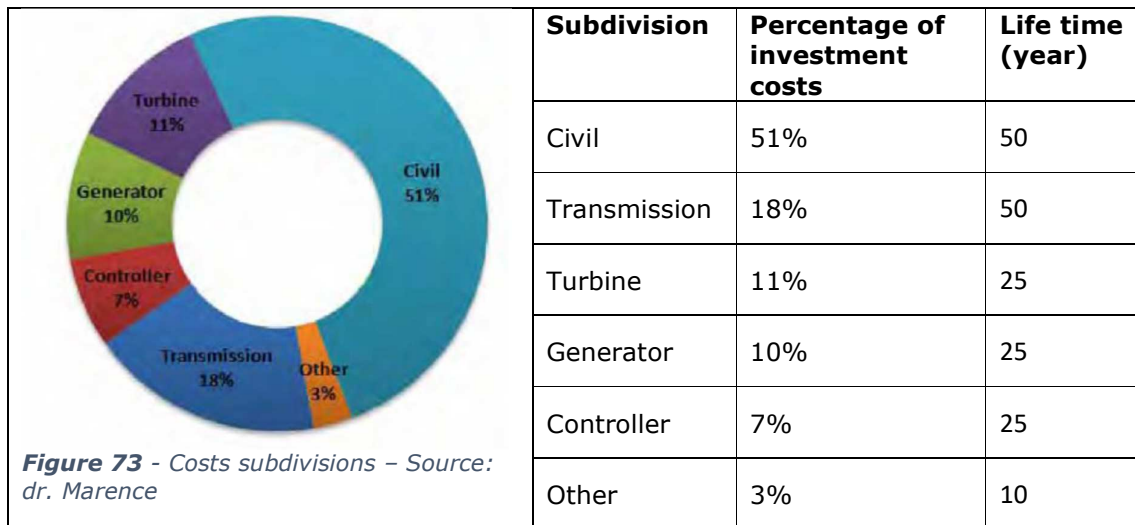


Figure 73 - Costs subdivisions – Source: dr. Marence

The different parts of the costs have a different lifetime and certain parts need to be replaced later in the life-cycle. The present value of these returning expenses have been calculated in the following way:

$$“Major\ expense”(year_x) = Expense(year_0) * \left(\frac{1+inflation}{1+r}\right)^x$$

For instance for design variant 0 (copy of Maurik) the investment costs are 19,3 Million. The “other” expenses are 3% of that (€579.000,-) and repeat every 10 years. According to “Worldwide Inflation Data” [41] inflation in the Netherlands was an average 2% the

last several decades. Using this, the present value of the expense in the 10th and 20th year are:

$$\text{"Major expense"}(\text{year } 10) = 579.000 * \left(\frac{1+0,02}{1+0,033}\right)^{10} = \text{€}510.126,-$$

$$\text{"Major expense"}(\text{year } 20) = 579.000 * \left(\frac{1+0,02}{1+0,033}\right)^{20} = \text{€}449.444,-$$

For the revenue the same is done, only here the SDE subsidy comes into play. This is given per kWh of sustainable energy that is produced. There are a few "fases" that have different rates. The base rate is the only one that is considered here to give a conservative estimation. The base amount is €0,09/kWh with a correction in 2019 of €-0,046/kWh, so effectively €0,044/kWh [42]. The subsidy is given for the first 15 years of the lifetime of the hydropower plant. The yearly operational cost have been taken as 4%.

In general the present value of the revenue is calculated as:

$$\text{revenue}_{+SDE}(\text{jaar}_x) = (E_{\text{annual}} * (PoE + SDE) - OC) * \left(\frac{1+\text{inflation}}{1+r}\right)^x$$

Where:

PoE = Price of electricity in [€/kWh]

OC = Operational costs in [€]

For design variant 0 an LCOE was found of €0,174/kWh, so then the present value of the revenue in the 1st, 10th and 20th year is as follows:

$$\text{revenue}_{+SDE}(\text{jaar}_1) = (6.669.000 * (0,174 + 0,044) - 46.446) * \left(\frac{1+0,02}{1+0,033}\right)^1 = \text{€}1.390.408,-$$

$$\text{revenue}_{+SDE}(\text{jaar}_{10}) = (6.669.000 * (0,174 + 0,044) - 46.446) * \left(\frac{1+0,02}{1+0,033}\right)^{10} = \text{€}1.038.101,-$$

$$\text{revenue}_{+SDE}(\text{jaar}_{20}) = (6.669.000 * (0,174 + 0) - 46.446) * \left(\frac{1+0,02}{1+0,033}\right)^{20} = \text{€}593.949,-$$

A design life-time of 50 years is taken. See for LCOE values **Table 34** of **chapter 7**.

The Archimedes screws have the highest cost of electricity and the regular Kaplan the lowest.

6.9.3 Internal rate of return

To indicate profitability of the investment (and thus how likely parties are willing to invest).

Using a cost of electricity of €0,207/kWh that design variant has as LCOE to normalise things. Only the 2nd design variant of the AST's is not able to get to zero after 50 years considered lifetime even with an interest rate of 0.

The best performing is design variant 4 of the regular Kaplan turbines with 6,7%. A close second is design variant 1 with 6,1%, which is interesting, because this was also the one with the lowest investment costs.

7 RESULTS TABLE

Results table		Variants								
Description	unit	Kaplan 1988	Kaplan Pentair				Kaplan Venturi		Archimedes Screw Turbine (AST)	
Design variant	-	DV CoM	DV1	DV2	DV3	DV4	DV2	DV4	DV1	DV2
Nr. Of turbines	#	4	2	3	4	5	3	5	11	23
Diameter of turbine	m	4,00	2,80	3,40	3,60	3,90	3,45	3,90	4,00	4,00
Land use (width of powerhouse)	m	45,0	17,0	29,5	41,0	54,8	30,7	56,3	77,0	161,0
Land use (minimum area of power house)	m ²	1.760	431	954	1.426	2.091	1.961	4.176	616	1.288
Rated Power	kW	2.975	1.475	2.642	3.031	3.160	2.909	3.977	1.712	3.580
Power per turbine	kW/#	744	738	881	758	632	970	795	156	156
Annual Energy	MWh	6.669	3.559	5.843	7.003	7.879	7.105	9.256	4.460	6.770
Capacity factor	%	25,6%	27,5%	25,2%	26,3%	28,4%	27,9%	26,6%	29,7%	21,6%
Estimated investment	Mln €	19,3	9,6	17,1	19,6	20,5	20,4	27,9	17,1	35,8
Investment cost per kW	€/kW	6.480	6.480	6.480	6.480	6.480	7.020	7.020	10.000	10.000
Investment cost per kWh per year	€/kWh/year	2,89	2,69	2,93	2,80	2,60	2,87	3,02	3,84	5,29
LCOE with r=3,3% and fase 1 SDE subsidy	€/kWh	0,174	0,161	0,176	0,178	0,154	0,173	0,182	0,238	0,336
LCOE with r=5,3% and fase 1 SDE subsidy	€/kWh	0,207	0,191	0,210	0,199	0,183	0,205	0,217	0,283	0,400
IRR with POE= €0,207/kWh and fase 1 SDE subsidy	%	5,3%	6,2%	5,2%	5,7%	6,7%	5,4%	4,8%	1,7%	0,0% (Loss)
Fish mortality rate	%	13%	2%	2%	2%	2%	< 2%	< 2%	5%	5%

Table 34 - Results table for all considered variants - POE=price of electricity

- Page intentionally left blank -

8 CONCLUSION AND RECOMMENDATIONS

8.1 CONCLUSIONS

First theory has been reviewed and theoretical model was produced that was able to match a Hill-chart of the Hydro-power plant in Maurik. The model uses turbo-machinery theory and hydraulic theory for pipe-systems.

8.1.1 Location

The location at Driel was assessed and an in depth analysis of the flow was performed. From this, a flow duration curve with related head-differences was produced. This was used for estimating production of various design variants.

Also spatially the location has been reviewed. For head based variants the possible locations are between the weir and the primary flood defence near the village of Driel. Between the weir and the lock there are several possibilities and North of the ship lock also some space is available. At the latter special attention needs to be paid to the present nature reserves and protected areas.

Another interesting find was that a mid-range voltage (10kV) cable runs through the weir. Connecting a hydro-power plant to this doesn't require lengthy wiring and accompanying costs and can be used given this cable can take the output power of the plant.

Shipping is a relevant factor for this location. Although more shipping goes over the Waal river, the Nederrijn also sees between 10 to 15 thousand ship movements per year, most of it going up stream. Professional shipping is quite constant throughout the year and recreational shipping is present mostly in the summer.

8.1.2 Flow analysis

The production was sought in flow regime b (partially closed), where the amount of opening of the weir gate(s) can be changed to divert flow to the turbines of a hydro-power plant. The weir functions as the main regulator valve for water distribution in the Netherlands. It's safe to assume that it is too complex to consider to change the weir operations for flow regimes "a" (fully closed) and "c" (fully open), as well as changing the moments when they happen. This because they affect many processes and regimes throughout the country ranging from flood defence at a national level to ground water regulation and agriculture on a local level.

Within flow regime "b" a generic turbine was designed, where no specific turbine type was assigned yet. After making several assumptions to reduce the amount of variables, 5 design variants were found with a certain discharge area and maximum discharge. One of these design variants resembles a copy of the turbines in Maurik. The other 4 were chosen more or less arbitrarily, sub-dividing the "annual production per discharge area"-curve.

A maximum to the discharge area was set to be 50m², because it can be concluded beforehand that power-plants much larger than Maurik (43,2m²) will not be economically feasible. Their production is half that of Maurik and the cost are the same or more, which leads to them being eliminated before further analysis.

After that the optimal speed ratio was investigated and it was found that using this optimal speed ratio an increase in power produced was reached between 9,7% and 16,6%. This optimal speed ratio is determined by the head ratio, which produces

maximum power when it is the largest value of either $2/3$ or 1 minus the normalised hydraulic losses (normalised with respect to available head difference).

8.1.3 Kaplan turbines

Building further on the generic turbine analysis, the Kaplan type was assessed. Diameters were determined from the discharge area and these dimensions were fed into the hydraulic models. This yielded a more precise energy estimation for the design variants.

The regular Kaplan turbines perform very well both technically and economically. Especially design variant number 4 that with 3,16 MW installed capacity produces the most energy of the regular Kaplan design variants. This variant also has the lowest LCOE of all the designs made.

8.1.4 Venturi turbines

The design variants for the Venturi enhanced Kaplan turbine are based on the regular Kaplan turbines, the difference being that they have an additional bypass pipe. This way the variants from the venturi enhanced turbines and the regular Kaplan can be compared and it is clear that with the enhancement more power and with that more energy is produced.

The enhancement does indeed increase the head difference over the turbine at the cost of discharge, if it has the right configuration regarding area ratio and turbine resistance. Given the right configuration, the amount of power lost is generally less than the power gained. Opening the bypass is therefore beneficial for most flow situations.

The challenge with the design of this variant was that extra parameters that came into play, like the ratio of area between the bypass and the turbine tube. An ambitious designer could even include a regulation valve to make the area ratio also variable during operation of the turbine.

All these degrees of freedom meant that some assumptions had to be made to get to one unique solution per variant within the time bounds of this research. The VET can easily be a thesis subject in and of itself.

Technically the Venturi performs really well, producing the most energy of all the variants. However, due to the high power capacity the estimated costs were also high. Economically the Venturi scores slightly worse than the regular Kaplan for this reason.

Further development and optimisation of this design is required to make it competing with the regular Kaplans.

8.1.5 Archimedes screw turbines

The Archimedes screw turbine (AST) was assessed using the reference project the "Dommelstroom". This project costs in total 1 million euros for 1 AST of 120 kW, producing in theory 600 MWh/year, but current production figures show more in the range of 370MWh.

An array of AST's of 23 "Dommelstroom" turbines appears to utilise the available flow quite well. Going by the reference project this would cost 35 million euros and yield on average 6770 MWh per year, good for about 1900 households (at 3500kWh/hh).

However, the costs per kilowatt are the largest of all variants and this makes the variant economically the least attractive. Perhaps with a more detailed cost analysis a reduction can be found in the fact that so many screws need to be produced. Having reoccurring designs generally reduces costs, both in mechanical and civil works.

8.1.6 Overall conclusions

To answer the main research question, all variants are technically able to extract energy from the very low head situation at Driel. As predicted beforehand the challenge lies in the economic feasibility. With sufficient SDE subsidy the regular Kaplan turbines can be made feasible. Of these design variant number 4 scores the best on LCOE and IRR. However, for HI design variant 1 might be more interesting as it has the lowest investment costs as well as the second best LCOE and IRR.

The Venturi enhancement is interesting technologically and potentially economically too. It needs further development to be competitive. The AST is performing the worst and, although it was able to get the same energy output figures, it didn't live up to the expectations of being the cheapest variant.

The method used for analysis at Driel can also be used for other low head run of river plants. When the choice is made to use pressurised flow with a turbo-machine based turbines the hydraulic models used in this thesis are applicable for similar situations and also the first estimation using the generic turbine can be very useful to get an idea of the size and amount of the turbines. The optimal head ratios and related speed ratios are also valid for other situations as the turbo machinery theory is specifically defined as being applicable for many different situations and types of turbo-machines.

However, when using a turbine with a fixed geometry, so not being able to for instance change the blade inclination can limit the range with which the speed ratio can actually be varied. The used theory is therefore most useful when designing double regulable Kaplan turbines.

8.2 RECOMMENDATIONS

As also mentioned in the conclusions, further development of the VET turbine design is highly recommended. The operational range of the Kaplan is increased and also the power produced. The configuration and calculation of energy yield can be further optimised. Also what should be looked into is how to optimise the head gain. For instance CFD analysis and/or lab tests showing the limits and benefits of the conflux behind a turbine tube.

Another recommendation is to look into other turbine types. In this study the Archimedes screw was at first considered a technologically more simple and thus cheaper power source, but turned out to be more expensive compared to the yield. Perhaps waterwheels can still be a competitive designs as they tend to have a very stable efficiency curve. Just like for the AST the flow capacity will be an interesting challenge for that type.

Also any further developments in low head turbine technologies could be investigated.

Location specific recommendations are: looking into combining water storage from high flow situations, so that this water flowing down the river is not wasted. In the locations analysis paragraph some suggestions have been made for storage areas. Being next to one of the few hills in the Netherlands, pumped storage could also be an option here. Challenge with that will be fitting it into the environment with nearby nature reserves and inhabitants.

Besides that, a study into fish friendliness for the future turbines will be greatly beneficial to the furthering the plans of realising the hydro power plant in Driel. For this working together with Hydro-power-plant Maurik is advised as they have both the same problem and more experience with it.

What also has to be kept in mind is that making a hydro-power station at Driel means that there are two active hydro power plants in the Nederrijn. Interaction and how to use the resources as an ensemble is something worth studying as well. Studying this system on a more national level could also include the IJssel lake and the locks and pump stations discharging water into the North-sea.

REFERENCES

- [1] Deepwater-Energy b.v., "Oryon Watermill," Deepwater-Energy b.v., [Online]. Available: <http://www.oryonwatermill.com/energy/productkenmerken>. [Accessed 05 12 2018].
- [2] United Nations, "Paris Agreement," in *Paris Agreement*, Paris, 2015.
- [3] Central Bureau of Statistics (Dutch) - CBS, "Open data CBS," 18 December 2018. [Online]. Available: <https://opendata.cbs.nl/statline/#/CBS/en/dataset/83140eng/table?ts=1546853268142>. [Accessed 7 January 2019].
- [4] Centraal Bureau voor de Statistiek (CBS), Den Haag; PBL Planbureau voor de Leefomgeving, Den Haag; RIVM Rijksinstituut voor Volksgezondheid en Milieu, Bilthoven; en Wageningen University and Research, Wageningen., "Inzet energiedragers en bruto elektriciteitsproductie (Dutch, translation: "Use of energy carriers and gross electricity production.")," 29 January 2019. [Online]. Available: <https://www.clo.nl/indicatoren/nl0019-inzet-energiedragers-en-bruto-elektriciteitsproductie>. [Accessed 07 May 2019].
- [5] Energie-opwek, "Energie Opwek .nl," Netbeheer Nederland, Tennet, Gasuni, SER, [Online]. Available: <https://energieopwek.nl/#over-het-energieakkoord>. [Accessed 10 12 2018].
- [6] Centraal Bureau voor de Statistiek, "Hernieuwbare energie in Nederland 2017 (Dutch, translation: "Renewable energy in the Netherlands 2017")," Centraal Bureau voor de Statistiek, Den Haag, 2018.
- [7] Fraunhofer-Gesellschaft, "Energy-charts.de," Fraunhofer-Gesellschaft, 03 May 2019. [Online]. Available: <https://www.energy-charts.de/osm.htm>. [Accessed 07 May 2019].
- [8] A. Moser, D. Wemyss, R. Scheidegger, F. Fenicia, M. Honti and C. Stamm, "Modelling biocide and herbicide concentrations in catchments of the Rhine basin.," *Hydrology and Earth System Sciences.*, vol. 22, no. 8, pp. 4229-4249, 2018.
- [9] W. Boiten, *Hydrometry: IHE Delft Lecture Note Series*, 3rd revised ed., Lisse: Swets & Zeitlinger B.V., 2003.
- [10] A. Kumar, T. Schei, A. Ahenkorah, R. Caceres Rodriguez, J.-M. Devernay, M. Freitas, D. Hall, Å. Killingtveit and Z. Liu, *Hydropower*. In *IPCC Special Report on Renewable Energy Sources and Climate Change*, O. Edenhofer, R. Pichs-Madruga, Y. Sokona, K. Seyboth, P. Matschoss, S. Kadner and T. Zwickel, Eds., Cambridge, New York: Cambridge University Press, 2011.
- [11] RWS (computer system), "Actuele overzichten watersystemen - Landelijk," RWS, [Online]. Available: <https://waterberichtgeving.rws.nl/water-en-weer/actuele-overzichten-watersystemen/landelijk-overzicht>. [Accessed 10 12 2018].
- [12] RWS - (computer system), "Actuele overzichten watersystemen - Nederrijn-Lek," RWS, [Online]. Available: <https://waterberichtgeving.rws.nl/water-en-weer/actuele-overzichten-watersystemen/nederrijn-lek>. [Accessed 10 12 2018].

- [13] T. Van Den Noortgaete, M. van Heereveld and L. Claassen, "Onderzoek potentie energie uit waterkracht in Provincie Gelderland," Haskoning Nederland B.V., Nijmegen, December 27, 2016.
- [14] M. Tukker and K. Kooij, "Bijlagen - Hydraulisch ontwerp en beheer afvalwatertransportsystemen (EN: Hydraulic design and maintenance of sewage-transport-systems)," in *CAPWAT Handboek v2*, 2nd ed., Delft, Deltares, 2012, pp. Appendix pages 6-13.
- [15] W. H. Hager, "Chapter 2 - Losses in flow," in *Wastewater Hydraulics - Theory and Practice*, 2nd ed., Berlin Heidelberg, Springer-Verlag, 2010, pp. 17-54.
- [16] I. E. Idel'chick, Handbook of Hydraulic Resistance - coefficients of local resistance and of friction, D. Grunauer and IPST-staff, Eds., Washington D.C.: U.S. Atomic Energy Commission and National Science Foundation - Israel Program for Scientific Translations Ltd., 1966.
- [17] S. Dixon, Fluid Mechanics, Thermodynamics of Turbomachinery, Fourth edition in SI/Metric units ed., Oxford: Butterworth-Heinemann - A division of Reed Educational and Professional Publishing Ltd - Reed Elsevier plc group, 1998.
- [18] E. W. Weisstein, "Newton's Method," MathWorld, 15 May 2019. [Online]. Available: <http://mathworld.wolfram.com/NewtonsMethod.html>. [Accessed 22 May 2019].
- [19] RIZA - Rijkswaterstaat - Directie Gelderland, De Rijn, Amsterdam: Drukkerij Mart. Spruijt, March 1993.
- [20] iisg; Boontje, Marcel;, "De waarde van de gulden / euro (EN: the value of the Guilder / Euro)," Een Instituut van de Koninklijke Nederlandse Akademie van Wetenschappen (KNAW), 2016. [Online]. Available: <http://www.iisg.nl/hpw/calculate-nl.php>. [Accessed 10 June 2019].
- [21] DEC Dommelstroom, "de waterkracht centrale (EN: the hydro power plant)," [Online]. Available: <https://dommelstroom.com/de-waterkrachtcentrale/>. [Accessed 16 June 2019].
- [22] A. J. Kozyn, *Power Loss Model for Archimedes Screw Turbines*, Guelph, Ontario: The University of Guelph - Faculty of Graduate Studies, 2016.
- [23] Kadaster, "Basisregistratie topografie with CC Licence," 01 September 2012. [Online]. Available: <http://chmodarch.com/nlindwg/>. [Accessed 27 May 2014].
- [24] Rijkswaterstaat - Ministerie van Infrastructuur en waterstaat, "waterinfo.nl," 2017 (daily updated data). [Online]. Available: <https://waterinfo.rws.nl>. [Accessed 11 March 2019].
- [25] Voorlichting Verkeer en Waterstaat - Rijkswaterstaat, *Stuwen is varen - De kanalisatie van de Neder-Rijn en Lek*, 2nd ed., Zutphen: Voorlichting Verkeer en Waterstaat, 1990.
- [26] van den Heuvel, Teha; VormVijf - Den Haag; RWS, "Brochure - Renovatie Stuwensemble - Nederrijn en Lek - Design & construct contract," Rijkswaterstaat, 12th March 2014. [Online]. Available: <https://www.tenderned.nl>. [Accessed 2nd May 2019].

- [27] T&W; RWS, "Iconische stuwen in Nederrijn en Lek in 2020 weer als nieuw," *Techniek & Wetenschap*; Webdesign by Insyde, 30th November 2016. [Online]. Available: <https://www.technischweekblad.nl/partnercontent/iconische-stuwen-in-nederrijn-en-lek-in-2020-weer-als-nieuw/item9733>. [Accessed 2nd May 2019].
- [28] H. Elbers and Hanselpedia, "Wikipedia - photo of weir complex Amerongen," 15 March 2011. [Online]. Available: <https://commons.wikimedia.org/w/index.php?curid=14615789>. [Accessed 30 May 2019].
- [29] H. Behrens, "Uitwerking informatiebehoefte waterstanden Rijkswaterstaat (translation: "Elaboration of information demand waterlevels Rijkswaterstaat")," Rijkswaterstaat, Deventer, 2008.
- [30] H. G. Tuin, "New canalization of the Nederrijn and Lek – Design of a weir equipped with fibre reinforced polymer gates which is designed using a structured design methodology based on Systems Engineering (Master Thesis)," Technical university of Delft, Delft, 2013.
- [31] Esri Nederland, "Actueel Hoogte Bestand Nederland (AHN)," Esri Nederland, community Maps Contributors, February 2019. [Online]. Available: <http://ahn.arcgisonline.nl/ahnviewer/>. [Accessed April 2019].
- [32] A. A.M.S. and H. J., "Statistisch overzicht van de Scheepvaart 2005," Ministerie van Verkeer en Waterstaat - Rijkswaterstaat Oost-Nederland, Arnhem, 2006.
- [33] van Blijderveen, Maarten; Liandon, "Geldersenergieakkoord - Bijlage 5 - Alliander [translation: Province of Gelderland energy agreement - appendix 5 - Alliander (electric-network-company)]," 23 December 2016. [Online]. Available: https://www.geldersenergieakkoord.nl/images/uploads/Bijlage_5_-_Alliander.pdf. [Accessed 05 October 2018].
- [34] Geldersch Landschap & Kasteelen - Afdeling Landschap en Kastelen en werkgebied Zuid Veluwe, "Beheervisie - Doorwerth," 13 December 2017. [Online]. Available: <https://assets.glk.nl/docs/da8142d7-2a8a-4313-8c4b-d94a95bf8897.pdf>. [Accessed 10 April 2019].
- [35] OpenStreetMap, "OpenStreetMap," OpenStreetMap, n.d. [Online]. Available: <https://www.openstreetmap.org/#map=16/51.9749/5.4100>. [Accessed 04 April 2019].
- [36] B. Pandey and A. Karki, *Hydroelectric energy - Renewable Energy and the Environment*, A. (. e. Ghassemi, Ed., Boca Raton: CRC Press - Taylor & Francis Group, 2016.
- [37] A. Betz, *Introduction to the Theory of flow machines*, Oxford: Pergamon Press, 1966.
- [38] Roberts, Peter; VerdErg Renewable Energy Ltd; Daly, Tim;BHR Group, "Venturi-Enhanced Turbine Technology," in *International Conference on Ocean energy*, 2014.

- [39] Landustrie, "Landustrie (company website)," 06 Oktober 2015. [Online]. Available: https://www.landustrie.nl/fileadmin/user_upload/LANDY_Hydropower_Screws.pdf. [Accessed 16 January 2019].
- [40] Triodos Bank, "Renewables europe fund - beleggen," Triodos Bank, 30 06 2019. [Online]. Available: <https://www.triodos.nl/beleggen/renewables-europe-fund>. [Accessed 14 07 2019].
- [41] Triami Media BV and HomeFinance, "Historische geharmoniseerde inflatie Nederland - HICP," Triami Media BV and HomeFinance, 2019. [Online]. Available: <https://nl.inflation.eu/inflatiecijfers/nederland/historische-inflatie/hicp-inflatie-nederland.aspx>. [Accessed 2019].
- [42] Rijksdienst voor Ondernemend Nederland, "Water SDE+ voorjaar 2019," 2019. [Online]. Available: <https://www.rvo.nl/sites/default/files/2019/02/Tabel%20Water%20SDE%20voorjaar%202019.pdf>. [Accessed 2019].
- [43] S. Bozhinova, V. Hecht, D. Kisliakov, G. Müller and S. Schneider, "Hydropower converters with head differences below 2,5m," in *Proceedings of the Institution of Civil Engineers - Energy*, 2013.
- [44] EDF Luminus, "Infopaneel centrales EDF Luminus," 2016. [Online]. Available: <https://www.google.com/url?sa=t&rct=j&q=&esrc=s&source=web&cd=1&ved=2ahUKewjOrbWG17njAhVCzKQKHAYMA34QFjAAegQIARAC&url=https%3A%2F%2Fedf.luminus.edf.com%2Fsites%2Fdefault%2Ffiles%2FLOT%25203%2FEDF%2520LUMINUS%2FANDENNE%2FPDF%2Ffr-infopaneel.pdf&usq=AOvVaw13>. [Accessed 2019].
- [45] H. Bakker, "Presentation - Lowering fish mortality at hydropower stations in Dutch rivers," 2016. [Online]. Available: http://fishmarket.fiskmarknad.org/images/Presentations/Harriet-BAKKER_Lowering-fish-mortality-at-hydropowerstations-in-Dutch-rivers.pdf. [Accessed 2019].
- [46] S. Dalley and J. P. Oleson, "Sennacherib, Archimedes, and the Water Screw: The Context of Invention in the Ancient World," *Technology and Culture*, vol. 44, no. 1, pp. 1-26, 2003.
- [47] T. Koetsier and H. Blauwendraat, "The Archimedean Screw-Pump: A Note on its Invention and the Development of the Theory," in *International Symposium on the History of Machines and Mechanisms*, Dordrecht/Boston/London, 2004.
- [48] K.-A. Radlik, "Hydrodynamic screw for energy conversion - uses changes in water supply to regulate energy output". Germany Patent DE4139134A1, 04 December 1997.
- [49] K. Brada, "Wasserkraftschnecke ermöglicht Stromerzeugung über Kleinkraftwerke," *Maschinenmarkt*, vol. 14, pp. 52-56, 1999.
- [50] D. Nuernbergk and C. Rorres, "Bestimmung des Durchflusses in Archimedischen Schnecken (German, in English: Calculation of the discharge of Archimedes Screws)," *Wasserkraft und Energie (Hydro-power and energy)*, vol. 20, no. 3, pp. 37-47, 2014.

- [51] J. Muysken, "Berekening van het nuttig effect van de vijzel. (Dutch, in English: Calculation of the nett effect of the screw.)," *De Ingenieur*, vol. 21, pp. 77-91, 1932.
- [52] J. Weisbach, *Lehrbuch der Ingenieur - und Maschinen-Mechanik*. (German, in English: Textbook of engineering and machine mechanics), 1st edition ed., Braunschweig: F. Vieweg und Sohn, 1855.
- [53] D. M. Nuernbergk, "Wasserkraftschnecken. Berechnung und optimaler Entwurf von Archimedischen Schnecken als Wasserkraftmaschine. (Hydropower screws - Calculation and Design of Archimedes Screws used in Hydropower)," Schäfer Verlag, Detmold, 2012.
- [54] J. Giesecke and E. Mosonyi, *Wasserkraftanlagen - Planung, Bau und Betrieb*, 5. edition, Ed., Singen: Springer, 2009.
- [55] W. Müller, "Die eisernen Wasserräder, Erster Teil: Die Zellenräder & Zweiter Teil: Die Schaufelräder (The iron water wheels, Part 1: the cell wheels & Part 2: the paddlewheels, in German)," Veit & Comp., Leipzig, 1899.
- [56] W. Müller, "Die eisernen Wasserräder: Atlas (The iron water wheels: technical drawings, in German)," Veit & Comp., Leipzig, 1899.
- [57] G. Müller, "WATER WHEELS AS A POWER SOURCE," pp. 1-9, 2004.
- [58] W. Fairbairn, *Treatise on Mills and Mill-Works*, 3rd ed., vol. Part 1, London: Longmans, Green & Co., 1874.
- [59] DINOLOket - TNO Geologische Dienst Nederland , "DINOLOket," n.d.. [Online]. Available: <https://www.dinoloket.nl/ondergrondgegevens>. [Accessed 08 April 2019].
- [60] Rijksdienst voor Ondernemend Nederland - Ministry of Agriculture, Nature and food quality, "Natura 2000," Alterra, August 2018. [Online]. Available: <https://www.synbiosys.alterra.nl/natura2000/googlemapszoek2.aspx>. [Accessed 03 April 2019].
- [61] Dutch Ministry of Argriculture, Nature and Food-quality - Rijksdienst voor Ondernemend Nederland, "Overzichtskaart ligging Natura 2000-gebieden - [translation: Overview map of location of Natura-2000 areas]," 03 May 2018. [Online]. Available: https://www.synbiosys.alterra.nl/natura2000/documenten/gebieden/A0_RVO_N2000_RV_20180503.pdf. [Accessed 04 April 2019].

